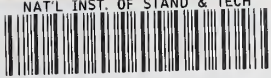


NAT'L INST. OF STAND & TECH



A11106 071106

NIST
PUBLICATIONS

NISTIR 6464

Counting Yields for Beta and Alpha Particle Sources

Martin J. Berger

U.S. DEPARTMENT OF COMMERCE
Technology Administration
National Institute of Standards
and Technology
Ionizing Radiation Division
100 Bureau Drive, Stop 8462
Gaithersburg, MD 20899-8462

QC
100
.U56
#6464
2000 c.2

NIST

Counting Yields for Beta and Alpha Particle Sources

Martin J. Berger

U.S. DEPARTMENT OF COMMERCE
Technology Administration
National Institute of Standards
and Technology
Ionizing Radiation Division
100 Bureau Drive, Stop 8462
Gaithersburg, MD 20899-8462

January 2000



U.S. DEPARTMENT OF COMMERCE
William M. Daley, Secretary

TECHNOLOGY ADMINISTRATION
Dr. Cheryl L. Shavers, Under Secretary of
Commerce for Technology

NATIONAL INSTITUTE OF STANDARDS AND
TECHNOLOGY
Raymond G. Kammer, Director

Counting Yields for Beta and Alpha Particle Sources*/

Martin J. Berger
National Institute of Standards and Technology
Gaithersburg, MD 20899

This report deals with the calculation and tabulation of the counting yields of beta- and alpha-particle sources. The counting yield is defined as the fraction of the emitted particles that emerge from the source and are counted by a 2 detector. This fraction is determined by the backscattering of particles from the backing, and their absorption within the backing. The counting yields were calculated with Monte Carlo transport codes that simulate the multiple scattering and slowing down of electrons and positrons in extended media. The calculated results apply (a) to very thin planar layers of beta-emitter at the surface of, or at various depths in the backing; (b) to beta-emitters distributed uniformly in a top layer of the backing.

* This work was supported by the U.S. Air Force under contract USAF-CCG:CCG-321.

1. Introduction

The purpose of this report was to tabulate counting yields of beta- and alpha-particle sources. The tables were calculated by Monte Carlo methods developed in earlier investigations [1-3]. The sources under consideration consist of a very thin layer of radioactive material deposited on top of, or at a specified depth within a thick backing, or radioactive material distributed uniformly in surface layer of the backing.

The counting yield, Y , is defined as the fraction of the emitted particles that emerge from the source and are counted by a 2π detector.*/ Knowledge of the counting yield is of importance for the calibration of detectors. When the backing is very thin, Y is very close to 0.5, because 50% of the particles are emitted toward the 2π detector, and the absorption of particles in the backing is negligible. With a planar source on top of a thick backing, Y is increased above 0.5, due to the contribution of backscattered particles. However, if the planar source is sufficiently deep in the backing, or if the radioactivity is distributed in a top layer of sufficient thickness in the backing, a significant fraction of the particles emitted toward the detector can be absorbed within the backing, so that Y can fall below 0.5.

Calculations of the counting yield can be done most expeditiously by the Monte Carlo method, i.e. by simulating the penetration, diffusion and slowing down of charged particles with use of random numbers. Many particles with initial energy E are started in random directions at a depth x below the surface of a semi-infinite medium. The emitted particles undergo many Coulomb interactions with atomic nuclei and with atomic electrons, which result in angular deflections and energy losses. Eventually the particles either emerge from the medium, or they are trapped in it because their residual range becomes too small for them to escape. The counting yield $Y(x,E)$ is equal to the average fraction of the sampled particle tracks which emerge from the semi-infinite medium.

The Coulomb collisions are extremely numerous, so that it is not feasible to simulate them individually in the Monte Carlo calculation. Instead, the so-called condensed-random-walk model is used [4,5]. The particle tracks are divided into a moderate number of segments (typically about 100), such that many Coulomb collisions occur in each segment. The angular deflection per segment is sampled from a multiple-scattering distribution, and the energy loss per track segment is calculated as the product of segment length times the stopping power. The use of stopping powers implies use of the continuous-slowning-down approximation. The neglect of energy-loss straggling can be shown to have a very small effect on the magnitude of the calculated counting yields.

* In earlier publications [1-3] this quantity was called the counting efficiency of the source. We prefer here to use the term counting yield, first used by radiochemists in the Manhattan project concerned with Pu-239 alpha-particle sources [6,7].

2. Counting Yields of Beta Sources

2.1. Monoenergetic Sources

The transport of electrons and positrons in extended media was treated with the Monte Carlo code ETRAN, which is based on the condensed random-walk model [4]. Descriptions of this code have been given by Seltzer [8,9]. The calculations were done with a special version of the ETRAN code which uses elastic-scattering cross sections from the computer code RELEL developed by Riley [10,11]. RELEL uses a screened Coulomb potential which is derived from electron density distributions generated with a relativistic Hartree-Fock program of Desclaux [12]. The accuracy of the condensed-random-walk model, in application to reflection and transmission coefficients and other quantities, has been verified in extensive comparisons [13,14].

Counting yields for monoenergetic isotropic sources, $Y(x,E)$, were calculated for plane isotropic electron sources at various depths $x \geq 0$ in Be, C, Al and Fe backings. Similar calculations were done for planar isotropic positron sources in Al and Fe backings. The calculations were done for 18 source energies up to 2.896 MeV. The results for electrons can also be extended, by interpolation with respect to atomic number, to compounds and mixtures. Trial calculations for compounds indicate that this interpolation can be done accurately by assigning to a compound an effective atomic number

$$Z_{\text{eff}} = \frac{\sum_j w_j (Z_j)^2 / A_j}{\sum_j w_j Z_j / A_j}, \quad (1)$$

where w_j is the fraction by weight, and Z_j and A_j are the atomic number and weight of the j 'th constituent.

2.2. Beta Spectra

Nuclear decay data for many radionuclides were compiled at the Oak Ridge National Laboratory by M. J. Martin [15]. This compilation was later extended to a larger number of radionuclides and incorporated into the ENDSDF file maintained at the National Nuclear Data Center at the Brookhaven National Laboratory. Using this ENDSDF file, and also the LOGFT program supplied by the National Nuclear Data Center, S. M. Seltzer at the National Institute of Standards and Technology calculated beta spectra which were stored in two large files, one for 649 beta(-) emitters, the other for 472 beta(+) emitters. These files were the source of information used in the present work.

Tables 1 and 2, for beta(-) and beta(+) emitters, respectively, list intensities, half lives, and the average and maximum energies of the beta spectra considered in this report. For radionuclides which emit several beta spectra with different endpoint energies, the tabulated maximum energy is that for the component spectrum with the largest endpoint energy. The tabulated average energy is an average (weighted by the intensities) of the average energies of the component spectra. Table 3 lists the maximum ranges of beta(-) and beta(+) particles in various materials, i.e. rectified path lengths evaluated the maximum energy of the beta spectra.

The counting yield for a planar beta source at depth x in the backing, $Y_b(x)$, is obtained as an integral over the beta spectrum $S(E)$:

$$Y_b(x) = \int_0^{E_{max}} Y(x, E) S(E) dE. \quad (2)$$

The evaluation of Eq(2) requires interpolation of $Y(x, E)$ with respect to E . This interpolation can be facilitated by tabulating the scaled counting yield $Y(x/r_0, E)$, where r_0 is the range at energy E . Plots of $Y(x/r_0, E)$ as a function of x/r_0 are shown in Fig.1 for Be, C, Al and Fe backings, for $E = 8, 512$ and 2048 keV. It can be seen that the scaled yields are rather insensitive to the value of E .

2.3. Tables of Counting Yields of Planar Beta Sources

A computer program CORBET is described in the Appendix, which interpolates in tables of $Y(x/r_0, E)$, and can be used to evaluate Eq(2) for any beta spectrum $S(E)$ with endpoint energy up to 2.896 MeV. Values of $Y_b(x)$ for 24 beta(-) emitters are given in Table 4 for Al backings, and in Table 5 for Fe backings. Values of $Y_b(x)$ for 12 beta(+) emitters are given in Table 6 for Al backings, and in Table 7 for Fe backings. In all these tables, the source depths are in units of microns. Illustrative plots of $Y_b(x)$ for Al-28, Sr-90/Y-90, Co-60 and C-14 sources are shown in Figs.2a-d for source depths x up to 20 microns in Be, C, Al and Fe backings,

A more economical description of the counting yields for beta spectra as a function of the source depth is obtained by tabulating the scaled quantity $Y_b(x/r_{max})$, where r_{max} is the maximum range at the endpoint energy of the spectrum (given in Table 3). Such scaled yields are shown in Fig.3a-d for Al-28, Sr-90/Y-90, Co-60 and C-14 sources, for Be, Al and Fe backings, and are tabulated for 24 beta(-) emitters are presented in Tables 8 to 11 for source with Be, C, Al and Fe backings.

Counting yields are of interest not only for the calibration of detectors, but also for determining the amount of radioactivity residing in surfaces contaminated with beta emitters. To provide input for illustrative applications of this kind, Tables 12 to 15 present scaled yields $Y_b(x/r_{max})$ for 24 beta(-) emitters located at various depths in four materials: sand, loam, dry soil and human skin (whose assumed compositions and effective atomic numbers are given in Table 3).

Finally, scaled yields for 12 beta(+) emitters are listed in Tables 16 and 17 for sources with Al and Fe backings.

2.4. Counting Yields for Sources with a Mylar Overlayer

In order to apply the results in Tables 4 to 17 to sources distributed in a top layer of the backing, one must know the source density $f(x)$ as a function of depth x . The counting yield for such a layer source is the average quantity

$$\langle Y_b \rangle = \int f(x) Y_b(x) dx. \quad (3)$$

Information about the depth distribution $f(x)$ may be difficult to obtain from the manufacturer of the source. However, it has been shown in Ref[3] that indirect information about $f(x)$ can be obtained by placing an overlayer of a plastic (such as mylar) on top of the source, and measuring

the relative transmission of the emerging particles as function of the overlayer thickness.

The greater the depth x in the backing where the beta particles originate, the harder is the spectrum of the emerging particles, due to the increased absorption of low-energy particles. This hardening of the emerging particle spectrum increases of the relative transmission through the mylar overlayer. This is illustrated in Fig.4, which compares the relative transmission through mylar for Co-60 beta particles originating at the surface ($x = 0$) and at depth $x = 10$ microns in an aluminum backing. Tables 18, 19 and 20, pertaining to C-14, Co-60 and Al-28 beta spectra, compare the relative transmission through mylar for sources located at many different depths x in an aluminum backing. Results for other radionuclide sources can be obtained with the program YLDBET2 discussed in the Appendix.

The transmission data can be conveniently summarized in terms of the half-value layer, i.e. the thickness of the mylar overlayer required to reduce the relative transmission by a factor two. The relation between the half-value layer and the depth of the source within an aluminum backing is illustrated in Fig.5 for the beta(-) emitters Fe-59, Cs-137, Tl-204 and Au-198. Table 21 lists mylar half-value layers for 24 beta(-) emitters, for 35 source depths x in Al from 0 to 20 microns. The computer programs for YLDBET3 in the Appendix can be used for calculating the half-value layer as a function of source depth.

Measured values of the half-value layer can be utilized as follows to estimate the counting yield. Lacking direct information about the source depth distribution $f(x)$, one assumes that the actual radioactive source distribution can be replaced by an effective plane source. The depth of this effective plane source is determined by relation between half-value layer and x in Table 21. The counting yield for this effective depth can then be obtained from Table 4.

Ref[3] describes extensive numerical experiments with a variety of assumed shapes of the density distribution $f(x)$. These trials indicate that the errors of the yield estimates based on the assumption of an effective plane source are generally small, often 1 - 2 % or less. However, for low-energy beta emitters such as C-14 or S-35 these errors are several times larger.

2.5. Application to Layer Sources in Sand, Loam, Dry Soil and Skin

The results in Tables 12 to 15 have been used in a model study to generate counting yields for 24 beta(-) emitters distributed in a top layer of thickness x_0 in sand, loam, dry soil and human skin, assuming a density distribution $f(x) = 1/x_0$ for $0 \leq x \leq x_0$. The average counting yields $\langle Y_b(x_0) \rangle$ for these four materials are given in Tables 22 to 25. Plots of $\langle Y_b(x_0) \rangle$ for layer sources in sand and human skin are shown in Figs.6a-b.

3. Counting Yields for Alpha Sources

3.1. Features of the Calculation

A description of the condensed-random-walk Monte Carlo code used to calculate the backscattering of alpha particles can be found in Ref[3]. The stopping powers used as input generated with the TRIM program [16] which implements and updates semi-empirical procedures developed by Ziegler, Biersack and Littmark [17]. The elastic scattering cross section for alpha particles was obtained by using classical mechanics, by calculating the relation between the collision impact parameter and the center-of-mass deflection angle. This was done using the numerical procedure developed by Everhart, Stone and Carbone [18]. The screened Coulomb potential required as input was taken to be universal atom-atom potential developed by Ziegler, Biersack and Littmark [17].

3.2. Counting Yields for a Po-210 Source

Assuming an energy of 5.3045 MeV for Po-210 alpha particles, the backscattering coefficient B, and the corresponding yield

$$Y(0) = 0.5*(1 + B), \quad (4)$$

were calculated for 37 elemental backings, for a plane source at the surface ($x = 0$). Various least-squares fitting procedures were tried to explore the dependence of $Y(0)$ on the atomic number Z or the atomic weight A of the backing. A linear fit of $Y(0)$ as function of Z is shown in Fig.7a, and a quadratic fit in Z in Fig.7b. A more satisfactory fit, shown in Fig.7c, was obtained by assuming a linear dependence on a power of A, setting $B = A^{\underline{n}}$, with $\underline{n} = 0.628$. This dependence is in approximate agreement with an earlier theory developed by Crawford [19] which predicts a backscattering coefficient proportional to $A^{3/4}$.

In the plot in Fig.7c, some residual irregularity of the A-dependence is evident. This is not surprising in view of fact that the alpha-particle stopping powers and ranges have a irregular A-dependence, due to the effect of atomic shell structure. The raw and fitted backscattering coefficients and counting yields from Fig.7c are compared in Table 26. The differences between the raw and fitted counting yields are no greater than about 0.1 percent.

3.3. Counting Yields at Energies from 9 MeV to 3 MeV

For plane sources at the surface of twelve elemental backings (with atomic numbers Z = 4, 13, 14, 26, 29, 47, 73, 74, 78, 79, 82 and 92) the backscattering coefficient B and the counting yield Y were calculated at more than twenty energies E, covering the energy region from 9 MeV to 3 MeV. For each value of Z, B was fitted as a function of 1/E by a cubic-spline least-squares algorithm. This fit was used to tabulate B at 61 equidistant energies between 9 MeV and 3 MeV. Finally, at each of these 61 energies the backscattering coefficient was fitted as a function of the atomic weight A, assuming that $B = aA^{\underline{n}}$. The parameters \underline{a} and \underline{n} , shown in Fig.8, are slowly varying functions of the energy. The value of \underline{n} in Fig.8 at 5.3 MeV, based on 12 Z-values, is 0.619, slightly lower than the value 0.628 obtained previously by fitting B-values at 5.3045 MeV for 37 values of Z.

A set of counting yields at 31 energies from 9 MeV to 3 MeV, obtained with the fitting coefficients \underline{a} and \underline{n} , is given in Table 27 for 30 values of Z. To obtain yields at intermediate energies, one can either interpolate in Table 27, or use the interpolation computer program YLDPOL described in the Appendix, which is based on a yield table at 61 energies. The energy dependence of Y(0) is illustrated in Fig.9 for eight elemental backings.

3.4. Counting Yields for Sources below the Surface of the Backing

Calculations were also made of the counting yields Y(x,E) for plane sources as a function of the source depth x. This was done for E = 9.2, 6.4, 4, and 3 MeV, for many values of x up to 5×10^{-5} g/cm², for Z = 4, 13, 26, 47, 78 and 92. Of particular interest is the ratio Y(x)/Y(0), which is a measure of the yield reduction resulting from a shift of the source plane from the surface to depth x. The percent reduction $100 [1 - Y(x)/Y(0)]$ is given in Table 28. By interpolation with the program THICKPOL, described in the Appendix, the reduction factor Y(x)/Y(0) can also be obtained at other energies and for other Z values. Plots of Y(x)/Y(0) are shown in Figs.10a-b, for Z = 4, 13, 26 and 78.

THICKPOL can also be used to obtain ratio $Y_{av}(x_0)/Y(0)$, where $Y_{av}(x_0)$ is the average yield for a uniform layer sources extending to depth x_0 below the surface of the backing. Such results are listed in Table 29, and are illustrated in Figs.11a-b for Z = 4, 13, 26 and 78.

3.5. Comparison of Calculated and Measured Yields

Backscattered alpha particles emerge from the backing predominantly at grazing angles, in directions nearly parallel to the surface of the backing. This was already known to early workers [7.8], and was confirmed experimentally by Walker [20] and also by Monte Carlo calculations in Ref[3]. The counting yield can therefore be obtained experimentally by comparing the counting rates obtained with a 2π detector, and the corresponding rate obtained with a narrow-geometry detector. The latter should see only particles emerging at relatively large angles with respect to the surface of the backing, thus excluding backscattered particles.

The backscattering coefficient is affected by the roughness of the surface of the backing. When the surface is not carefully polished, some radioactive material is deposited in scratches in the surface, and some particles are absorbed instead of emerging from the backing. Such surface roughness effects would be difficult to include in the theoretical modeling. Therefore comparisons of experimental and calculated counting yields are best confined to circumstances in which the surfaces were as smooth as possible.

Comparisons of the counting rates obtained with 2π and 1π detectors were made by Hutchinson et al [21] for Po-210 sources (emitting 5.3045 MeV alpha particles). Their measurements were made with thin polonium layers deposited on unpolished and on highly polished backings, and also for polonium chloride in a thin (2μ g/cm²) collodion layer placed on top of highly polished metal backings. Results extracted from this experiment are

summarized in Table 30, and indicate that the surface roughness effects are somewhat irregular and can be of the order of 1% or even greater. In Ref[21] it was also shown that when the $2/1$ counting-rate ratios are plotted against the atomic number of the backing, the results for backings with unpolished and polished backing surfaces have a much larger spread than the results of polonium chloride in a thin collodion layer.

3.5.1. Activities of Uranium Fluoride Alpha Sources Mounted on Silicon Wafers

As part of a Neutron Standards program at NIST, activity measurements were made with several alpha sources consisting of thin layers of $^{233}\text{UF}_4$ on a silicon wafer. The average energy of the emitted alpha particles was 4.81 MeV. J. M. R. Hutchinson measured the activities of these sources with a 2π counter. D. M. Gilliam made measurements with narrow-geometry detector of accurately known geometric efficiency. This detector saw only particles emerging at angles greater than about 82 deg with respect to the surface of the silicon wafer, so that contributions of backscattered particles were entirely excluded. The results of these measurements were summarized in a memorandum from D. M. Gilliam [22], and a complete description of the experiment is currently being prepared.

In Ref [22] the 2 counting rates measured by Hutchinson were converted into activity values through division by counting yields obtained from a semi-empirical theory of Lucas and Hutchinson [23]. These activities were 0.7% to 0.8% larger than those obtained directly by Gilliam. The desire to reduce these discrepancies provided the motivation for the more detailed Monte Carlo calculations in Ref[3].

The surfaces of the silicon wafers were carefully examined at NIST by a method in which surface height variations were extracted from the measured variations in the phase of the light reflected from the surface. The roughness, expressed in terms of the root mean square value of height variations, was estimated to be 0.937 nm, which is very small compared to the range of 4.81-MeV alpha particles. The silicon wafers used as backings are both hard and smooth, and one can expect that surface-roughness effects will be at a minimum in this experiment.

The ^{233}U activity, according to Hutchinson (private communication), was $9.48 \times 10^{-3} \text{ Ci/g} = 3.51 \times 10^8 \text{ Bq/g}$. Let N_G be the activity measured with the narrow-geometry detector. Assuming that N_G does not require a backscattering correction, the mass of uranium in the source, $M(\text{U})$, is $N_G / (3.5076 \times 10^8) \text{ g}$. The atomic weight of ^{233}U is $A_U = 233.039628$ and that of F is $A_F = 18.998403$. The mass $M(\text{UF}_4)$ of the source is $M(\text{U}) (A_U + 4A_F) / A_U$. The experimental sources were disks with a radius of 1 cm, so that the thickness of the source, in g/cm^2 , is $M(\text{UF}_4) / \pi$.

Results of transport calculations are not available for alpha particles in a medium consisting of two layers of different composition (UF_4 and Si). Because the $^{233}\text{UF}_4$ layer is extremely thin, the condensed-random-walk model would not be the appropriate tool to take it into account, and all individual elastic collision should be are simulated when the particles are in or near the UF_4 layer. However, only a small correction is required to take into account the presence of the $^{233}\text{UF}_4$ layer. A simpler, more approximate, treatment was therefore deemed sufficient, which is based on

the following information: (i) the counting yield $Y(0)$ for a plane source at the surface of Si backing ($Y(0) = 0.50703$ at 4.81 MeV, a value obtained with the interpolation program YLDPOL described in the Appendix); (ii) the reduction factor $Y_{av}(x_o)/Y(0)$ for Si, where $Y_{av}(x_o)$ is the counting yield for a layer source of thickness x_o in Si; (iii) the corresponding reduction factor $Y_{av}(x_o)/Y(0)$ for UF_4 , obtained by a separate Monte Carlo calculation. Two alternative approximations were used:

- (a) Range scaling. The yield was calculated as product $Y(0)$ (for Si) times the ratio $Y(0)/Y_{av}(x_o')$ for Si, evaluated for a scaled thickness $x_o' = x_o [\text{range}(\text{Si})/\text{range}(\text{UF}_4)]$. Here x_o is the actual source thickness in UF_4 , $\text{range}(\text{Si}) = 5.200 \times 10^{-3} \text{ g/cm}^2$, and $\text{range}(\text{UF}_4) = 1.0142 \times 10^{-2} \text{ g/cm}^2$.
- (b) Use of a uranium fluoride reduction factor. The yield was calculated as the product $Y(0)$ (for Si) times the ratio $Y_{av}(x_o)/Y(0)$ for UF_4 .

Numerical details for these procedures are summarized in Table 31. The counting yields obtained with methods (a) and (b) differ by no more than 0.1%. However, the overall error of the yield values is estimated to be larger, perhaps 0.2%.

In Table 32, comparisons are made of the source activities obtained with narrow-geometry detectors, and those based on measurements with 2 detectors divided by counting yields from approximations (a) or (b). The percent differences between the two sets of results are of the order of 0.2 percent or smaller, which is consistent with the estimated uncertainties of the counting yields.

3.5.2. Yields for Po-210 Alpha Sources on Various Metal Backings

We consider next the measurements already mentioned above, made by Hutchinson et al [21] with Po-210 (5.3045 MeV) alpha-particle sources encapsulated in a thin layer of collodion placed on top of metal backings. Measurements were made with a 2π counter and 1π counter. The latter did not see backscattered alpha particles, which emerge predominantly at very small angles with respect to the surface of the collodion layer. The geometric efficiency of the 1π counter was not determined directly.

The ratio of the counting rates of the 2π and 1π detectors is

$$N_{2\pi}/N_{1\pi} = K (1 + B), \quad (5)$$

where K is the ratio of the geometric efficiency of the 2π counter to that of the 1π counter, and B is the backscattering coefficient. These ratios were measured for backings with $Z = 4, 13, 26, 29, 47, 48, 78$ and 79 , and also for brass and monel.

In Section 3.2 it was shown that calculated counting yields for 37 elements could be approximated closely by a linear least-squares fit as a function of $A^{0.628}$, where A is the atomic number. For this reason, the ratio in N_2/N_1 was also fitted as a linear function of $A^{0.628}$:

$$N_2/N_1 = a + b A^{0.628}, \quad (6)$$

with $a = 2.5019$ and $b = 0.004519$. The quality of this fit is illustrated in Fig.12. Assuming that B would vanish for A approaching zero, and comparing Eqs(5) and (6), one can identify the parameter a with the geometric-efficiency ratio K . The experimental counting yield is therefore

$$Y = 0.5 (1 + B) = (N_{2\pi}/N_{1\pi})/K = 0.5 \{1 + (b/a) A^{0.628}\}. \quad (7)$$

In Table 33, the experimental counting yields for eight elemental backings, obtained from Eq(7) are compared with calculated counting yields. The latter were obtained with interpolation program YLDPOL described in the Appendix, and then dividing the results by 1.001. This reduction factor was obtained with program THICKPOL, and takes into account that the polonium chloride source is spread in a collodion layer of thickness 2 g/cm^2 . It can be seen in Table 33 that the differences between experimental and calculated counting yields increase with the atomic number of the backing, and lie between 0.1 and 0.3%, which is consistent with the estimated combined theoretical and experimental uncertainties.

The situation is not quite so favorable in comparisons with other experimental results. Combining the yield for a platinum backing in Table 33 with the surface-roughness effect in Table 30, one would arrive at an estimated yield of 0.5212 for a Po-210 source deposited directly on polished platinum. However, in a later experiment involving measurements with a 2π counter and an 0.8 counter of known geometric efficiency, Hutchinson *et al* [24] obtained for this situation a yield 0.5176, which is smaller by 0.69%. On the other hand, in Ref. [24] the yield of Gd-148 (3.1828 MeV) alpha particles was determined by measurements with a 2π detector and a calibration with a silicon surface-barrier detector, leading to a yield 0.5242, which is only 0.32% smaller than the calculated value of 0.5259 from Table 27.

In earlier experiments, Cunningham *et al* [7] and Parsons *et al* [8], using Pu-239 (5.1481 MeV) thin alpha particle sources on platinum, obtained counting yields with magnitudes 0.520 and 0.518, respectively. These results are 0.59%, respectively 0.96% smaller than the calculated value of 0.523 from Table 27. It is possible that surface-roughness effects are responsible for these differences.

Appendix: Software and Data Files

1. Computer Programs for Use with Beta Sources

1.1. Program BETASPEC

BETASPEC extracts beta spectra from the database files BETA.MIN (for 649 beta(-) emitters) or BETA.PLS (for 472 beta(+) emitters). BETA.MIN and BETA.PLS are binary direct-access files for use in Fortran programs, and were generated from a database prepared by S. M. Seltzer (National Institute of Standards and Technology), who used the ENSDF file and computer programs from the National Nuclear Data Center at the Brookhaven National Laboratory.

Each radionuclide included in BETA.MIN or BETA.PLS has an identification (ID) number. The names of all beta emitters and their ID

numbers are contained in files BETAM.ID (for beta(-) emitters) and BETAP.ID (for beta(+) emitters). These files also contain the half life, the maximum and average energy, and the intensity (number of particles emitted per disintegration).

The user of BETASPEC must indicate 1) whether the radionuclide of interest is a beta(-) or beta(+) emitter, and 2) whether the ID number of the emitter of interest is known. If the answer to 2) is negative, the user has the choice of inspecting the BETAM.ID or BETAP.ID files on the monitor screen, and can then return to the BETASPEC program by hitting the escape key. Finally, the user is prompted to supply the name of the file in which the beta spectrum is to be stored.

The output from BETASPEC consists of a scaled beta spectrum at 41 equally spaced energies between 0 and the endpoint energy. The quantity tabulated is the product $E_{\max} S(E/E_{\max})$, where S is the spectrum, E is the spectral energy and E_{\max} is the endpoint energy. Even though the beta spectrum may consist of several components with different endpoint energies, BETASPEC provides only a single combined spectrum.

1.2. Program CORBET

CORBET evaluates the counting yield $Y_b(x)$ for a beta source according to Eq(2), using the interpolation and approximation methods described in Ref[1]. Due to limitations of the input data, CORBET is applicable only to beta sources with endpoint energies smaller than 2.896 MeV.

The following input data are needed: 1) A file with the beta-spectrum file for the radionuclide of interest, generated with program BETASPEC; 2) a file with a list of source depths (distances from the surface of the backing); 3) a stopping-power/range file, SRE.nnn (for electrons) or SRP.nnn (for positrons); 4) a yield file for mononenergetic isotropic sources, CORFAC.nnn (or equivalent CORPOL.nnn files for compounds), where nnn indicates the ID number of the beta emitter. The following files are available:

- a. For electrons in Be, C, Al or Fe: SRE.0nn and CORFAC.Enn,
for nn = 04, 06, 13 and 26.
- b. For positrons in Al or Fe: SRP.0nn and CORFAC.Pnn,
for nn = 13 and 26.
- c. For electrons in compounds: SRE.nnn and CORPOL.nnn. Such files are available for the following ID numbers:

nnn	Material	nnn	Material
169	Pyrex glass	223	Lucite
245	Sand (silica)	276	Water
301	Concrete	302	Plate glass
303	Typical loam	304	Dry soil
305	Skin		

CORBET is an interactive program. When prompted, the user must 1) indicate whether the depths x are to be specified in microns or in g/cm^2 ; 2) provide the name of the file containing the set of depths; 3) indicate

whether the radionuclide of interest is a beta (-) or beta (+) emitter; 4) For a beta (-) emitter, the user must specify whether the backing has atomic number $Z = 4, 6, 13$ or 26 , or whether the backing material is a material with an effective atomic number (between 4 and 26). For a beta (+) emitter there are only the choices $Z = 13$ or 26 .

A file containing a set of depths must be prepared in advance of running CORBET. The first line of this file should contain an integer specifying the number of depths, and subsequent lines should list the depths.

1.3. Program CORPOL

If the backing material of interest is a compound or mixture (or is an element other than Be, C, Al or Fe) a file CORPOL.nnn (where nnn is the ID number for the compound) must be generated by running program CORPOL. The CORFAC.nnn for elements, with nnn = 004, 006, 013 and 026, are used as a basis for interpolation with respect to Z , using the effective atomic number Z_{eff} from Eq(1). Due to the limitations of the available calculated input data this is only possible for beta (-) emitters, for backing materials with Z_{eff} between 4 and 26 .

1.4. Program DPAX11G

For a compound or mixture, DPAX11G must be used to generate the required stopping-power/range file SRE.nnn. DPAX11G prompts the user to name a run file, a print file, and an output data file. The latter is used only as input for the Monte Carlo program ETRAN, is unnecessary in the present context, and can be designated "NUL". By editing one can extract from the print file a stopping-power/range file.

Listed below as an example is the run file DRYSOIL.RUN used by DPAX11G to generate a print file for "dry soil":

```

1      1
DPAX11, Dry Soil, 4.096-0.001 MeV,electrons.
8
15.23000      AL-2,0-3/145.2/
62.58000      SI,0-2/139.2/
 3.10000      FE-2,0-3
 5.10000      CA,0
 3.71000      NA-2,0
 3.11000      K-2,0
 3.45000      MG,0
 3.72000      FE,0
0  1 1.50000E 00      1.00000      20.00000
 1      1      0      0      +1      1      4      1      8      96 4.09600E 00

```

Line 1 is fixed, line 2 is a title, and line 3 indicates that there are 8 constituent compounds in dry soil. The next 8 lines give the chemical formulas of these constituents. The numbers in brackets, /145.2/ and /139.2/ are mean excitation energies for compounds recommended in ICRU Report 37 [12]; slightly different values would be used if the numbers in brackets were omitted. The next to the last line gives other material properties. For generating a stopping-power/range table for a solid compound, the only

significant number is the third one, 1.5, representing the density of the material in g/cm³. In the last line, the significant number is +1, which indicates that the incident particle is an electron. For positrons this number should be replaced by +2. The significance of the various input parameters in the run file is explained in more detail in the file DATAPAC.DOC included in the archive file DATAPAC.ARC.

Lines 623 to 723 of the output print file from DPAX11G produced with the run file listed above contain the stopping-power/range file SRE.304 for dry soil. However, one must insert two additional lines at the beginning of the file. The first line should contain the name of the material, and the second line the effective atomic number Z_{eff} (defined by Eq.1), followed by the density in g/cm³.

1.5. Program YLDBET1

YLDBET1, a specialized version of a program CORBET, calculates the counting yield of plane beta sources located at a set of depths beneath the surface of an aluminum foil. The output file contains a table with source depths (in microns) and counting yields, and has the extension YLD. For example, if the file containing the beta spectrum is called Co-60, the output file is called Co-60.YLD.

1.6. Program YLDBET2

YLDBET2 calculates the transmission of beta particles through a mylar layer adjacent to an anodized aluminum foil. These results are generated for plane beta(-) sources located at various depths beneath the aluminum-mylar interface. The file TRANSIT DAT must be available, which contains transmission data for monoenergetic isotropic electron sources, for many source depths in aluminum, and many mylar over-layer thicknesses. The output file produced by YLDBET2 has the extension TRA. For example, with a beta spectrum Co-60, the output file is called Co-60.TRA.

1.7. Program YLDBET3

YLDBET3 calculates a table consisting of the following three columns pertaining to plane beta(-) sources: (a) the depth x of the source in aluminum; (b) the corresponding half-value layer of mylar which reduces the transmission by a factor 0.5 (or 0.7 for Al-28); (c) the corresponding counting yield. Optionally, the program accepts as input a half-value layer of mylar (mg/cm²) (from transmission measurements of a source whose counting yield is to be determined). The program then calculates, by interpolation, the corresponding effective source depth and the counting yield.

YLDBET3 requires as input two files previously generated with YLDBET1 and YLDBET2. For example, for a spectrum Co-60, it uses Co-60.YLD and Co-60.TRA as input, and the output file is called Co-60.XSE.

2. Programs for Use with Alpha Sources

2.1. Program YLDPOL

For a plane source emitting alpha particles of energy E (between 3 MeV and 9 MeV), YLDPOL calculates the counting yield taking into account backscattering from backings with atomic numbers $Z = 4-6, 11-14, 19-34, 42, 46-50, 64, 73, 74, 78, 79, 82$ and 92. This is done by interpolating with respect to $1/E$ in a table with entries at 61 energies stored in file YLDARR.15.

2.2. Program THICKPOL

THICKPOL is an interpolation program that calculates the ratios $Y(x)/Y(0)$ and $Y_{av}(x_0)/Y(0)$, where $Y(0)$ is the counting yield for a plane source at the surface of a backing, $Y(x)$ is the counting yield for a plane source at a depth x in a backing, and $Y_{av}(x_0)$ is the counting yield for a uniform layer source that extends to a depth x_0 below the surface of the backing. By interpolation, THICKPOL obtains results for any Z , for energies E between 3 MeV and 9 MeV.

3. Files on Floppy Disks

This report is accompanied by two floppy 1.44 Mb disks with the following files:

DISK 1: BETASOFT.ARC	DISK2: DATAPAC.ARC
ALFASOFT.ARC	DATAPAC.LST
BETASOFT.LST	
ALFASOFT.LST	
ARCE.COM	

DISK 3: YREP.ARC	YREP.LST
YFIG.ARC	YFIG.LST
YTAB.ARC	YTAB.LST
ARCE.COM	

The files with extension ARC are compressed archive files. Those with extension LST list the individual files contained in the archive files. The program ARCE.COM (executable on a personal computer) can be used to extract the individual files from the archive files.

The BETASOFT files contain Fortran source code, executable files, and input data files for calculating counting yields for beta sources. The ALFASOFT files contain similar sets of files for calculating the yields of alpha sources. The TABLE files contain the content of Tables 1 - 29 of this report; they are ASCII files, with all escape codes stripped out.

The files in YREP.ARC contain the text of the report, and those in YTAB contain the tables. All these files were generated with the TEXTTRA word processor. The files in YFIG contain the figures, and are written in HPGL format.

References

1. M. J. Berger, M. P. Unterweger, and J. M. R. Hutchinson, The influence of backing and covering materials on the ^{239}Pu counting efficiencies of beta particle sources, Nucl. Inst. Meth A 369, 684-688 (1996).
2. M. J. Berger, A method of determining the ^{239}Pu counting efficiency of beta particle sources, Nucl. Instr. Meth. B 134, 276-286 (1998).
3. M. J. Berger, Backscattering of Alpha Particles, Contractor's Report to NIST, (April 1998)
4. Berger, M. J., Monte Carlo calculation of the penetration and diffusion of fast charged particles, in Methods of Computational Physics, Vol.1, p.135, Academic Press, N.Y. (1963).
5. Kawrakow, I. and Bielajew, A. F., On the condensed-history technique for electron transport, Nucl. Inst. and Methods B, 142, 253-280 (1998).
6. Cunningham, B. B., Ghiorso, A. and Hindman, J. C., Back-scattering of Pu-239 alpha particles from platinum. In The Transuranium Elements. G. T. Seaborg (Editor) National Nuclear Energy Series, Vol.14, Part II, p.1192, McGraw-Hill, New York (1949).
7. Parsons, J. H., Flatau, O., East, J. K., Dandl, R. and Borkowski, C. J., Note on back-scattering of Pu-239 alpha particles from platinum sample plates. In The Transuranium Elements. G. T. Seaborg (Editor) National Nuclear Energy Series, Vol.14, Part II, p.1197, McGraw-Hill, New York (1949).
8. Seltzer, S. M., An overview of ETRAN Monte Carlo methods for coupled electron/photon transport calculations, in Monte Carlo Transport of Electrons and Photons, pp.153 - 181 , Plenum, New York (1988).
9. Seltzer, S. M., Electron-photon Monte Carlo calculations: the ETRAN code, Appl. Radiat. Isot. 42, 917-941 (1991).
10. Riley, M. E., MacCallum, C. J. and Biggs, F., Theoretical electron-atom scattering cross sections, Atomic Data and Nuclear Data Tables 15, 443-476 (1975).
11. Riley, M. E., Relativistic, elastic electron scattering from atoms at energies greater than 1 keV, Report SLA-74-0107, Sandia National Laboratories (1974).
12. Desclaux, J. P., A multi-configuration relativistic Dirac-Fock program, Comp. Physics Commun. 9, 31 (1975).
13. Berger, M. J., ETRAN - experimental benchmarks, in Monte Carlo Transport of Electrons and Photons, pp. 183 - 219, Plenum, New York (1988).
14. M. J. Berger, Applicability of the condensed-random-walk Monte Carlo method at low energies in high-Z materials, Radiat. Phys. and Chem. 53,

191-201 (1998).

15. M. J. Martin, Appendix of NCRP Report 58 (1978).
16. Computer program package TRIM (Version 91.14), code SR (executable file dated 05-07-92, private communication from J. F. Ziegler (1992)).
17. Ziegler, J. F., Biersack, J. P. and Littmark, U., The stopping and range of ions in solids, Vol.3, Pergamon Press, Elmsford, N.Y. (1985).
18. Everhart, E., Stone, G. and Carbone, R. J., Classical calculation of differential cross section for scattering from a Coulomb potential with exponential screening, Phys. Rev. 99, 1287-1290 (1955).
19. Crawford, J. A. Theoretical calculations concerning back-scattering of alpha particles, in The Transuranium Elements. G. T. Seaborg (Editor) National Nuclear Energy Series, Vol.14, Part II, p.1307, McGraw-Hill, New York (1949).
20. Walker, D. J., An experimental study of the backscattering of 5.3-MeV alpha particles from platinum and monel metal, Int. J. appl. Radiat. Isotopes 16, 183-189 (1965).
21. Hutchinson, J. M. R., Naas, C. R., Walker, D. H. and Mann, W. B., Backscattering of alpha particles from thick metal backings as a function of atomic weight, Int. J. Appl. Radiat. Isotopes 19, 517-522 (1968).
22. D. M. Gilliam, Memorandum to J. Pauwels, CEC-JRC), 30 March 1995.
23. Lucas, L. L. and Hutchinson, J. M. R., Study of the scattering correction for thick uranium-oxide and other alpha-particle sources I. Theoretical. Int. J. Appl. Radiat. Isotopes 27, 35-42 (1976).
24. Hutchinson, J. M. R., Lucas, L. L. and Mullen, P. A., Study of the scattering correction for thick uranium-oxide and other alpha particle sources - II. Experimental, Int. J. Appl. Radiat. Isotopes 27, 43-45 (1976).

Figures

1. Scaled counting yield $Y(x/r_0, E)$ of a plane electron source emitting electrons of energy E uniformly in all direction. The source is located at the surface of a backing of atomic number Z . The yield is plotted as function of the scaled source depth x/r_0 , where r_0 is the range at energy E . The solid, dotted and dashed curves are for $E = 8, 512$ and 2048 keV, respectively.
2. Counting yields $Y_b(x)$ of plane beta sources, for selected beta(-) emitters on top of or at various depths in the backing.
 - a. Beryllium backing
 - b. Carbon backing
 - c. Aluminum backing
 - d. Iron backing
3. Counting yield $Y_b(x/r_{\max})$ of plane beta sources on Be, Al and Fe backings, as a function of the scaled depth x/r_{\max} , where r_{\max} is the range at the maximum energy of the beta spectrum.
 - a. Al-28
 - b. Sr-90/Y-90
 - c. Co-60
 - d. C-14
4. Relative transmission of Co-60 beta particles through a mylar overlayer, for source depths $x = 0$ and $x = 10$ microns in aluminum.
5. Relation between the half-value layer of mylar, h , and the source depth, x , in aluminum, for plane Fe-50, Cs-137, Tl-204 and Au-198 beta sources.
6. Average counting yield $\langle Y_b(x_0) \rangle$, for sources distributed uniformly to depth x_0 in backing, for Al-28, Sr-90/Y-90, Co-60 and C-14 beta sources.
 - a. For layer source in sand
 - b. For layer source in skin
7. Least-squares fit of counting yield Y as function of atomic number Z or atomic weight A , for 5.3045-MeV alpha particles.
 - a. Linear function of Z
 - b. Quadratic function of Z
 - c. Linear function of $A^{0.628}$
8. Energy dependence of the parameters a and n of the formula for the backscattering coefficient, $B = a + A^n$, where A is the atomic weight.
9. Counting yield, $Y(0)$, as a function of alpha-particle energy, for a plane source at the surface (depth $x = 0$) of a backing of atomic number Z .

10. Reduction ratio $Y(x)/Y(0)$ for plane sources at depth x .
 - a. For backings with $Z = 4$ and 13
 - b. For backings with $Z = 26$ and 78

11. Reduction ratio $Y_{av}(x_0)/Y(0)$ for uniform layer sources extending to depth x_0 below the surface of the backing.
 - a. For backings with $Z = 4$ and 13
 - b. For backings with $Z = 26$ and 78

12. Least-squares fit of the $2/1$ counting ratios measured by Hutchinson, Naas, Walker and Mann [21].

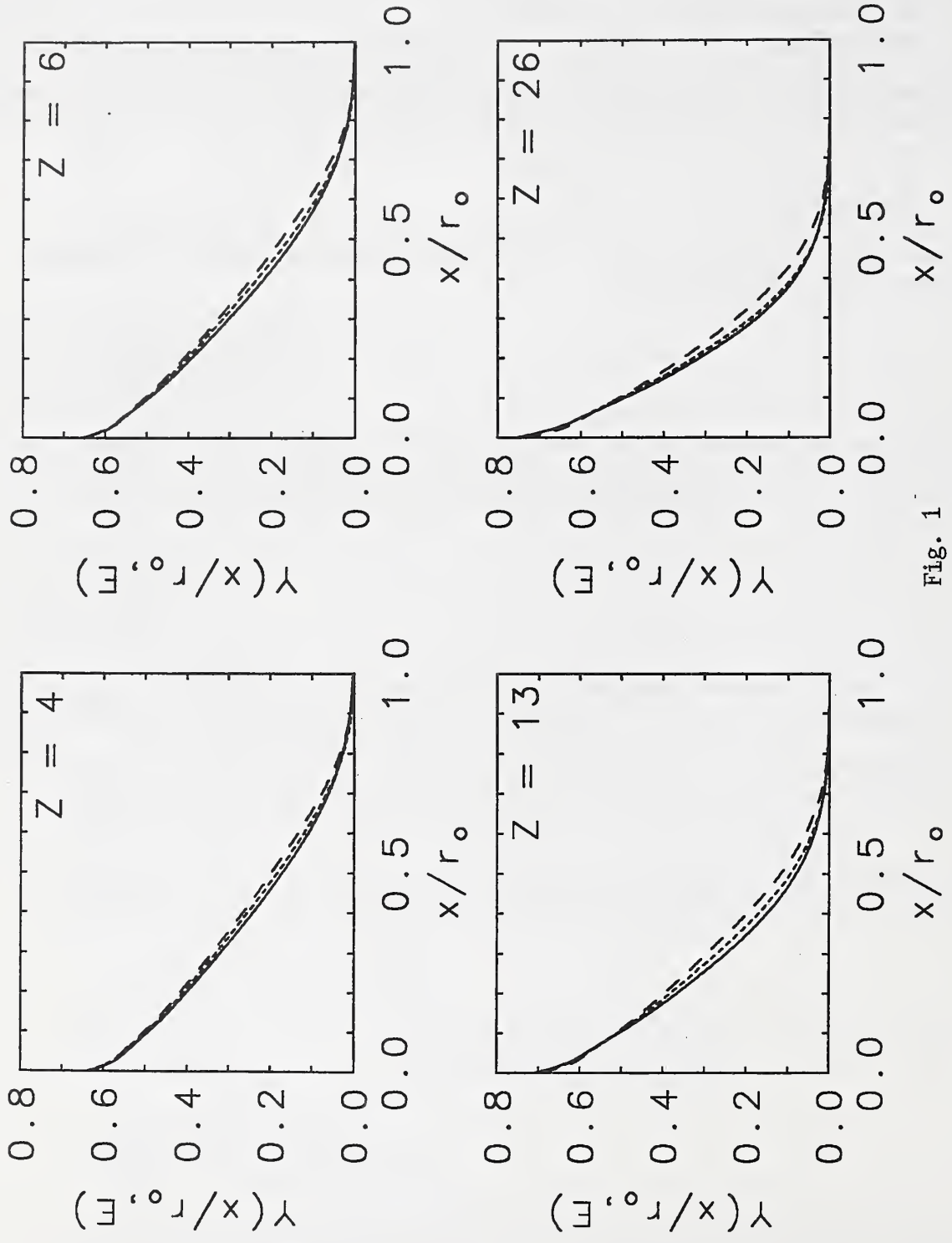


Fig. 1

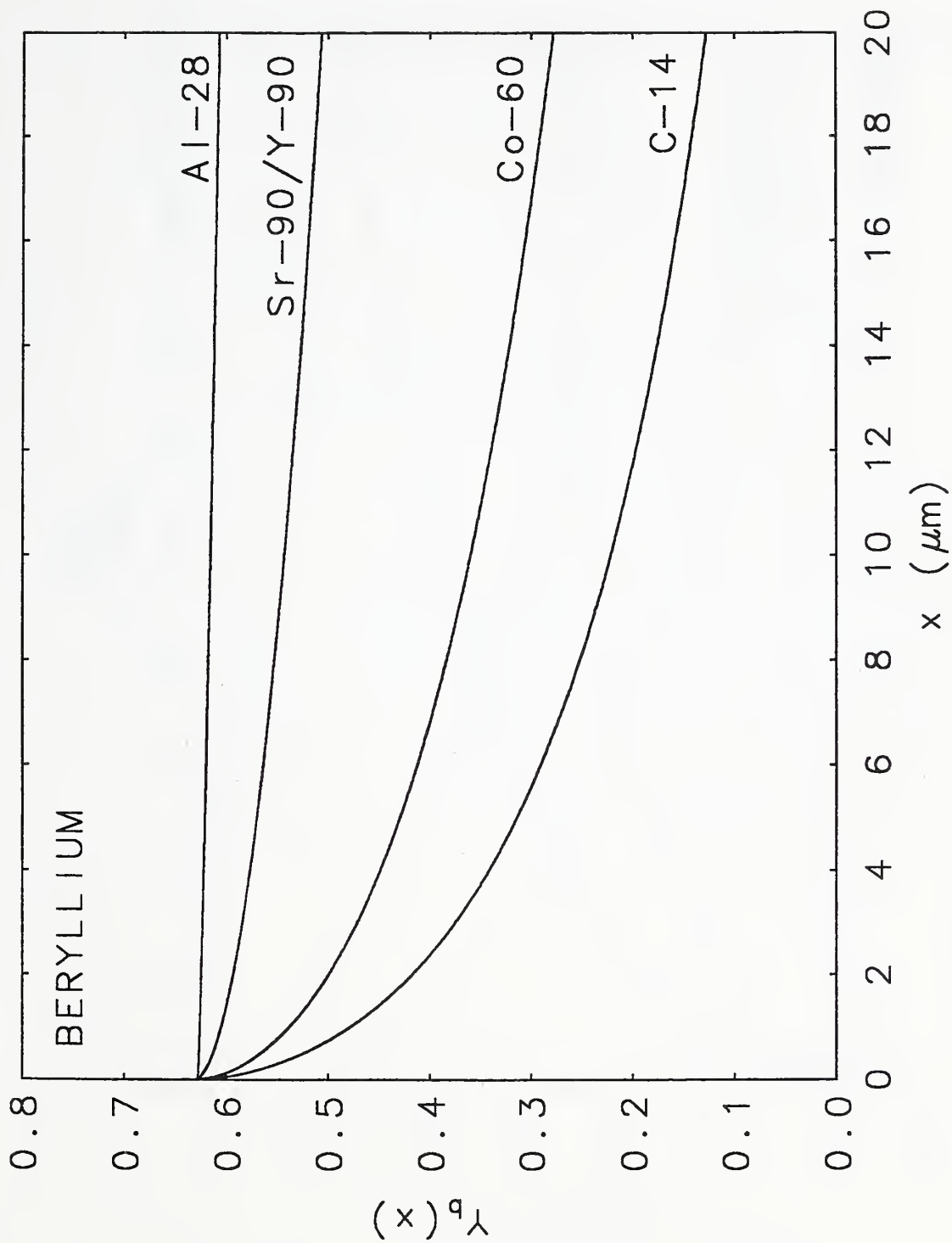


Fig.2a

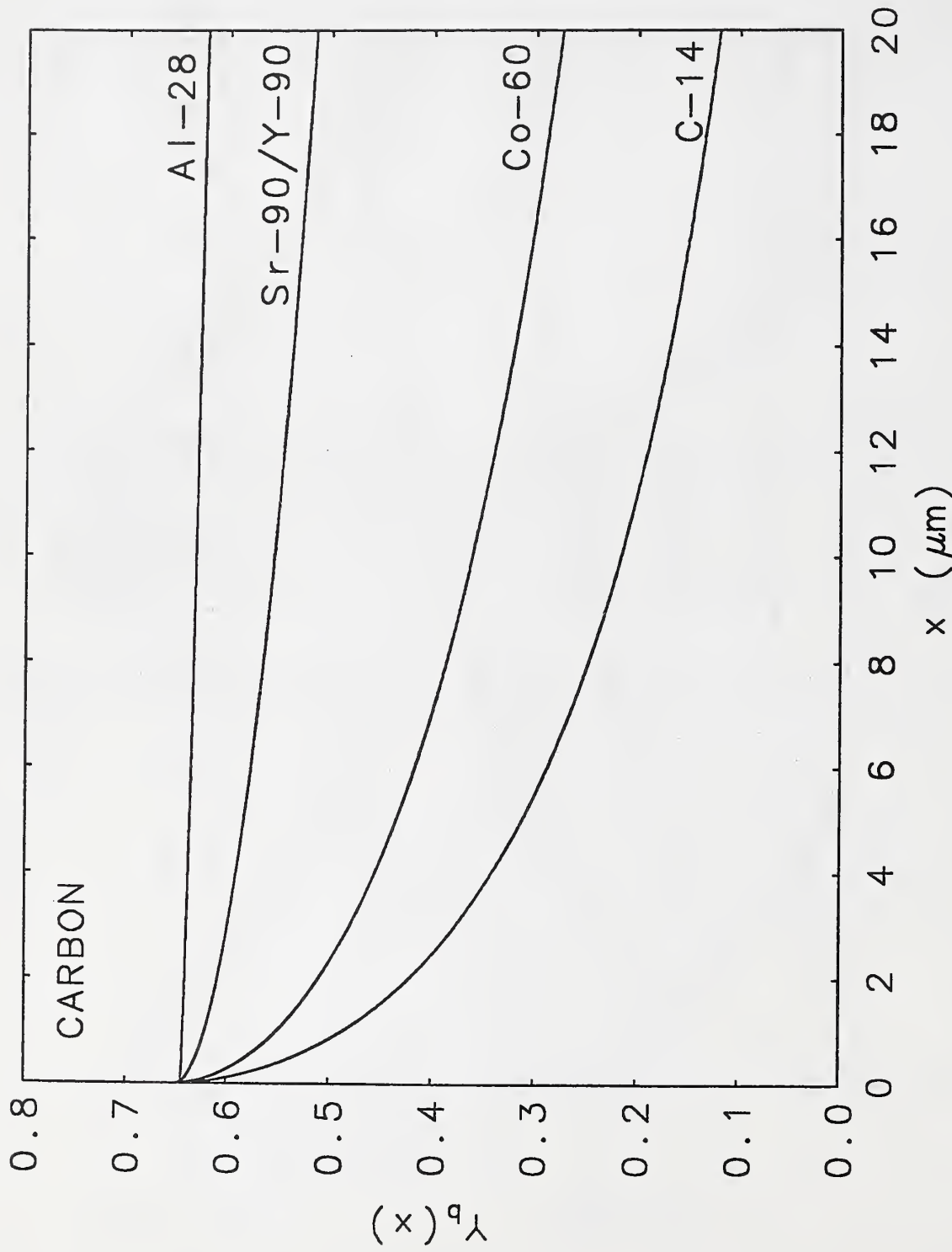


Fig.2b

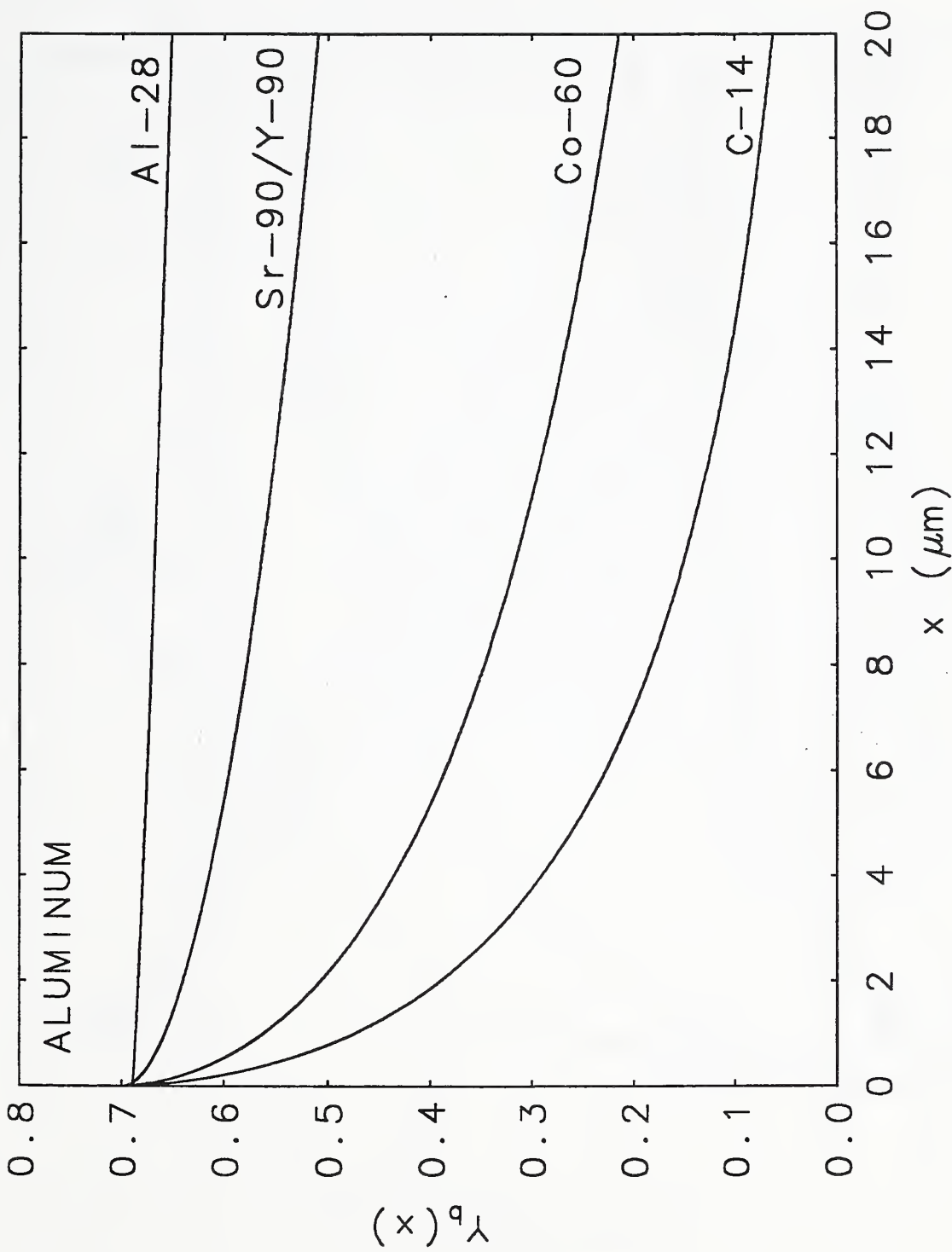


Fig.2c

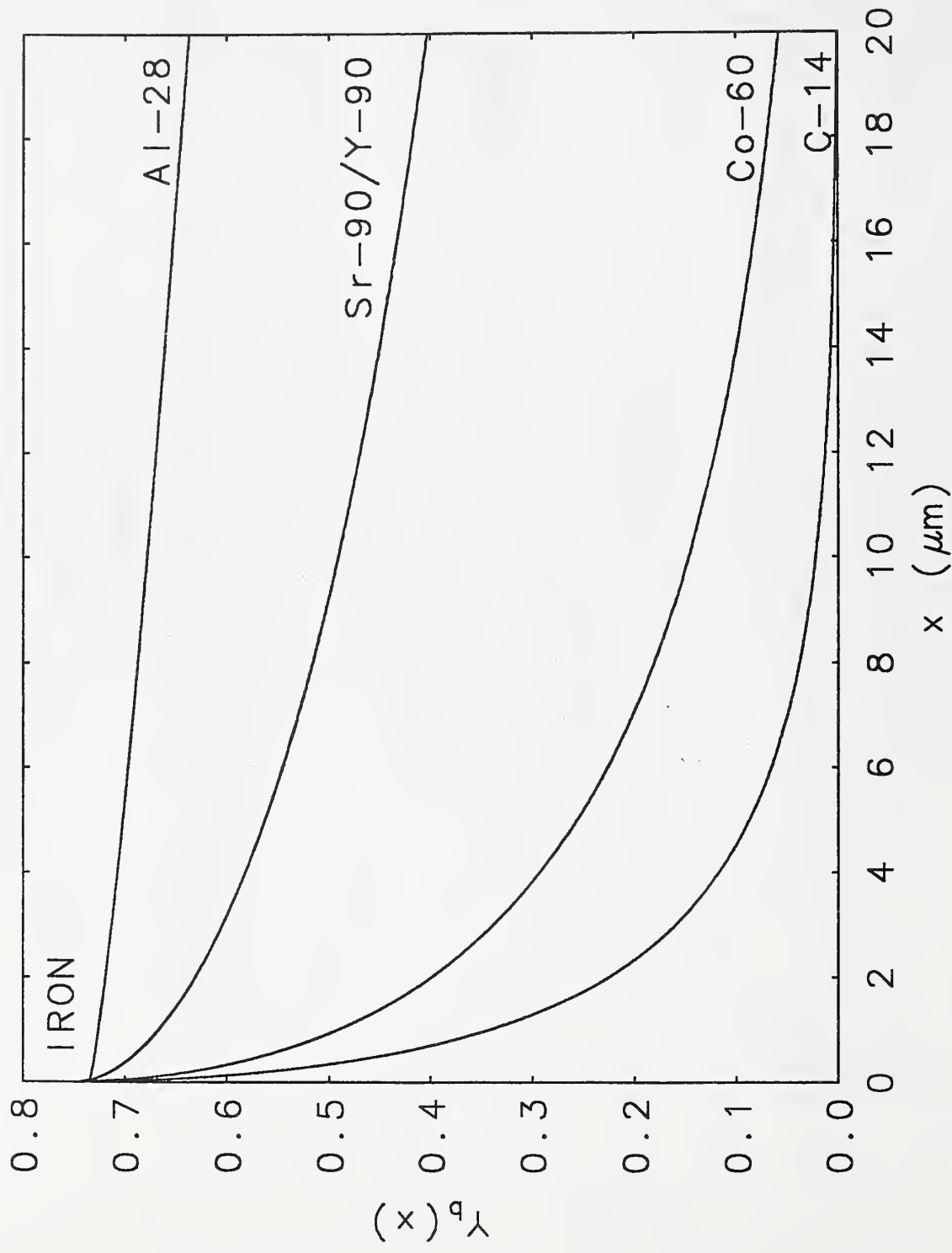


Fig.2d

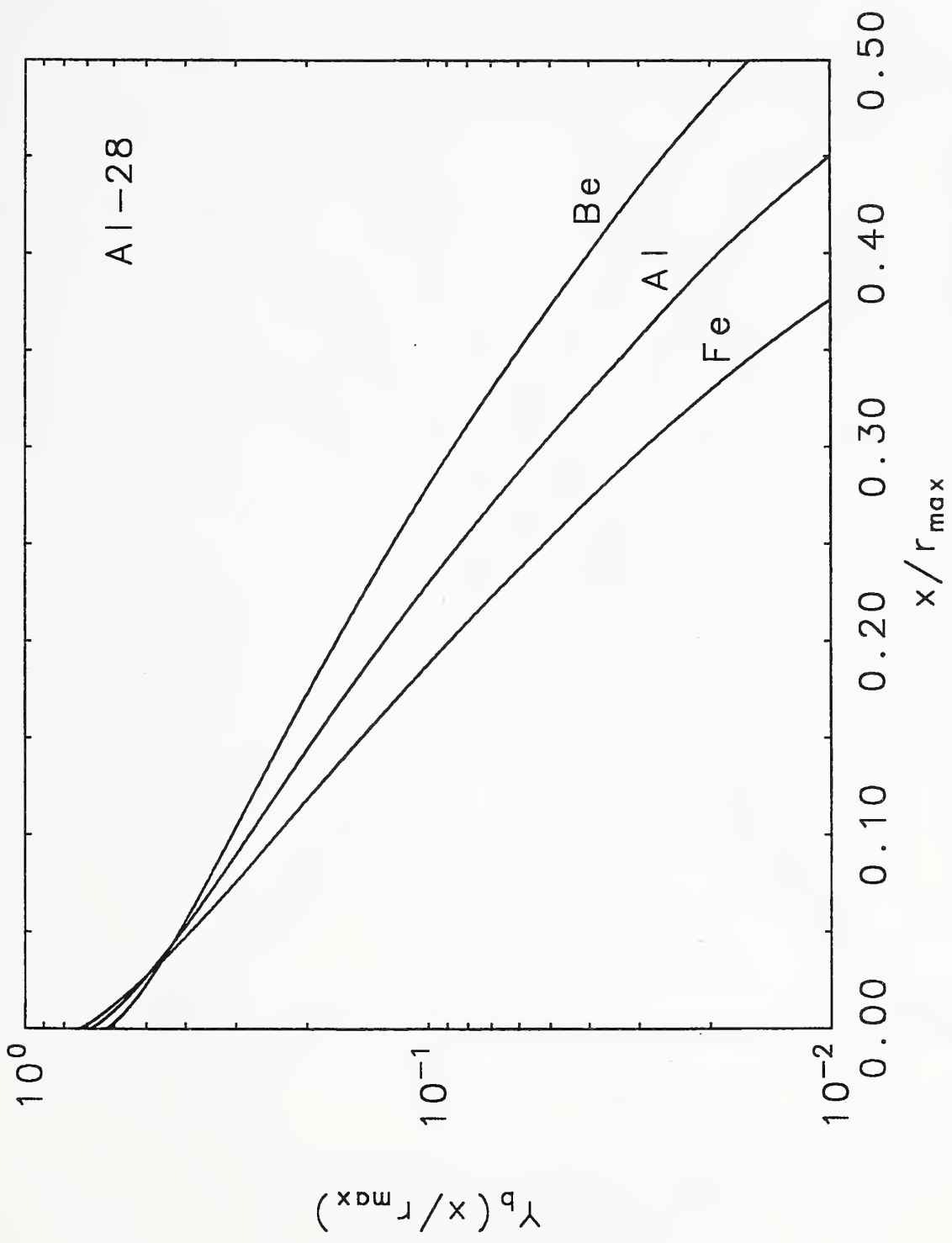


Fig.3a

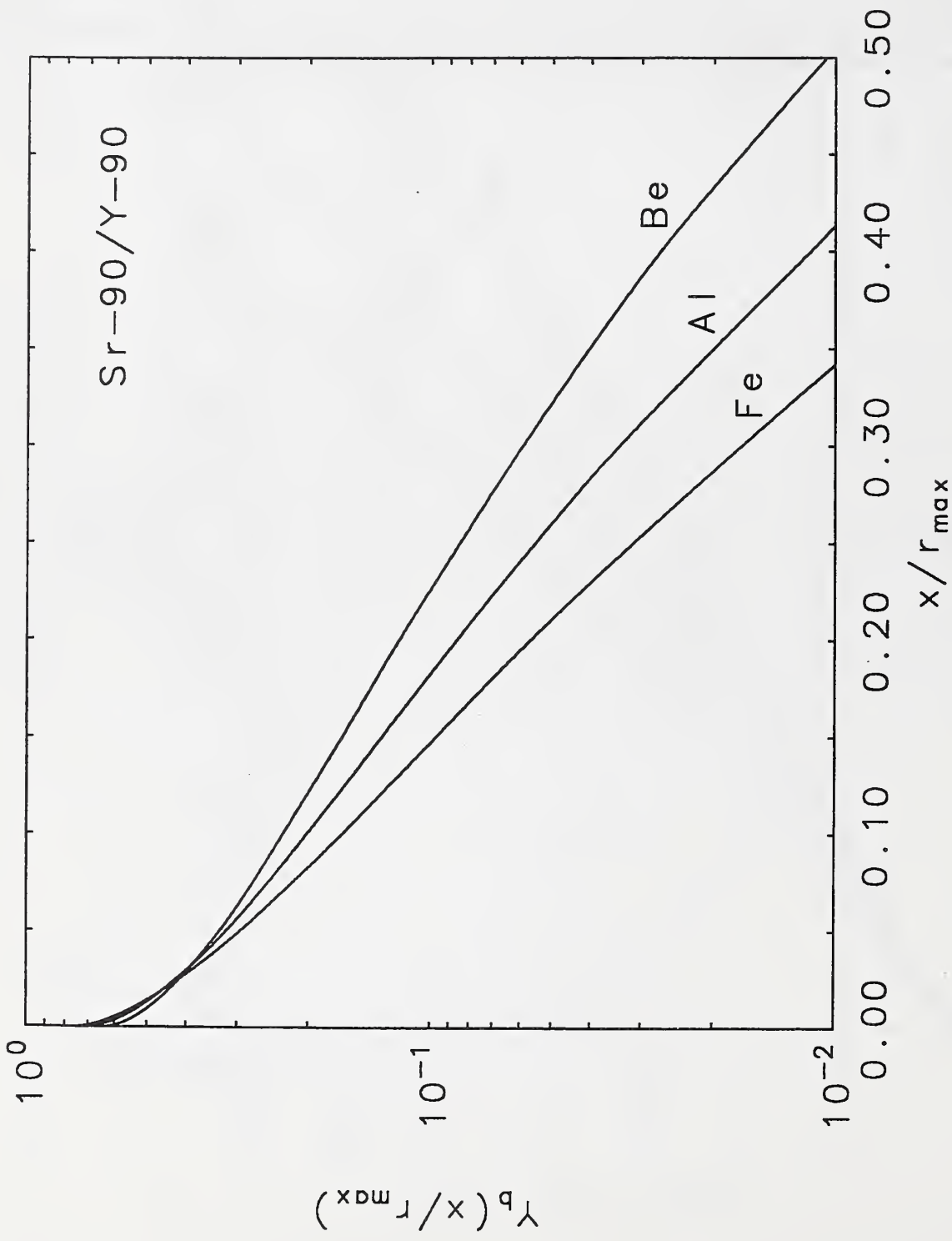


Fig.3b

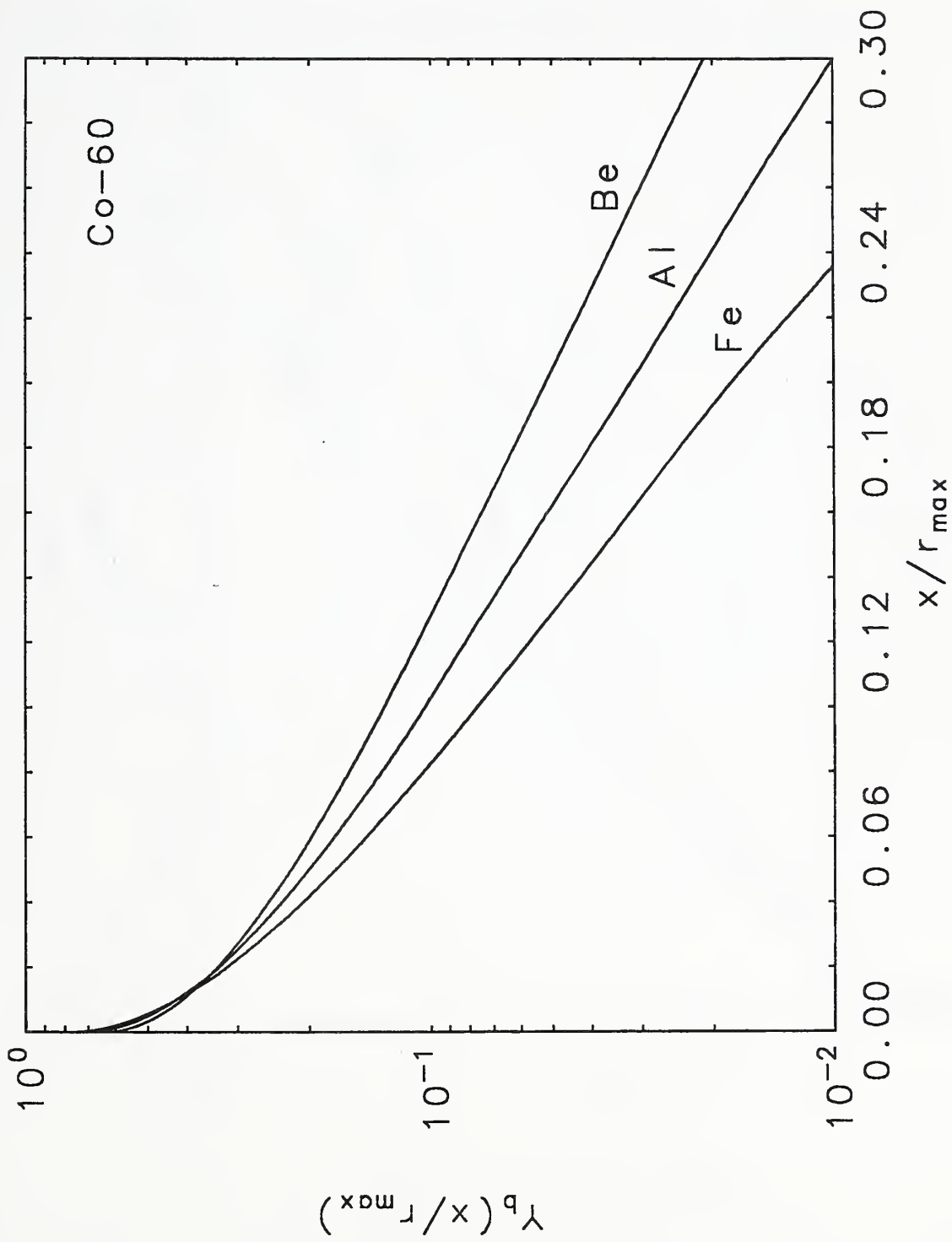


Fig. 3c

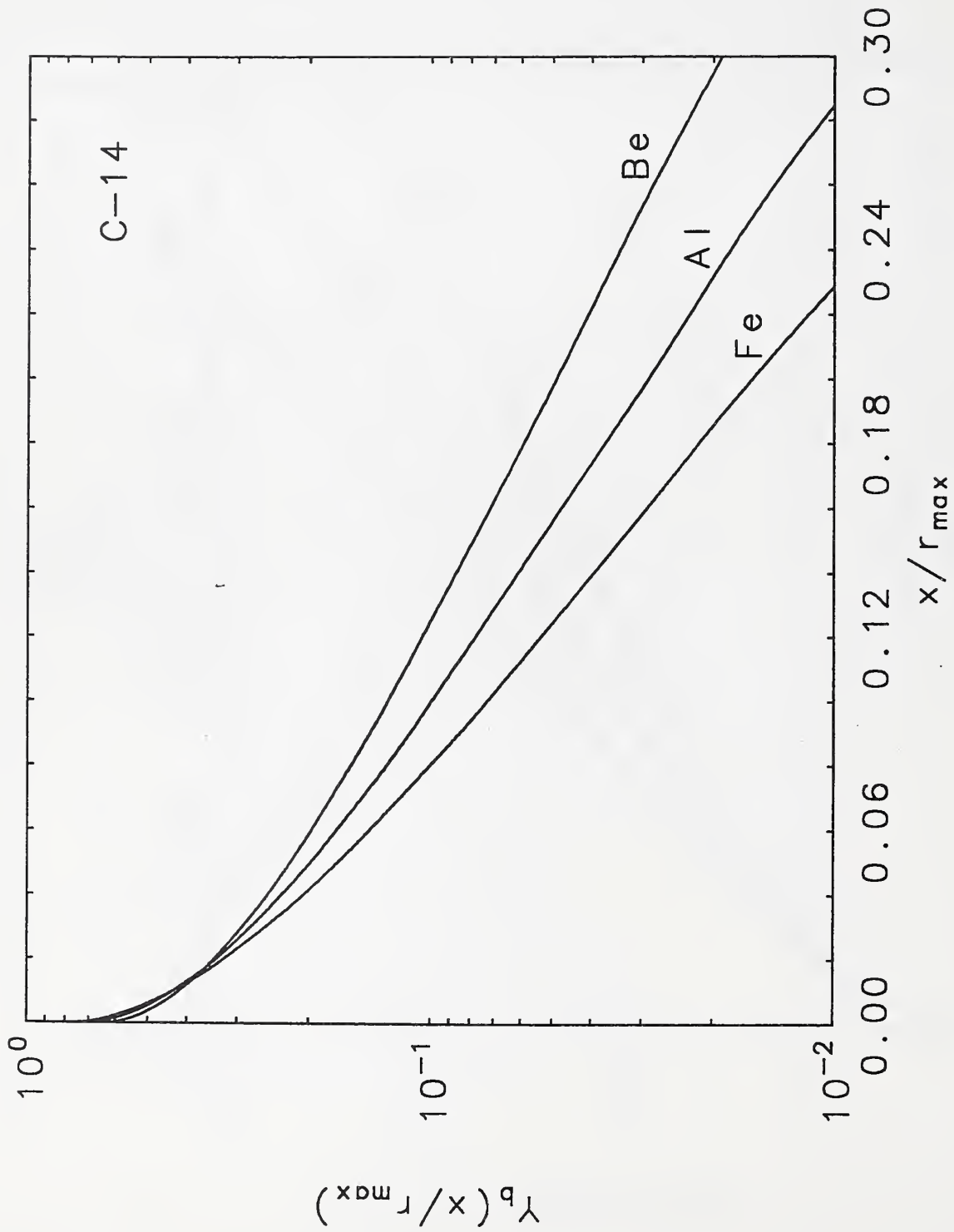


Fig.3d

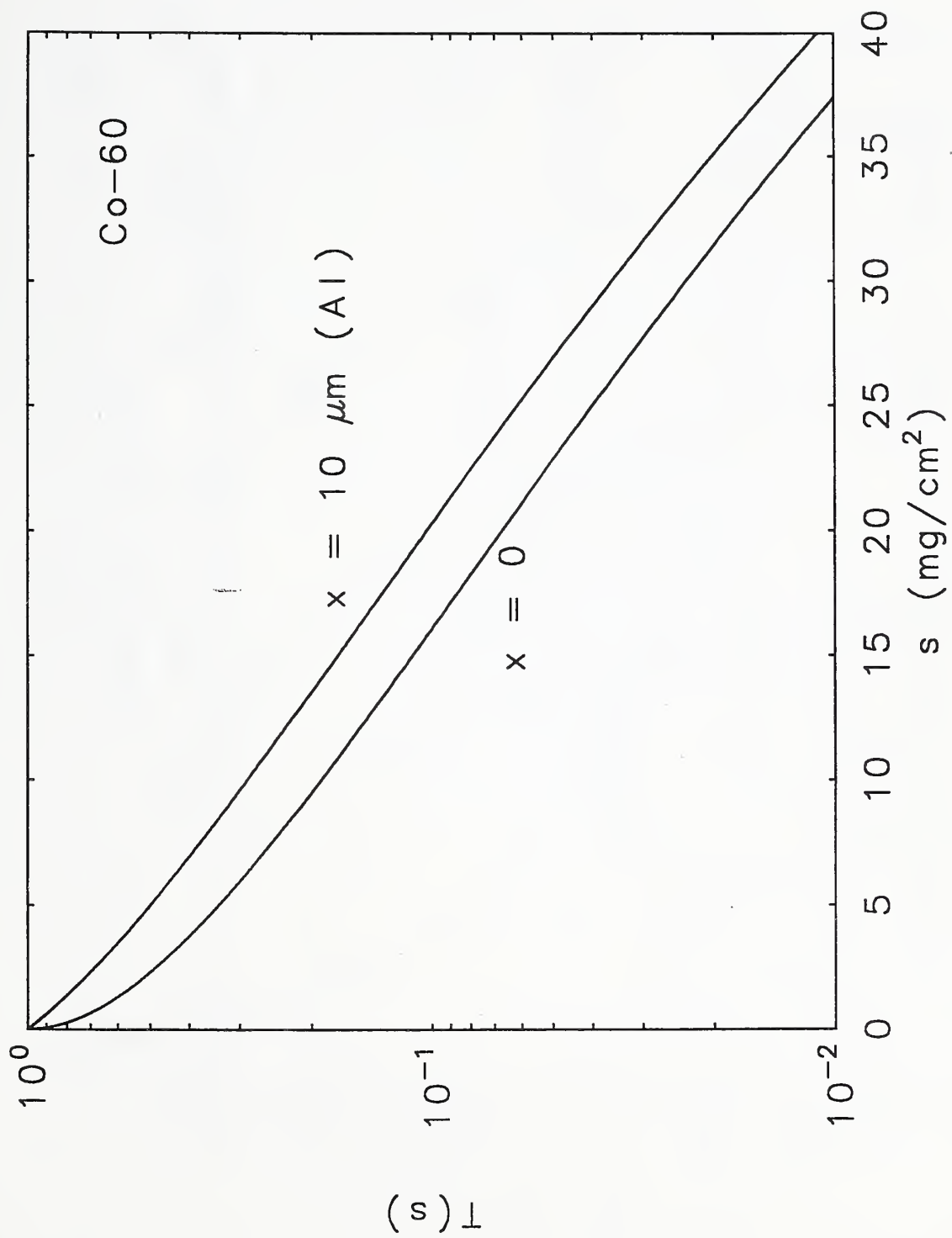


Fig.4

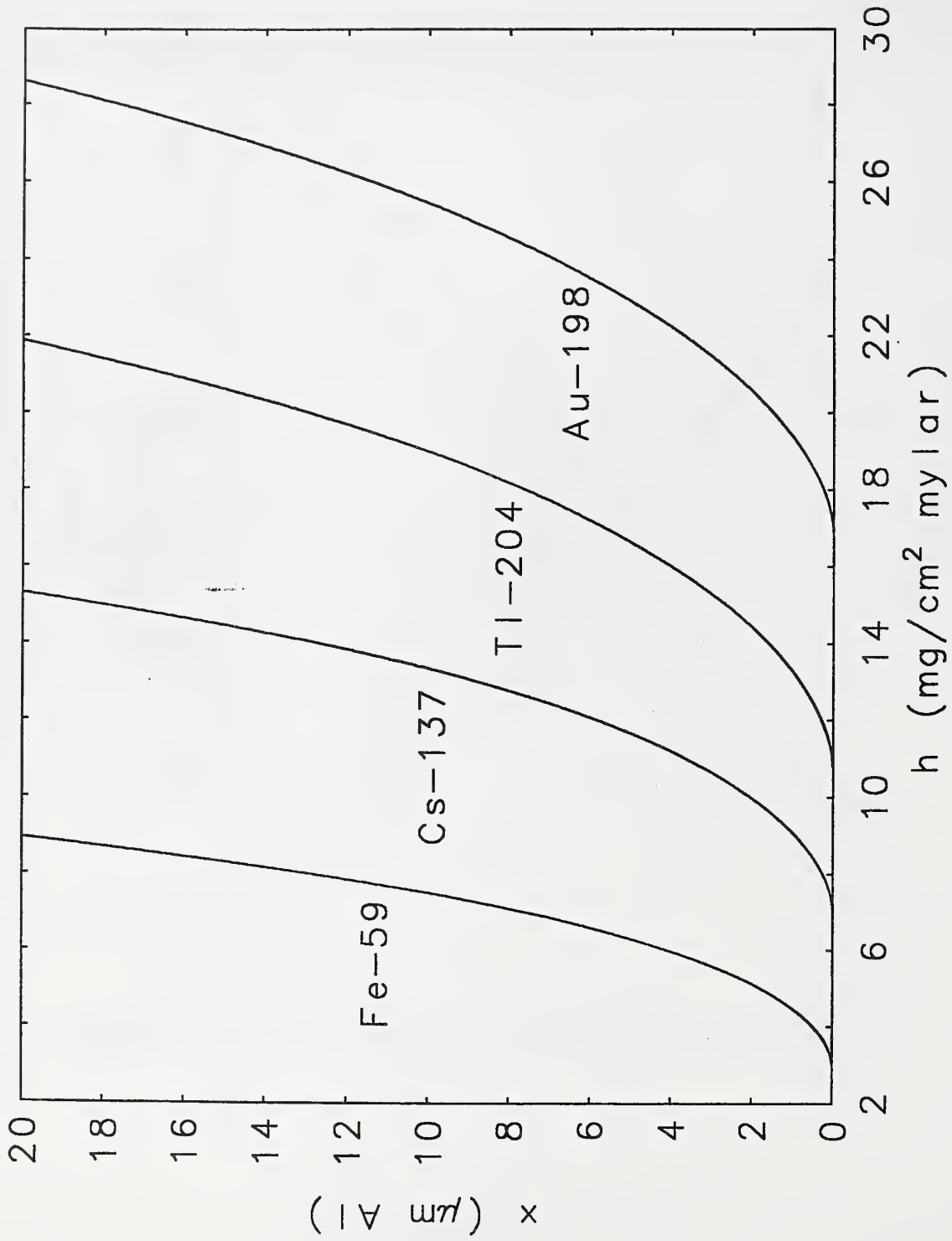


Fig.5

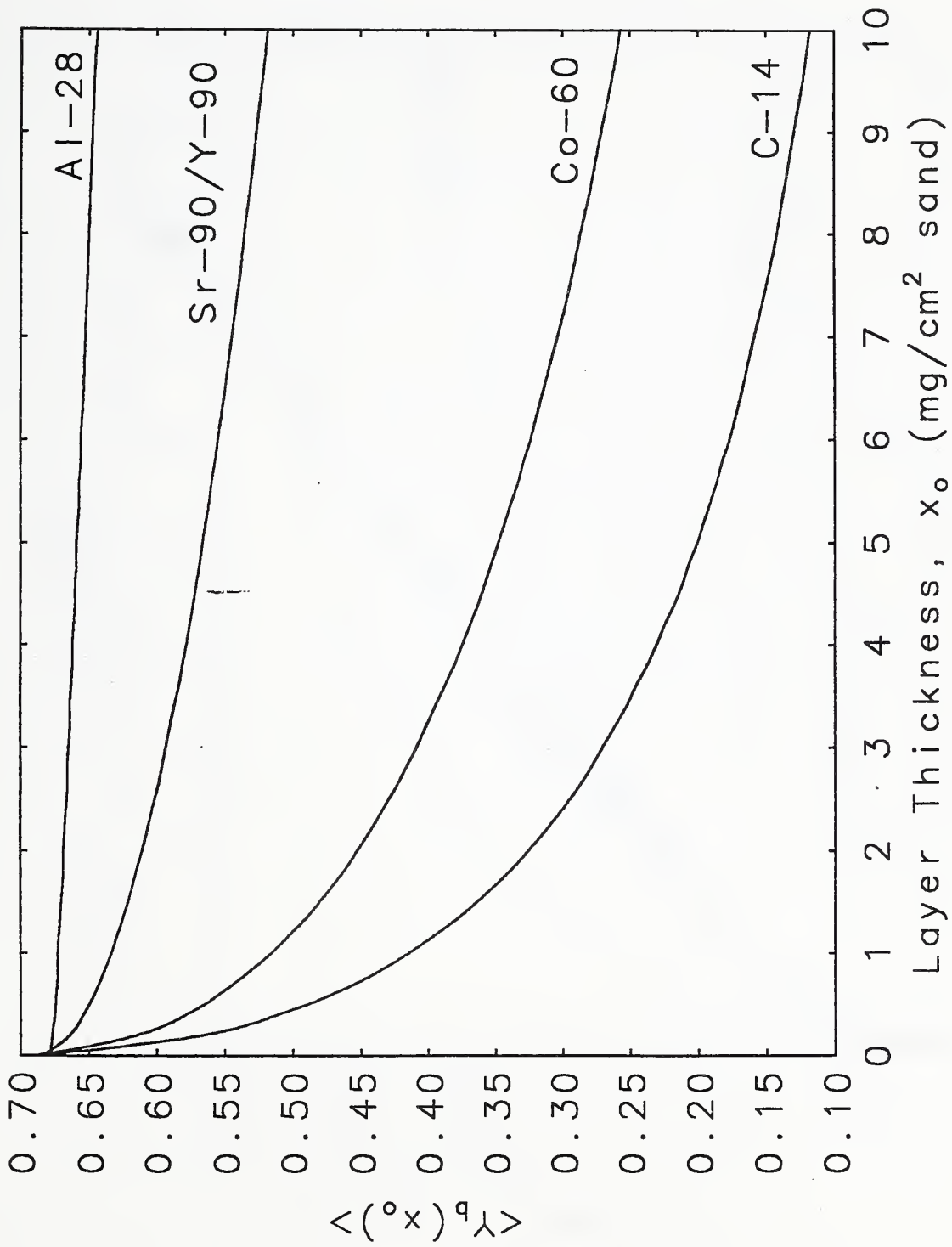


Fig.6a

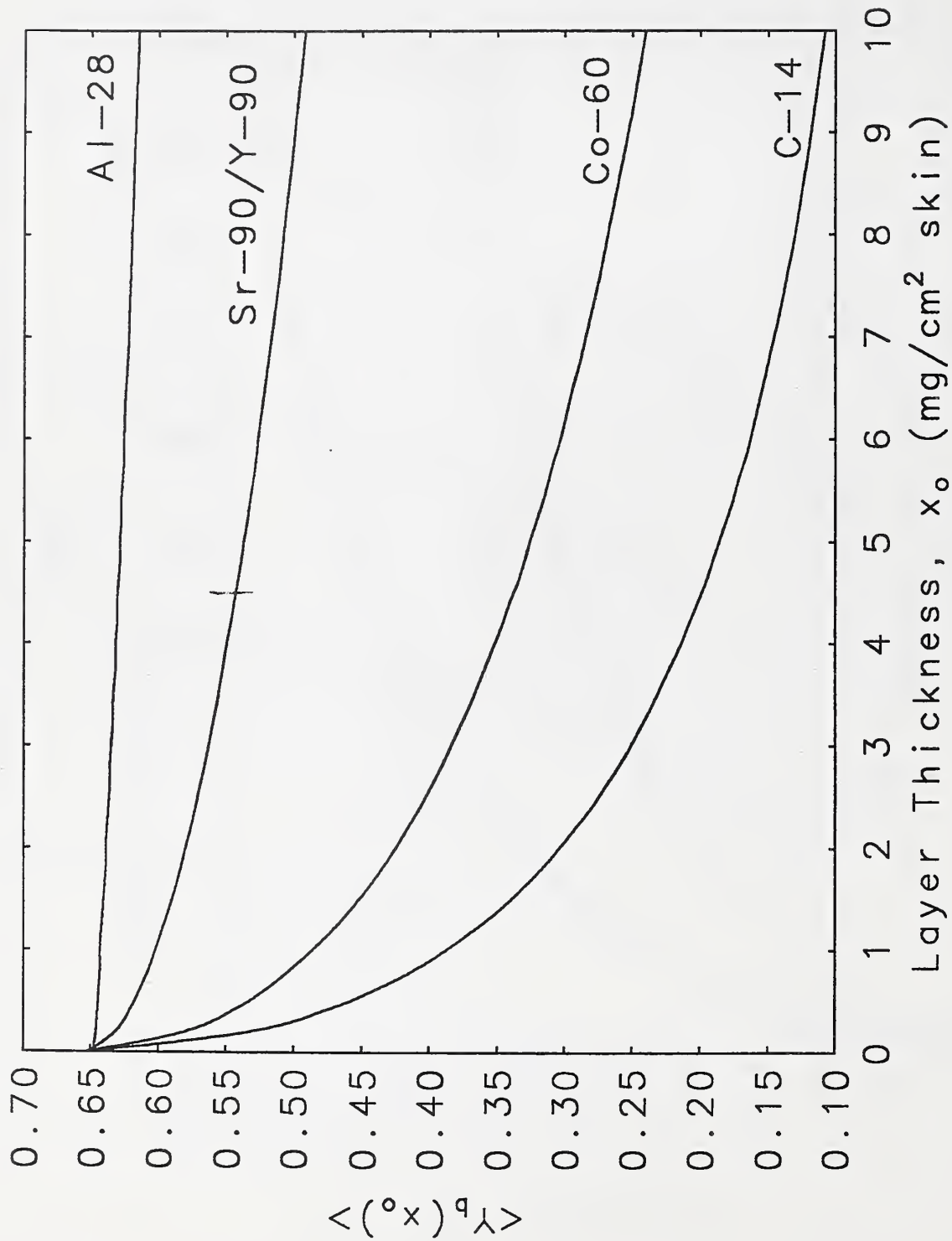


Fig.6b

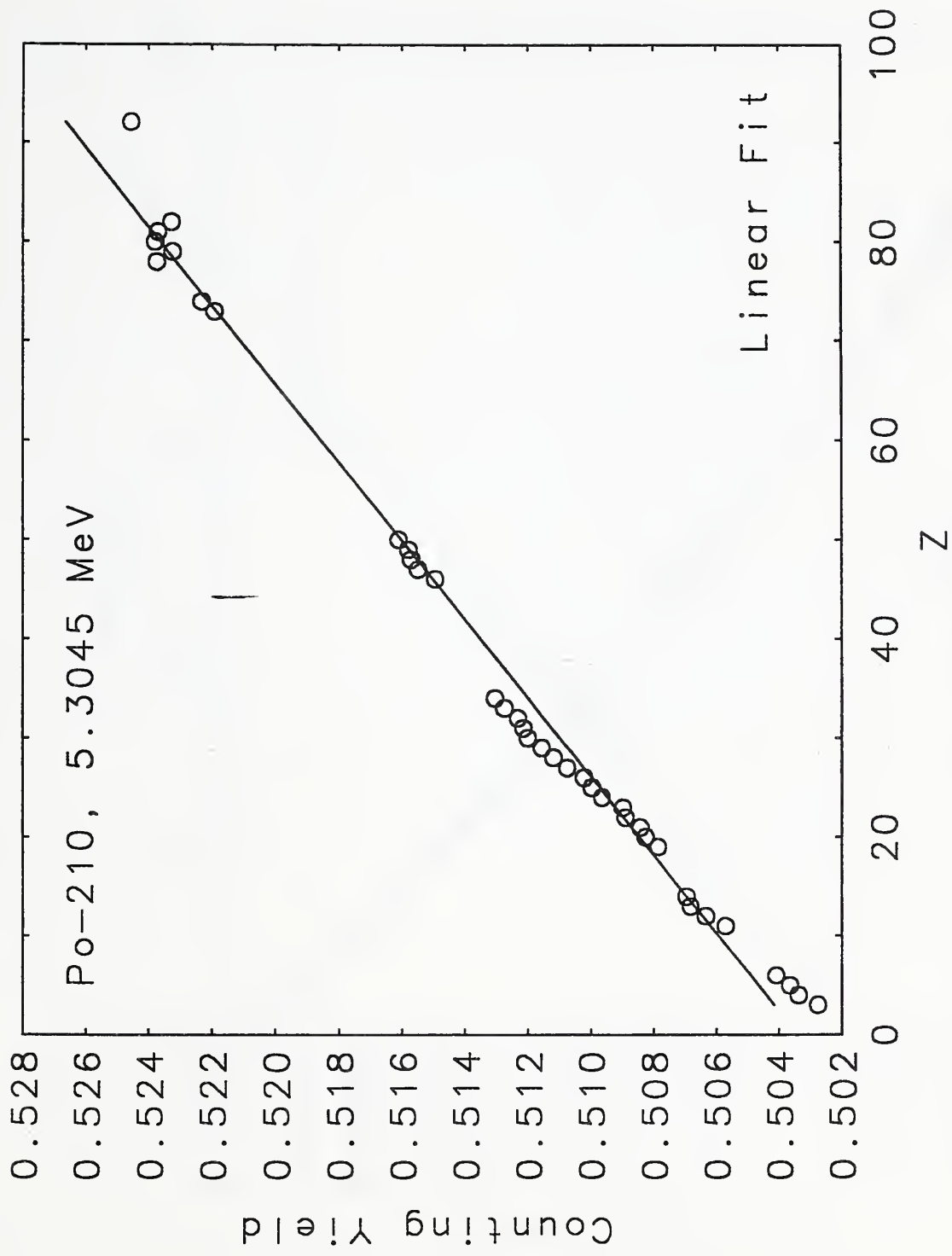


Fig.7a

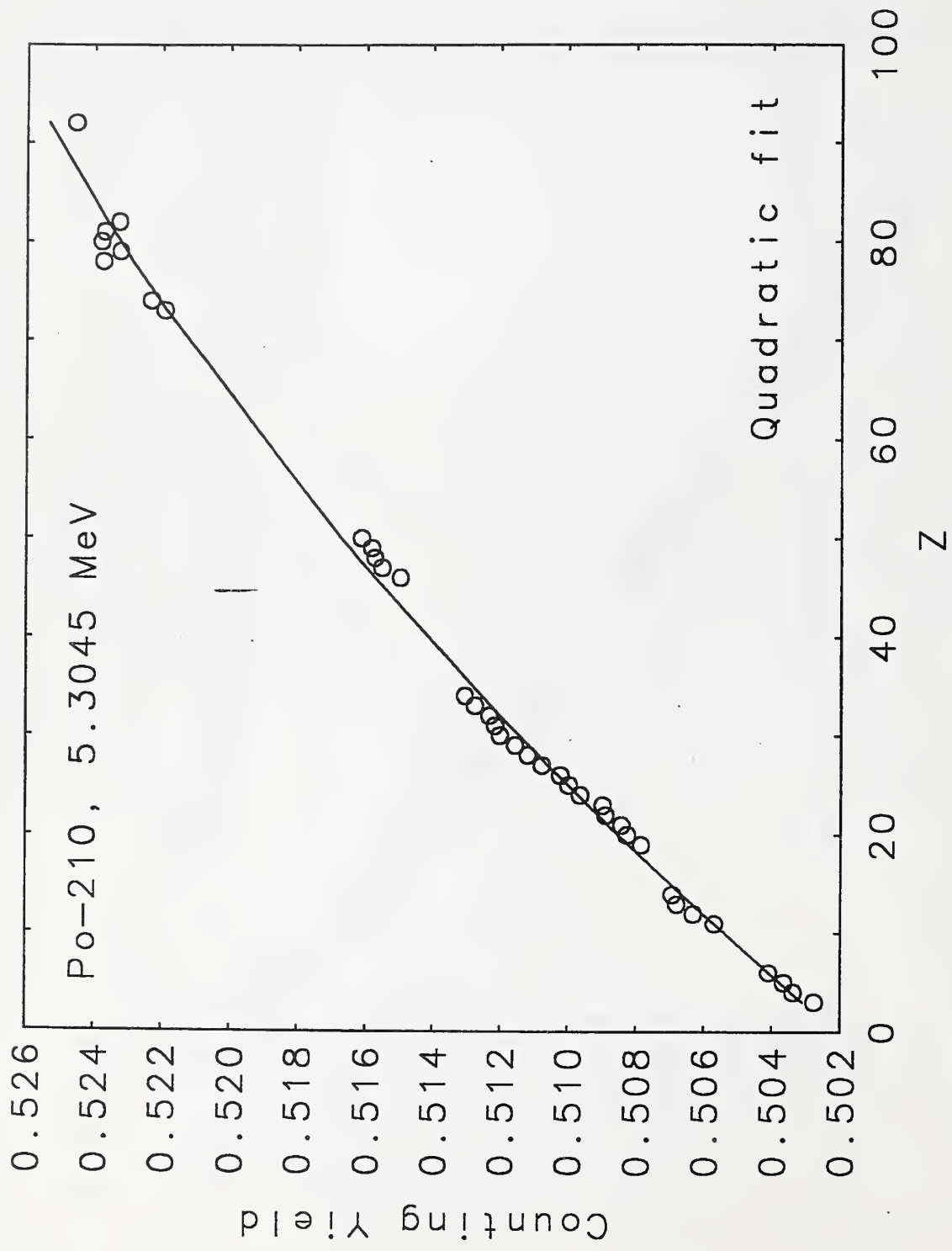


Fig.7b

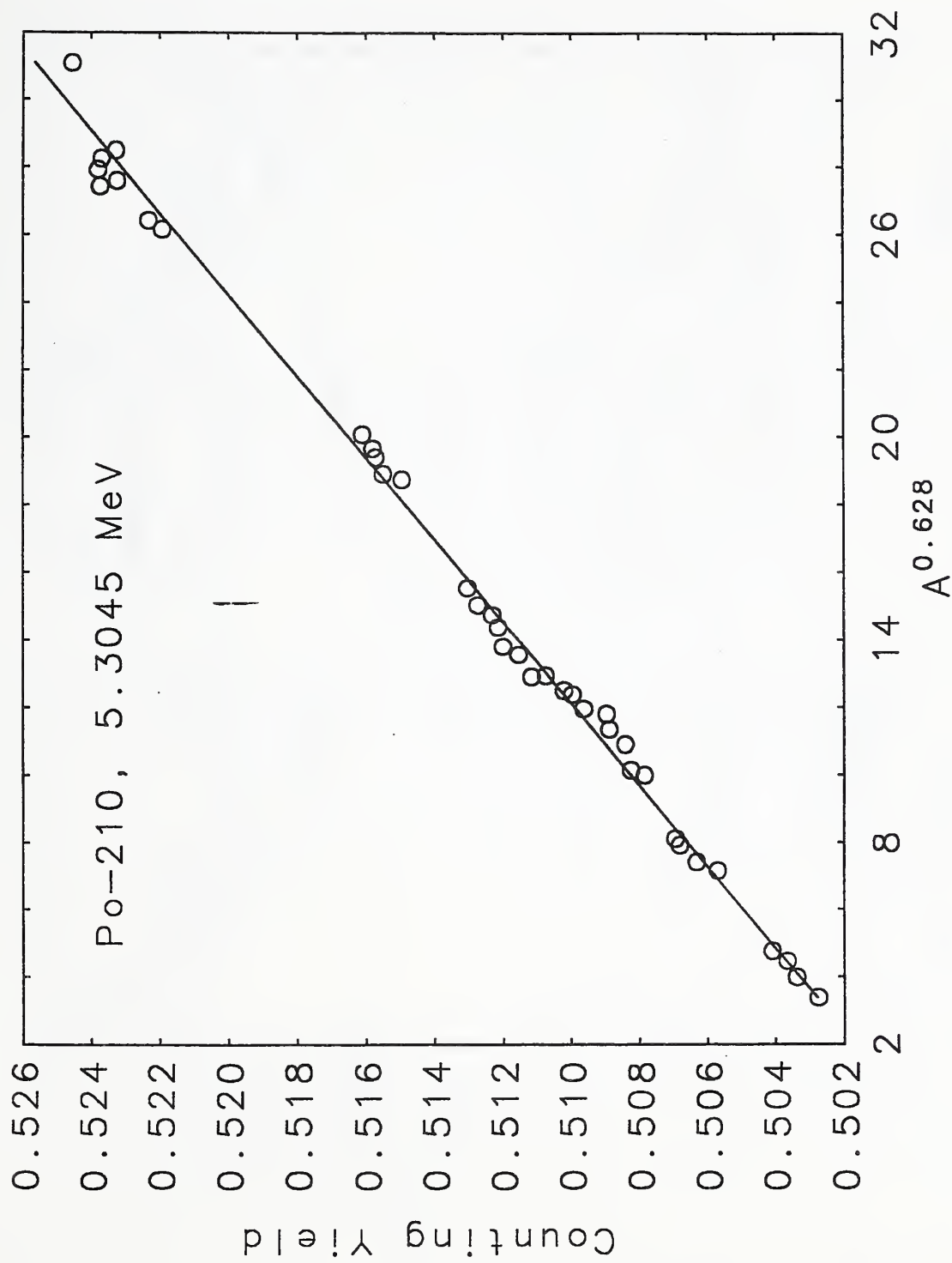


Fig.7c

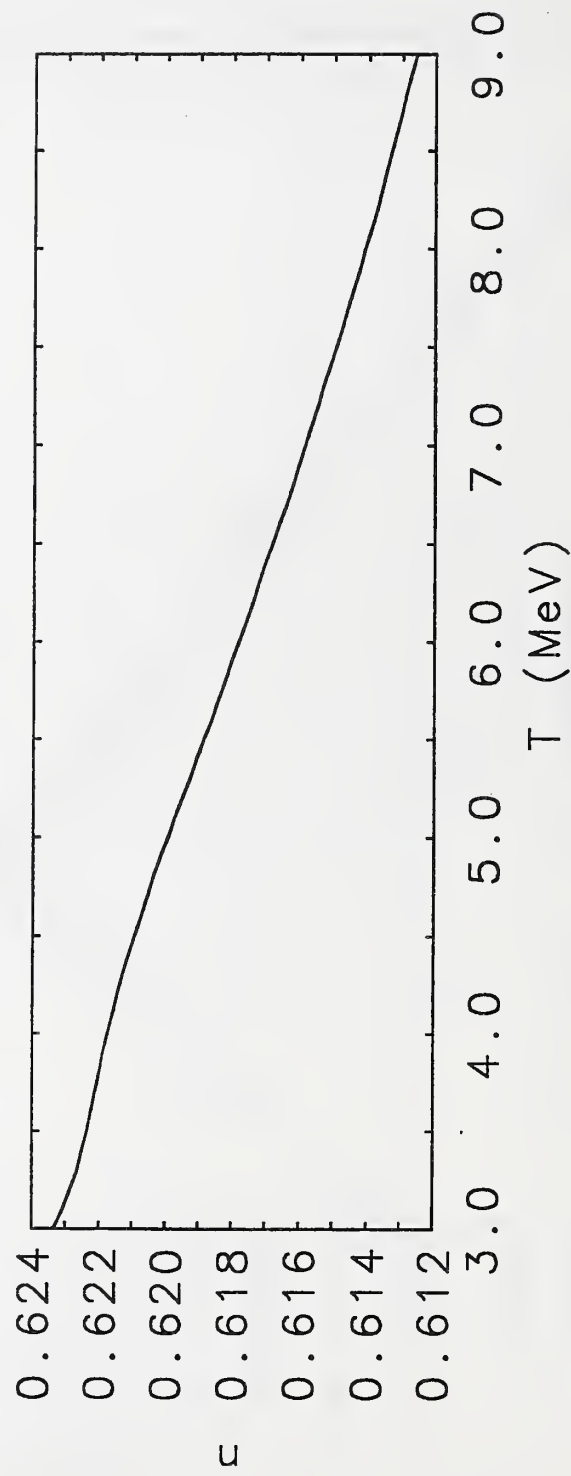
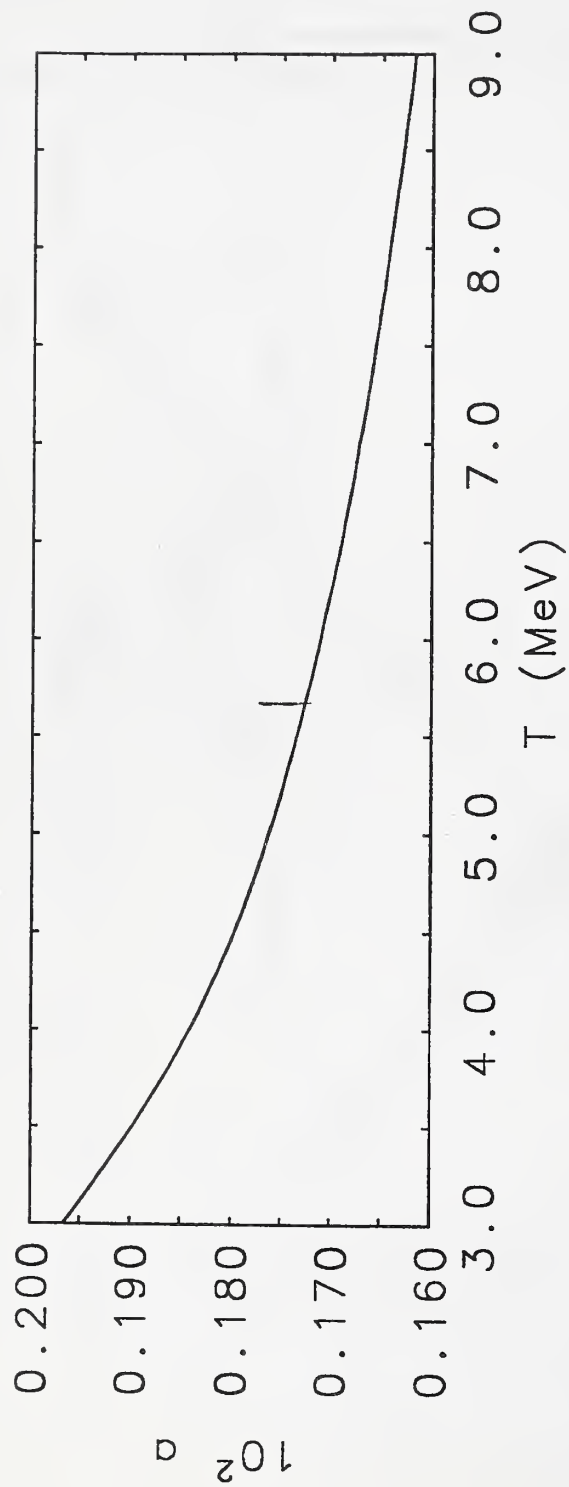


Fig.8

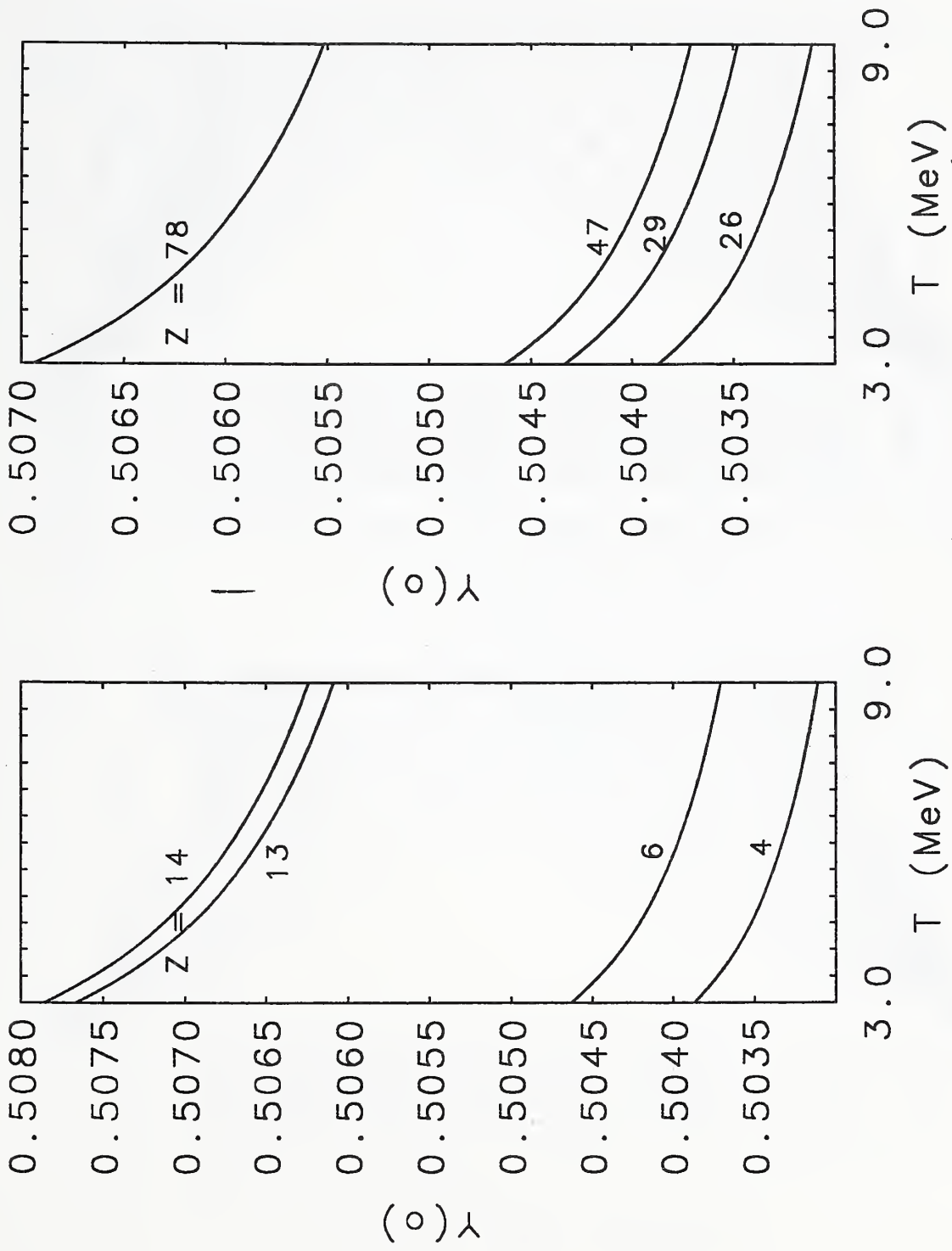


Fig.9

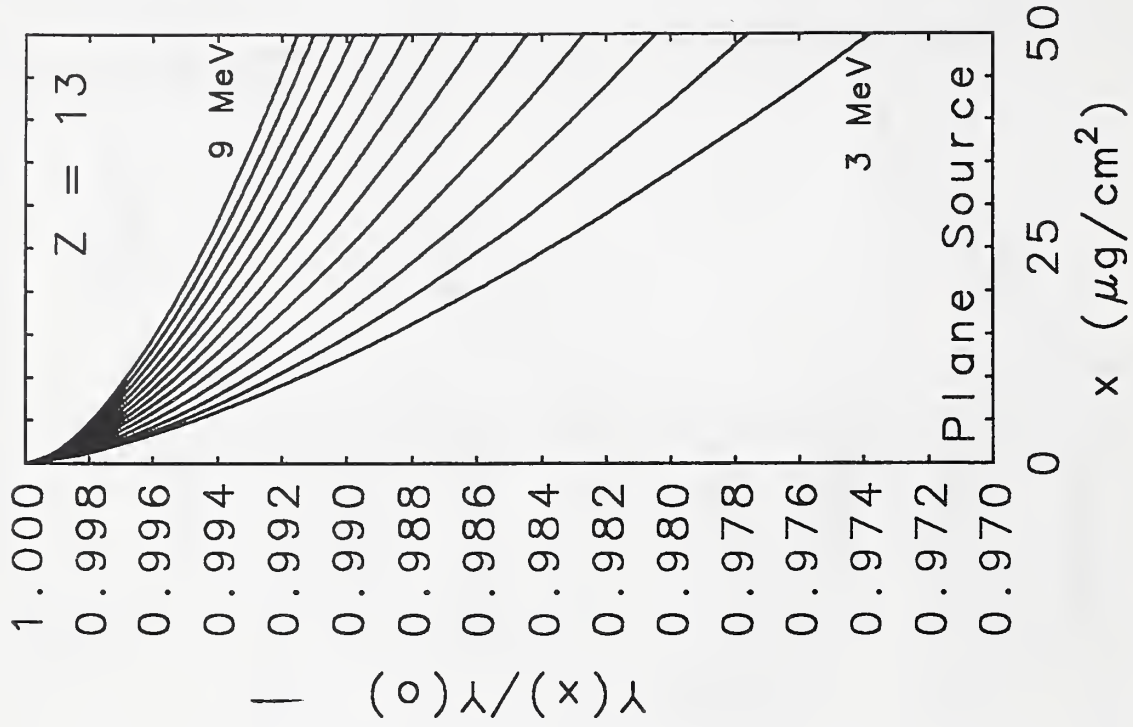
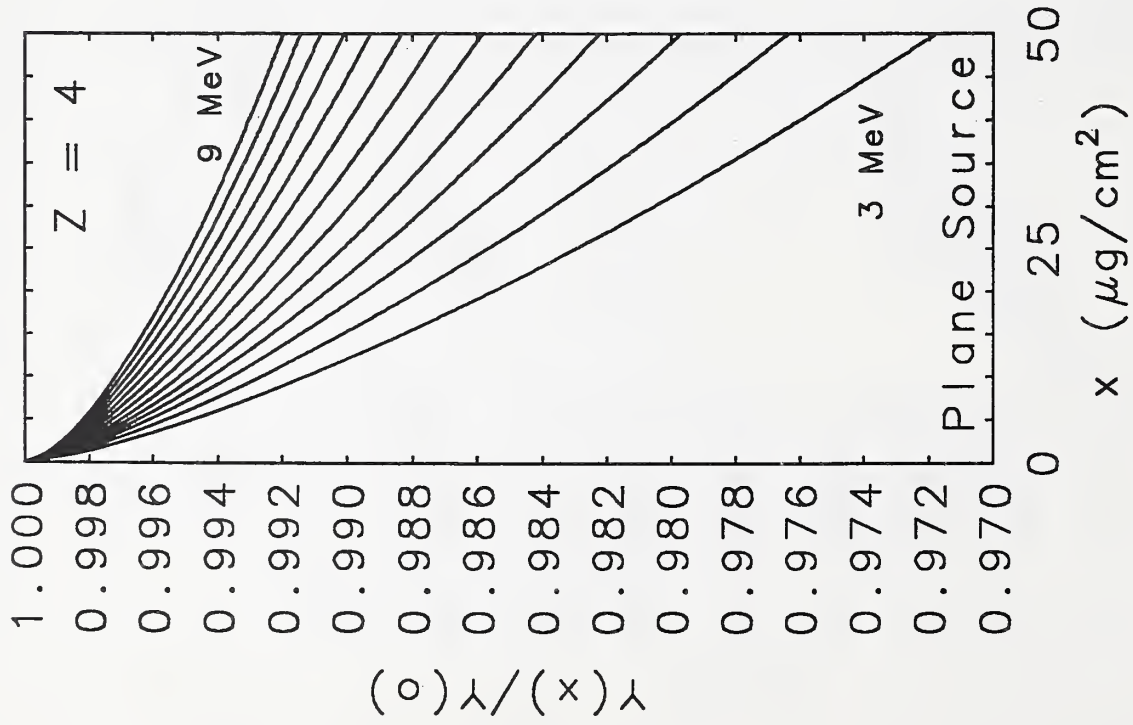


Fig.10a

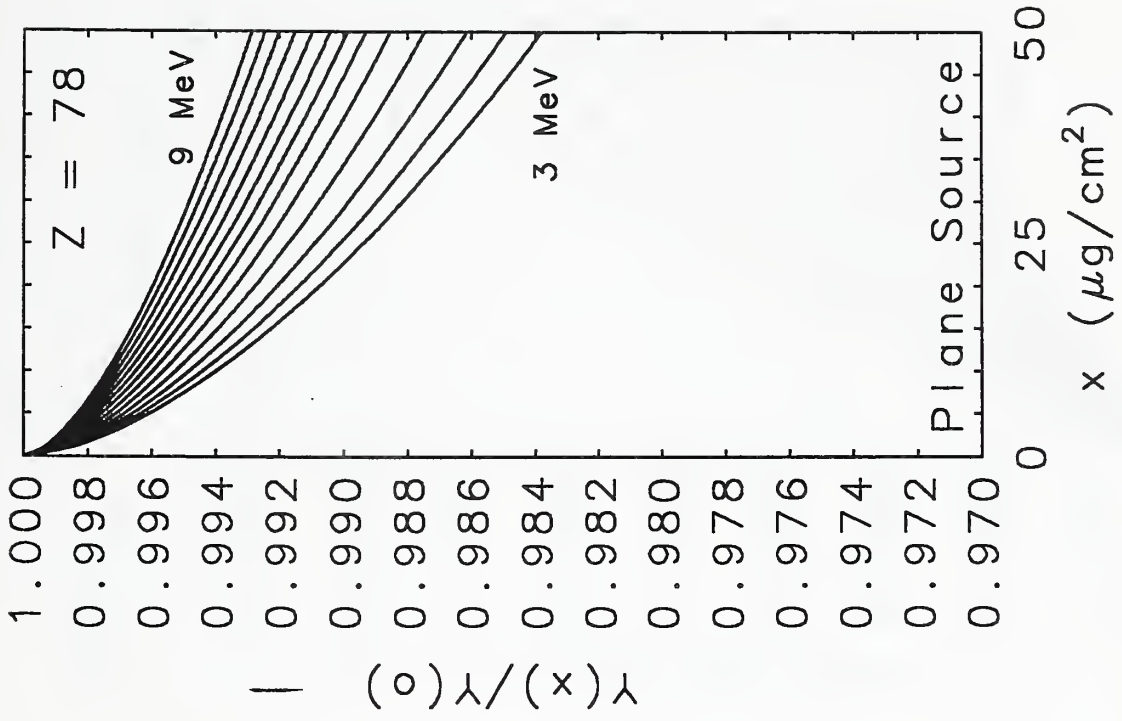
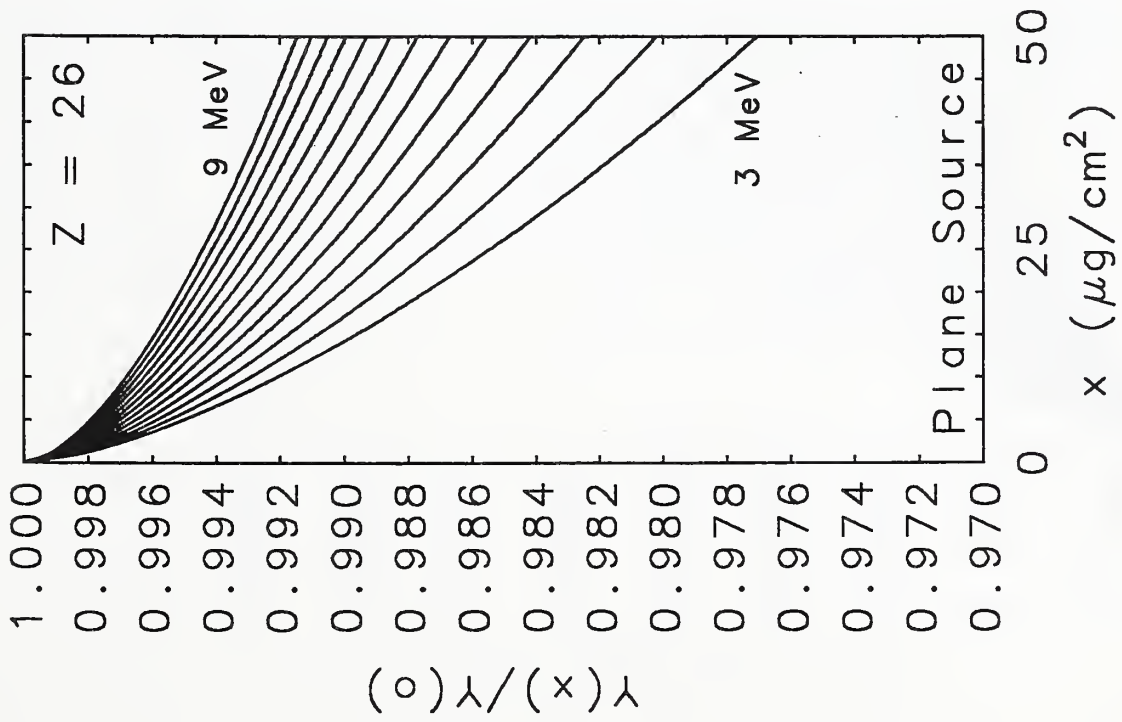


Fig.10b

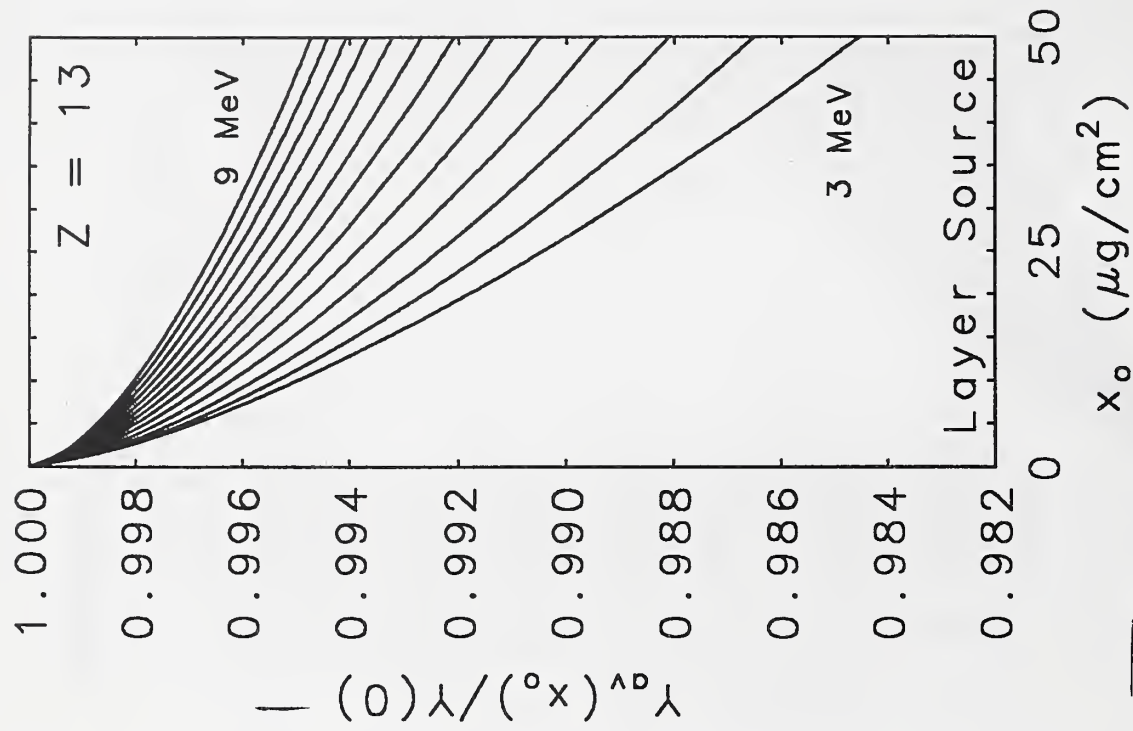
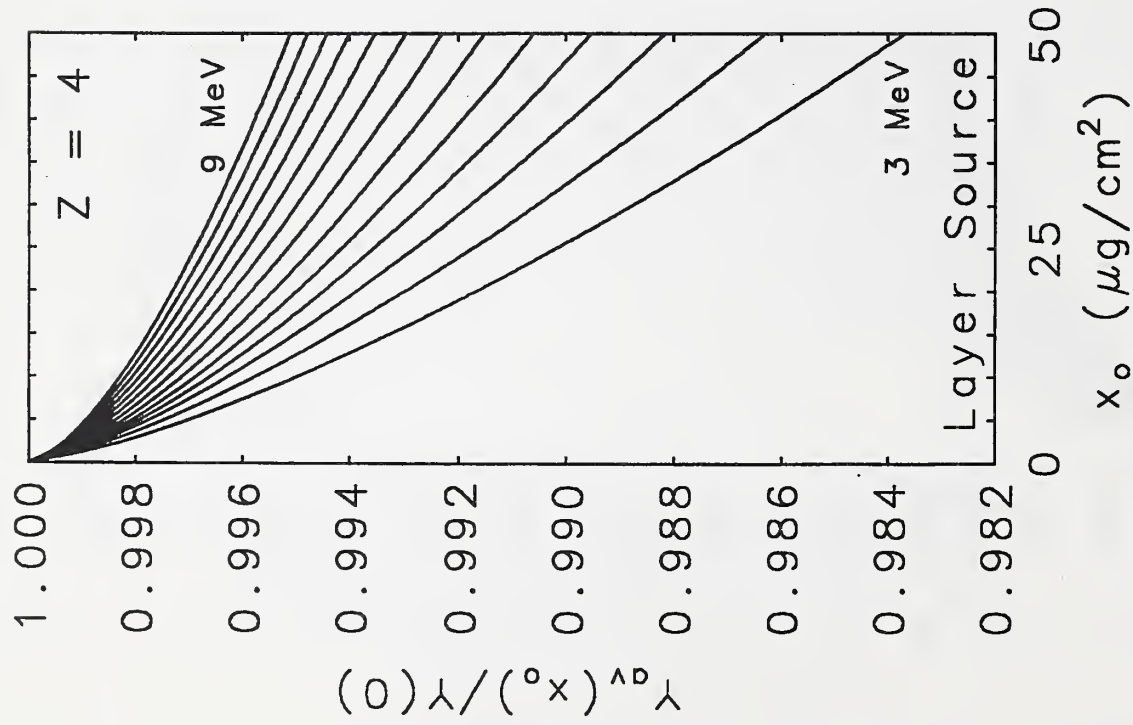


Fig.11a

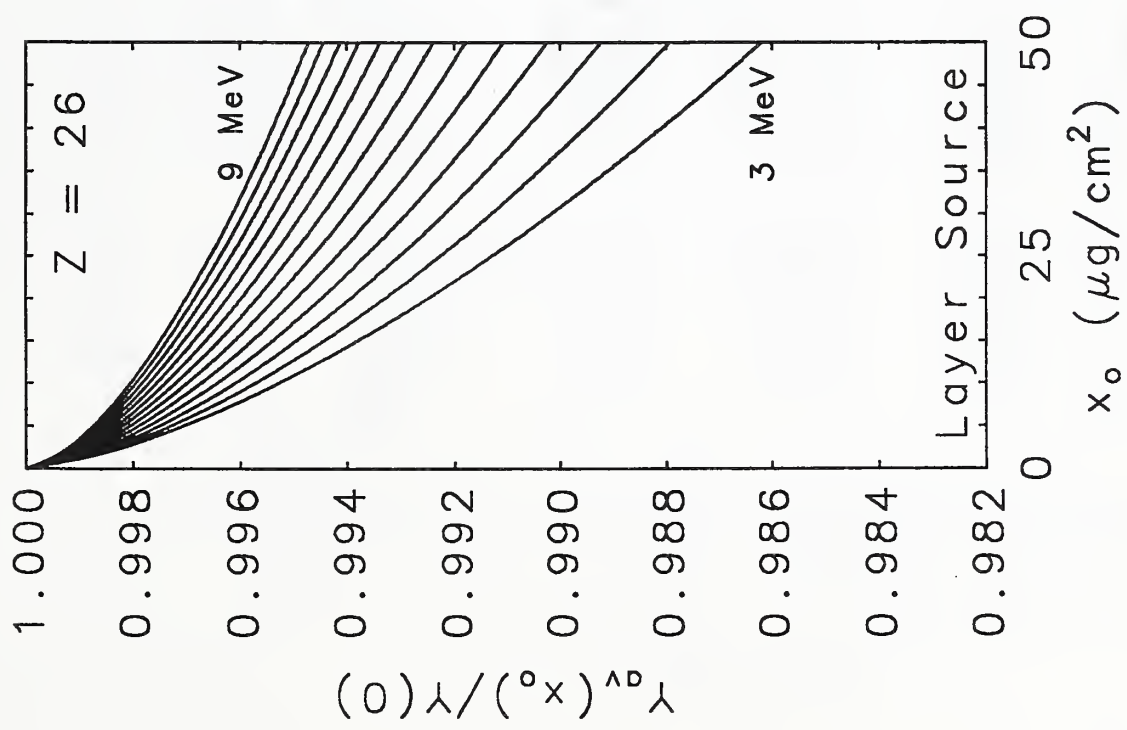
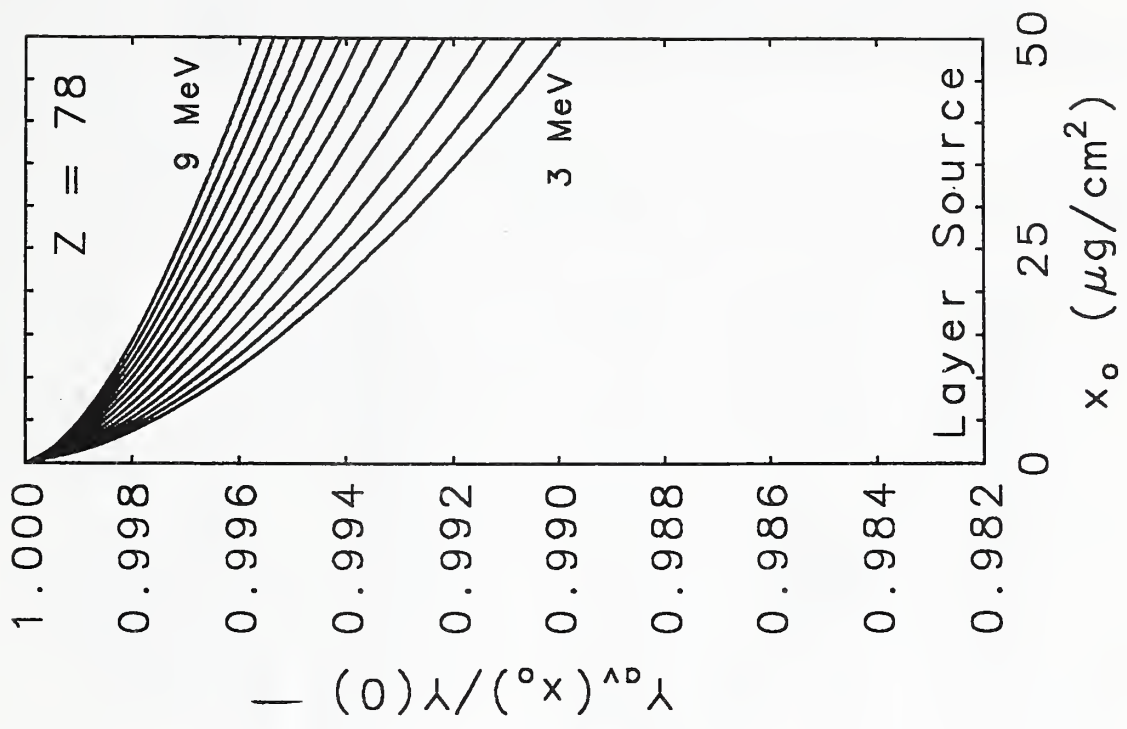


Fig.11b

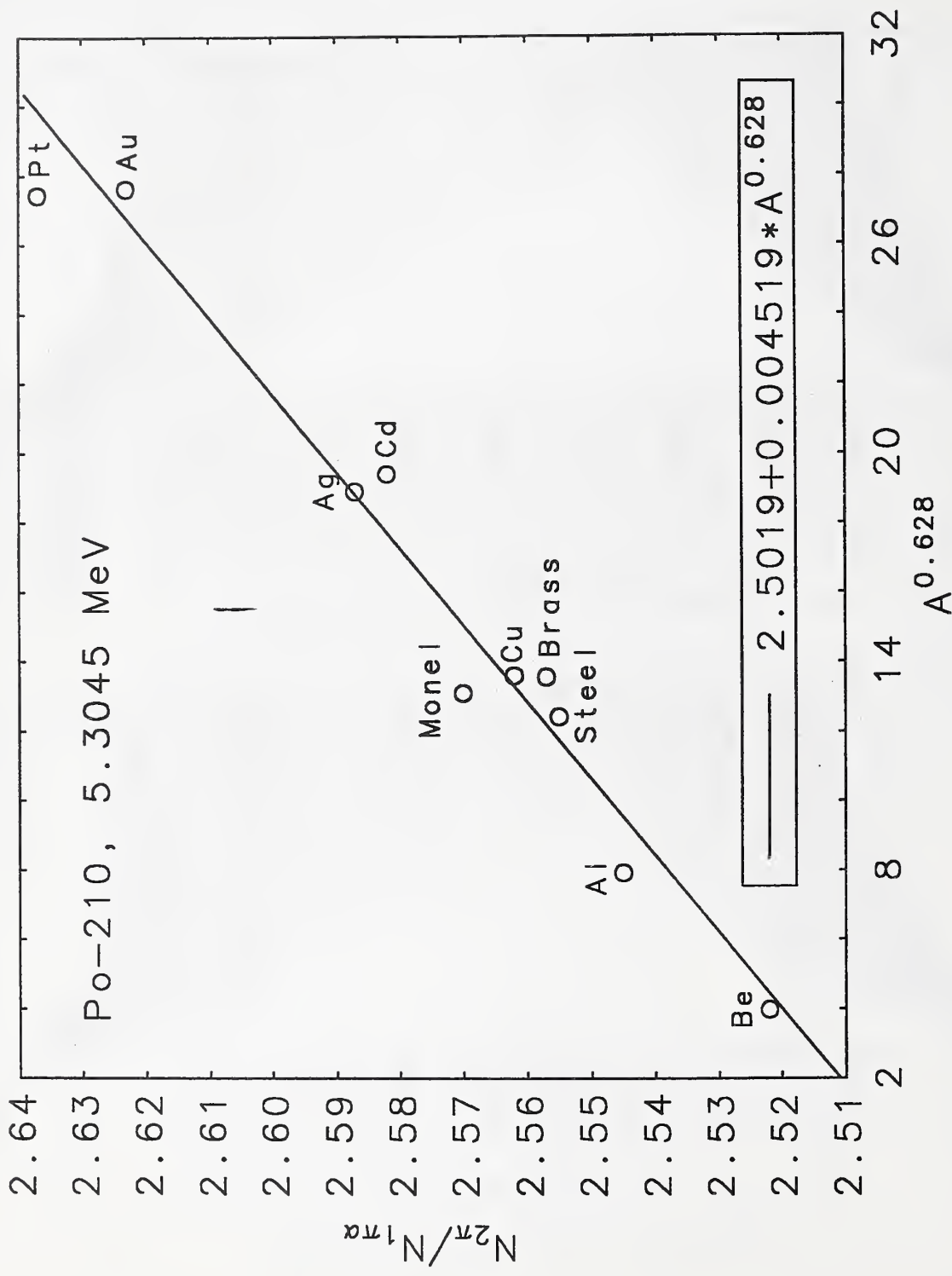


Fig.12

Table 1. List of beta(-) emitters for which counting yields are given in this report. ID is the identification number of the emitter in the spectrum database, $T_{1/2}$ is the half life, and E_{\max} and E_{av} are the maximum and average energies of the spectrum.

ID	Nuclide	$T_{1/2}$	E_{\max} (MeV)	E_{av} (MeV)	Intensity
2	1H3	12.33 Y	0.01857	0.00568	1.00000
14	6C14	5730 Y	0.15648	0.04947	1.00000
47	16S35	87.44 D	0.16747	0.04883	1.00000
445	61Pm147	2.6234 Y	0.22470	0.06196	0.99994
59	20Ca45	163.8 D	0.25690	0.07724	0.99998
235	43Tc99	2.111E+5 Y	0.29360	0.08459	0.99998
95	27Co60	5.2704 Y	0.31787	0.09578	0.99925
185	38Sr90	29.12 Y	0.54600	0.19577	1.00000
105	29Cu64	12.701 H	0.57820	0.19025	0.37100
543	77Ir192	73.831 D	0.67232	0.17979	0.95358
48	17Cl36	3.01E+5 Y	0.70950	0.25131	0.98100
569	81Tl204	3.78 Y	0.76340	0.24393	1.00000
373	53I131	8.04 D	0.80687	0.18172	0.99930
557	79Au198	2.696 D	0.96070	0.31157	1.00000
403	55Cs137	30.0 Y	1.17320	0.18692	1.00000
271	47Ag110	249.76 D	1.46794	0.06976	0.98838
92	26Fe59	44.496 D	1.56480	0.11750	0.99860
45	15P32	14.26 D	1.71040	0.69489	1.00000
55	19K43	22.6 H	1.81700	0.30888	1.00140
70	21Sc49	57.2 M	1.99400	0.81848	0.99940
77	22Ti51	5.76 M	2.15252	0.86849	1.00000
186	39Y90	64.1 H	2.27920	0.93264	0.99984
329	51Sb124	60.20 D	2.30227	0.38499	1.00168
37	13Al28	2.240 M	2.86419	1.24226	0.99990

Table 2. List of beta(+) emitters for which counting yields are given in this report. ID is the identification number of the emitter in the spectrum database, $T_{1/2}$ is the half life, and E_{\max} and E_{av} are the maximum and average energies of the spectrum.

ID	Nuclide	$T_{1/2}$	E_{\max} (MeV)	E_{av} (MeV)	Intensity
13	11Na22	2.602 Y	0.54552	0.21554	0.89840
80	29Cu64	12.701 H	0.65289	0.27813	0.17900
173	43Tc95	61 D	0.71689	0.29057	0.00310
52	26Fe52	8.275 H	0.80357	0.33993	0.56000
1	6C11	20.385 M	0.96009	0.38557	0.99759
63	27Co56	78.76 D	1.46124	0.60762	0.19670
34	21Sc44	3.927 H	1.47577	0.63270	0.94370
144	39Y86	48 M	1.51379	0.66696	0.00450
106	33As74	17.76 D	1.54009	0.44209	0.29100
136	37Rb84	32.87 D	1.65809	0.55630	0.25900
263	55Cs125	45 M	2.04799	0.84950	0.37820
247	53I119	19.1 M	2.09048	0.92620	0.53952

Table 3. Maximum ranges of beta particles, calculated in the continuous-slowng-down approximation at the maximum energy of the beta spectrum.

Nuclide	Maximum Range, g/cm ²			
	Be	C	Al	Fe
1H3	9.0992E-04	8.4140E-04	1.0288E-03	1.2255E-03
6C14	3.7002E-02	3.3825E-02	3.9197E-02	4.4410E-02
13Al28	1.8126E+00	1.6446E+00	1.7835E+00	1.9501E+00
15P32	1.0309E+00	9.3687E-01	1.0321E+00	1.1384E+00
16S35	4.1351E-02	3.7789E-02	4.3736E-02	4.9512E-02
17Cl36	3.5215E-01	3.2034E-01	3.6078E-01	4.0208E-01
19K43	1.1041E+00	1.0031E+00	1.1028E+00	1.2160E+00
20Ca45	8.1744E-02	7.4605E-02	8.5669E-02	9.6483E-02
21Sc49	1.2253E+00	1.1127E+00	1.2194E+00	1.3426E+00
22Ti51	1.3325E+00	1.2103E+00	1.3239E+00	1.4556E+00
26Fe59	9.3167E-01	8.4646E-01	9.3474E-01	1.0325E+00
27Co60	1.1326E-01	1.0326E-01	1.1816E-01	1.3272E-01
29Cu64	2.6750E-01	2.4358E-01	2.7549E-01	3.0766E-01
38Sr90	2.4729E-01	2.2518E-01	2.5495E-01	2.8490E-01
39Y90	1.4180E+00	1.2882E+00	1.4069E+00	1.5452E+00
43Tc99	1.0040E-01	9.1576E-02	1.0493E-01	1.1796E-01
47Ag110	8.6533E-01	7.8627E-01	8.6975E-01	9.6159E-01
51Sb124	1.4336E+00	1.3023E+00	1.4218E+00	1.5613E+00
53I131	4.1636E-01	3.7871E-01	4.2527E-01	4.7339E-01
55Cs137	6.6377E-01	6.0335E-01	6.7140E-01	7.4436E-01
61Pm147	6.6287E-02	6.0523E-02	6.9672E-02	7.8584E-02
77Ir192	3.2791E-01	2.9840E-01	3.3635E-01	3.7513E-01
79Au198	5.1944E-01	4.7229E-01	5.2818E-01	5.8686E-01
81Tl204	3.8757E-01	3.5253E-01	3.9641E-01	4.4146E-01

Table 3, continued.

Nuclide	Maximum Range, g/cm ²			
	Sand/ ^a	Loam/ ^b	Dry Soil/ ^c	Skin/ ^d
1H3	9.5288E-04	8.8778E-04	9.7585E-04	7.5438E-04
6C14	3.6760E-02	3.4771E-02	3.7440E-02	3.0383E-02
13Al28	1.7014E+00	1.6211E+00	1.7043E+00	1.4588E+00
15P32	9.7780E-01	9.2990E-01	9.8348E-01	8.3072E-01
16S35	4.1019E-02	3.8820E-02	4.1779E-02	3.3933E-02
17Cl36	3.3934E-01	3.2220E-01	3.4377E-01	2.8503E-01
19K43	1.0454E+00	9.9498E-01	1.0513E+00	8.8929E-01
20Ca45	8.0421E-02	7.6240E-02	8.1848E-02	6.6891E-02
21Sc49	1.1577E+00	1.1016E+00	1.1630E+00	9.8645E-01
22Ti51	1.2582E+00	1.1971E+00	1.2630E+00	1.0730E+00
26Fe59	8.8478E-01	8.4122E-01	8.9059E-01	7.5067E-01
27Co60	1.1087E-01	1.0519E-01	1.1281E-01	9.2468E-02
29Cu64	2.5884E-01	2.4581E-01	2.6266E-01	2.1699E-01
38Sr90	2.3951E-01	2.2749E-01	2.4313E-01	2.0068E-01
39Y90	1.3376E+00	1.2736E+00	1.3427E+00	1.1419E+00
43Tc99	9.8500E-02	9.3416E-02	1.0021E-01	8.2040E-02
47Ag110	8.2275E-01	7.8206E-01	8.2856E-01	6.9728E-01
51Sb124	1.3520E+00	1.2874E+00	1.3572E+00	1.1545E+00
53I131	4.0024E-01	3.8012E-01	4.0501E-01	3.3661E-01
55Cs137	6.3370E-01	6.0210E-01	6.3930E-01	5.3538E-01
61Pm147	6.5387E-02	6.1957E-02	6.6559E-02	5.4296E-02
77Ir192	3.1634E-01	3.0038E-01	3.2058E-01	2.6555E-01
79Au198	4.9772E-01	4.7275E-01	5.0297E-01	4.1943E-01
81Tl204	3.7296E-01	3.5415E-01	3.7758E-01	3.1347E-01

a. Silica, SiO₂. Density 2.2 g/cm²; effective atomic number $Z_{\text{eff}} = 10.8$.

b. Assumed composition (percentage by weight): 0.02 N₂; 9.04 H₂O; 16.87 Al₂O₃; 45.60 SiO₂; 1.37 Fe₂O₃; 1.34 CaCO₃; 1.10 Na₂O; 0.67 K₂O; 7.92 C₉H₁₂; 16.08 C₆H₁₀O₅. Density 1.5 g/cm³; effective atomic number $Z_{\text{eff}} = 9.31$.

c. Assumed composition (percentage by weight): 15.23 Al₂O₃; 62.58 SiO₂; 3.10 Fe₂O₃; 5.10 CaO; 3.71 Na₂O; 3.11 K₂O; 3.45 MgO; 3.72 FeO. Density 1.5 g/cm³; effective atomic number $Z_{\text{eff}} = 11.9$.

d. Assumed composition (percentage by weight): 61.538 H₂O; 3.173 H; 22.825 C; 4.642 N; 7.248 O; 0.007 Na; 0.006 Mg; 0.033 P; 0.159 S; 0.267 Cl; 0.085 K; 0.015 Ca; 0.001 Fe; 0.001 Zn. Density 1.1 g/cm³; effective atomic number $Z_{\text{eff}} = 6.32$.

Table 3, continued.

Nuclide	Maximum Range, g/cm ²	
	Al	Fe
6C11	5.3149E-01	5.9246E-01
11Na22	2.5296E-01	2.8322E-01
21Sc44	8.8770E-01	9.8559E-01
26Fe52	4.2438E-01	4.7381E-01
27Co56	8.7769E-01	9.7453E-01
29Cu64	3.2314E-01	3.6132E-01
33As74	9.3199E-01	1.0345E+00
37Rb84	1.0131E+00	1.1231E+00
39Y86	9.1389E-01	1.0145E+00
43Tc95	3.6587E-01	4.0874E-01
53I119	1.3078E+00	1.4453E+00
55Cs125	1.2790E+00	1.4140E+00

Table 4. Counting yield $Y_b(x)$ of plane beta(-) sources as a function of the source depth x in an aluminum backing.

x (microns)	6C14	13Al28	15P32	16S35	17Cl36	19K43
0.00	0.701	0.689	0.695	0.701	0.699	0.699
0.05	0.658	0.689	0.694	0.648	0.693	0.695
0.10	0.636	0.689	0.693	0.623	0.689	0.692
0.15	0.619	0.689	0.693	0.605	0.686	0.689
0.20	0.604	0.688	0.692	0.589	0.683	0.687
0.25	0.591	0.688	0.691	0.575	0.681	0.685
0.30	0.580	0.688	0.691	0.563	0.678	0.683
0.40	0.559	0.688	0.690	0.542	0.674	0.679
0.50	0.542	0.687	0.689	0.524	0.670	0.676
0.60	0.526	0.687	0.688	0.508	0.667	0.673
0.70	0.512	0.687	0.687	0.494	0.664	0.671
0.80	0.499	0.686	0.687	0.481	0.661	0.668
0.90	0.487	0.686	0.686	0.469	0.658	0.666
1.00	0.475	0.686	0.685	0.458	0.655	0.664
1.25	0.450	0.685	0.684	0.433	0.649	0.658
1.50	0.428	0.685	0.682	0.412	0.643	0.653
1.75	0.408	0.684	0.681	0.393	0.638	0.649
2.00	0.391	0.683	0.679	0.376	0.633	0.645
2.50	0.360	0.682	0.676	0.346	0.623	0.637
3.00	0.333	0.681	0.674	0.321	0.615	0.629
3.50	0.310	0.680	0.671	0.300	0.607	0.623
4.00	0.290	0.679	0.669	0.281	0.599	0.616
4.50	0.272	0.678	0.667	0.264	0.592	0.610
5.00	0.256	0.677	0.665	0.248	0.586	0.605
5.50	0.241	0.676	0.662	0.234	0.579	0.599
6.00	0.228	0.675	0.660	0.222	0.573	0.594
7.00	0.204	0.673	0.656	0.199	0.562	0.584
8.00	0.184	0.671	0.653	0.180	0.551	0.575
9.00	0.166	0.670	0.649	0.164	0.541	0.566
10.00	0.151	0.668	0.645	0.149	0.531	0.558
12.00	0.125	0.664	0.639	0.125	0.514	0.543
14.00	0.104	0.661	0.632	0.106	0.498	0.529
16.00	0.087	0.658	0.626	0.090	0.483	0.516
18.00	0.074	0.655	0.620	0.077	0.470	0.504
20.00	0.062	0.652	0.614	0.065	0.457	0.492

Table 4, continued.

x (microns)	20Ca45	21Sc49	22Ti51	26Fe59	27Co60	29Cu64
0.00	0.701	0.694	0.693	0.700	0.701	0.698
0.05	0.668	0.693	0.692	0.683	0.674	0.690
0.10	0.652	0.692	0.692	0.671	0.661	0.685
0.15	0.639	0.692	0.691	0.661	0.650	0.682
0.20	0.629	0.691	0.691	0.653	0.641	0.679
0.25	0.619	0.691	0.690	0.646	0.634	0.676
0.30	0.611	0.690	0.690	0.640	0.627	0.673
0.40	0.596	0.689	0.689	0.629	0.614	0.668
0.50	0.584	0.689	0.689	0.619	0.604	0.664
0.60	0.572	0.688	0.688	0.610	0.594	0.660
0.70	0.562	0.687	0.687	0.602	0.585	0.657
0.80	0.552	0.687	0.687	0.595	0.577	0.653
0.90	0.544	0.686	0.686	0.588	0.569	0.650
1.00	0.535	0.686	0.686	0.581	0.562	0.647
1.25	0.517	0.684	0.684	0.566	0.546	0.640
1.50	0.500	0.683	0.683	0.553	0.532	0.633
1.75	0.485	0.682	0.682	0.541	0.519	0.627
2.00	0.471	0.680	0.681	0.531	0.507	0.622
2.50	0.447	0.678	0.679	0.511	0.486	0.611
3.00	0.426	0.676	0.677	0.494	0.467	0.601
3.50	0.408	0.674	0.675	0.479	0.450	0.592
4.00	0.391	0.672	0.673	0.465	0.435	0.584
4.50	0.376	0.670	0.671	0.452	0.421	0.576
5.00	0.362	0.668	0.669	0.440	0.409	0.569
5.50	0.349	0.667	0.668	0.429	0.397	0.562
6.00	0.337	0.665	0.666	0.419	0.386	0.555
7.00	0.315	0.662	0.663	0.400	0.365	0.542
8.00	0.296	0.658	0.660	0.383	0.347	0.530
9.00	0.279	0.655	0.657	0.368	0.331	0.519
10.00	0.263	0.652	0.654	0.354	0.316	0.509
12.00	0.236	0.647	0.649	0.329	0.290	0.490
14.00	0.213	0.641	0.644	0.307	0.267	0.472
16.00	0.194	0.636	0.639	0.288	0.247	0.456
18.00	0.177	0.631	0.634	0.271	0.230	0.442
20.00	0.161	0.626	0.629	0.256	0.214	0.428

Table 4, continued.

x (microns)	38Sr90 39Y90	43Tc99	47Ag110	51Sb124	53I131	55Cs137
0.00	0.696	0.701	0.701	0.698	0.700	0.700
0.05	0.690	0.669	0.641	0.690	0.687	0.688
0.10	0.686	0.654	0.603	0.684	0.680	0.681
0.15	0.684	0.642	0.575	0.679	0.674	0.675
0.20	0.681	0.632	0.553	0.675	0.669	0.670
0.25	0.679	0.623	0.535	0.671	0.664	0.666
0.30	0.677	0.615	0.519	0.668	0.660	0.662
0.40	0.673	0.601	0.492	0.662	0.653	0.655
0.50	0.670	0.589	0.470	0.657	0.647	0.648
0.60	0.667	0.578	0.451	0.652	0.641	0.643
0.70	0.665	0.568	0.435	0.647	0.636	0.638
0.80	0.662	0.559	0.420	0.643	0.631	0.633
0.90	0.660	0.550	0.407	0.640	0.626	0.628
1.00	0.658	0.542	0.395	0.636	0.622	0.624
1.25	0.653	0.524	0.370	0.628	0.612	0.614
1.50	0.648	0.509	0.349	0.621	0.603	0.605
1.75	0.644	0.495	0.331	0.614	0.594	0.597
2.00	0.640	0.482	0.315	0.608	0.587	0.590
2.50	0.632	0.459	0.290	0.597	0.573	0.577
3.00	0.626	0.439	0.270	0.587	0.561	0.564
3.50	0.620	0.421	0.253	0.578	0.549	0.553
4.00	0.614	0.405	0.239	0.570	0.539	0.543
4.50	0.609	0.390	0.227	0.563	0.529	0.534
5.00	0.604	0.377	0.217	0.556	0.520	0.525
5.50	0.599	0.365	0.208	0.549	0.512	0.517
6.00	0.594	0.353	0.200	0.543	0.504	0.509
7.00	0.586	0.332	0.186	0.531	0.489	0.494
8.00	0.578	0.314	0.175	0.521	0.475	0.481
9.00	0.570	0.297	0.166	0.511	0.463	0.469
10.00	0.564	0.282	0.158	0.502	0.451	0.457
12.00	0.551	0.256	0.146	0.486	0.430	0.437
14.00	0.539	0.234	0.136	0.472	0.412	0.418
16.00	0.528	0.214	0.129	0.459	0.395	0.401
18.00	0.519	0.198	0.122	0.447	0.379	0.386
20.00	0.509	0.182	0.117	0.436	0.365	0.372

Table 4, continued

x (microns)	61Pm147	77Ir192	79Au198	81Tl204
0.00	0.701	0.700	0.699	0.699
0.05	0.657	0.686	0.692	0.689
0.10	0.636	0.678	0.688	0.683
0.15	0.620	0.672	0.685	0.679
0.20	0.606	0.667	0.682	0.675
0.25	0.595	0.662	0.680	0.671
0.30	0.584	0.658	0.678	0.668
0.40	0.566	0.650	0.674	0.662
0.50	0.551	0.644	0.670	0.657
0.60	0.537	0.638	0.667	0.653
0.70	0.525	0.632	0.664	0.649
0.80	0.513	0.627	0.661	0.645
0.90	0.503	0.622	0.658	0.641
1.00	0.493	0.618	0.656	0.638
1.25	0.471	0.608	0.650	0.630
1.50	0.452	0.598	0.645	0.622
1.75	0.435	0.590	0.640	0.616
2.00	0.420	0.582	0.635	0.610
2.50	0.393	0.568	0.626	0.599
3.00	0.371	0.555	0.619	0.589
3.50	0.351	0.544	0.612	0.580
4.00	0.333	0.533	0.605	0.571
4.50	0.317	0.524	0.599	0.563
5.00	0.302	0.514	0.593	0.556
5.50	0.289	0.506	0.587	0.549
6.00	0.277	0.498	0.582	0.542
7.00	0.255	0.483	0.572	0.530
8.00	0.236	0.469	0.562	0.519
9.00	0.220	0.456	0.554	0.508
10.00	0.205	0.445	0.545	0.499
12.00	0.179	0.424	0.530	0.481
14.00	0.158	0.405	0.516	0.465
16.00	0.141	0.388	0.503	0.450
18.00	0.126	0.373	0.492	0.437
20.00	0.112	0.359	0.481	0.424

Table 5. Counting yield $Y_p(x)$ of plane beta(-) sources as a function of the source depth x in an iron backing.

x (microns)	6C14	13Al28	15P32	16S35	17Cl36	19K43
0.00	0.752	0.735	0.743	0.752	0.750	0.749
0.05	0.664	0.734	0.740	0.649	0.735	0.738
0.10	0.621	0.734	0.738	0.603	0.727	0.731
0.15	0.588	0.733	0.737	0.569	0.720	0.726
0.20	0.561	0.732	0.735	0.542	0.714	0.721
0.25	0.537	0.732	0.734	0.518	0.709	0.716
0.30	0.516	0.731	0.733	0.497	0.704	0.712
0.40	0.480	0.731	0.731	0.462	0.695	0.705
0.50	0.450	0.730	0.729	0.433	0.687	0.698
0.60	0.424	0.729	0.727	0.408	0.680	0.692
0.70	0.400	0.728	0.725	0.385	0.673	0.687
0.80	0.380	0.727	0.723	0.366	0.667	0.681
0.90	0.361	0.727	0.721	0.348	0.661	0.676
1.00	0.344	0.726	0.719	0.332	0.655	0.671
1.25	0.306	0.724	0.715	0.296	0.642	0.660
1.50	0.276	0.722	0.711	0.267	0.630	0.650
1.75	0.249	0.721	0.708	0.243	0.619	0.640
2.00	0.227	0.719	0.704	0.222	0.608	0.631
2.50	0.190	0.716	0.698	0.187	0.589	0.615
3.00	0.160	0.713	0.691	0.159	0.572	0.600
3.50	0.137	0.710	0.685	0.137	0.556	0.586
4.00	0.117	0.707	0.680	0.118	0.541	0.573
4.50	0.101	0.705	0.674	0.103	0.527	0.561
5.00	0.087	0.702	0.669	0.090	0.514	0.550
5.50	0.076	0.699	0.664	0.079	0.502	0.539
6.00	0.066	0.697	0.659	0.069	0.490	0.529
7.00	0.050	0.692	0.649	0.054	0.469	0.510
8.00	0.038	0.687	0.640	0.042	0.449	0.492
9.00	0.029	0.682	0.632	0.033	0.431	0.476
10.00	0.023	0.678	0.623	0.026	0.415	0.461
12.00	0.013	0.669	0.607	0.016	0.385	0.433
14.00	0.008	0.661	0.593	0.010	0.358	0.408
16.00	0.004	0.652	0.579	0.006	0.334	0.386
18.00	0.002	0.645	0.565	0.004	0.313	0.365
20.00	0.001	0.637	0.553	0.002	0.293	0.347

Table 5, continued.

x (microns)	20Ca45	21Sc49	22Ti51	26Fe59	27Co60	29Cu64
0.00	0.752	0.741	0.740	0.751	0.752	0.749
0.05	0.686	0.739	0.738	0.709	0.698	0.732
0.10	0.655	0.737	0.737	0.686	0.672	0.723
0.15	0.631	0.736	0.736	0.667	0.652	0.715
0.20	0.611	0.735	0.734	0.652	0.635	0.709
0.25	0.594	0.734	0.733	0.639	0.620	0.703
0.30	0.579	0.733	0.733	0.627	0.607	0.698
0.40	0.553	0.731	0.731	0.606	0.585	0.688
0.50	0.530	0.729	0.729	0.588	0.565	0.679
0.60	0.510	0.727	0.728	0.573	0.548	0.671
0.70	0.492	0.726	0.726	0.558	0.532	0.664
0.80	0.476	0.724	0.725	0.545	0.518	0.657
0.90	0.461	0.723	0.723	0.533	0.504	0.651
1.00	0.447	0.721	0.722	0.522	0.492	0.645
1.25	0.416	0.718	0.719	0.496	0.464	0.630
1.50	0.390	0.715	0.716	0.474	0.440	0.617
1.75	0.367	0.712	0.713	0.455	0.419	0.605
2.00	0.346	0.709	0.710	0.437	0.400	0.594
2.50	0.311	0.703	0.705	0.406	0.367	0.574
3.00	0.282	0.698	0.700	0.380	0.339	0.555
3.50	0.257	0.693	0.695	0.356	0.314	0.539
4.00	0.235	0.688	0.691	0.336	0.293	0.523
4.50	0.216	0.684	0.686	0.318	0.274	0.509
5.00	0.199	0.679	0.682	0.301	0.257	0.496
5.50	0.184	0.675	0.678	0.286	0.241	0.483
6.00	0.170	0.671	0.674	0.272	0.227	0.471
7.00	0.147	0.663	0.666	0.248	0.202	0.449
8.00	0.128	0.655	0.659	0.227	0.181	0.430
9.00	0.111	0.648	0.652	0.209	0.163	0.412
10.00	0.098	0.640	0.645	0.192	0.147	0.395
12.00	0.075	0.627	0.632	0.165	0.120	0.365
14.00	0.059	0.614	0.620	0.143	0.100	0.339
16.00	0.046	0.602	0.609	0.125	0.083	0.316
18.00	0.036	0.590	0.597	0.110	0.069	0.295
20.00	0.028	0.579	0.587	0.097	0.058	0.277

Table 5, continued.

x (microns)	³⁸ Sr ⁹⁰ ³⁹ Y ⁹⁰	⁴³ Tc ⁹⁹	⁴⁷ Ag ¹¹⁰	⁵¹ Sb ¹²⁴	⁵³ I ¹³¹	⁵⁵ Cs ¹³⁷
0.00	0.745	0.752	0.752	0.747	0.751	0.750
0.05	0.731	0.688	0.617	0.728	0.722	0.724
0.10	0.724	0.659	0.555	0.715	0.707	0.709
0.15	0.718	0.636	0.512	0.705	0.696	0.697
0.20	0.713	0.617	0.479	0.697	0.686	0.688
0.25	0.709	0.601	0.452	0.690	0.677	0.679
0.30	0.705	0.586	0.430	0.683	0.669	0.672
0.40	0.698	0.561	0.394	0.672	0.655	0.658
0.50	0.692	0.540	0.365	0.662	0.643	0.646
0.60	0.686	0.521	0.342	0.653	0.632	0.635
0.70	0.681	0.504	0.323	0.645	0.622	0.625
0.80	0.676	0.488	0.306	0.638	0.612	0.616
0.90	0.671	0.474	0.292	0.631	0.604	0.608
1.00	0.667	0.461	0.279	0.624	0.595	0.600
1.25	0.656	0.432	0.254	0.610	0.577	0.582
1.50	0.647	0.407	0.234	0.597	0.560	0.565
1.75	0.639	0.384	0.218	0.585	0.545	0.551
2.00	0.631	0.365	0.206	0.574	0.531	0.537
2.50	0.617	0.331	0.186	0.555	0.507	0.513
3.00	0.604	0.303	0.171	0.539	0.485	0.492
3.50	0.593	0.278	0.160	0.524	0.466	0.473
4.00	0.582	0.257	0.150	0.511	0.448	0.455
4.50	0.572	0.238	0.143	0.498	0.432	0.440
5.00	0.563	0.222	0.136	0.487	0.418	0.425
5.50	0.554	0.207	0.131	0.477	0.404	0.411
6.00	0.546	0.193	0.126	0.467	0.391	0.398
7.00	0.530	0.170	0.117	0.449	0.368	0.375
8.00	0.516	0.150	0.110	0.433	0.347	0.354
9.00	0.503	0.133	0.103	0.418	0.328	0.336
10.00	0.491	0.119	0.098	0.405	0.311	0.319
12.00	0.469	0.095	0.088	0.382	0.282	0.289
14.00	0.450	0.077	0.079	0.361	0.256	0.263
16.00	0.433	0.062	0.072	0.343	0.234	0.240
18.00	0.417	0.051	0.065	0.327	0.215	0.221
20.00	0.403	0.042	0.060	0.313	0.198	0.203

Table 5, continued.

x (microns)	61Pm147	77Ir192	79Au198	81Tl204
0.00	0.752	0.751	0.749	0.750
0.05	0.665	0.720	0.734	0.727
0.10	0.626	0.705	0.726	0.715
0.15	0.597	0.693	0.719	0.706
0.20	0.573	0.682	0.714	0.699
0.25	0.552	0.673	0.709	0.692
0.30	0.534	0.665	0.704	0.685
0.40	0.504	0.651	0.696	0.674
0.50	0.478	0.638	0.689	0.665
0.60	0.455	0.627	0.682	0.656
0.70	0.435	0.616	0.676	0.648
0.80	0.417	0.607	0.670	0.640
0.90	0.401	0.598	0.665	0.633
1.00	0.386	0.590	0.660	0.627
1.25	0.353	0.571	0.648	0.611
1.50	0.326	0.554	0.637	0.598
1.75	0.302	0.539	0.627	0.586
2.00	0.282	0.525	0.618	0.574
2.50	0.247	0.500	0.601	0.554
3.00	0.219	0.478	0.586	0.536
3.50	0.195	0.459	0.572	0.520
4.00	0.175	0.441	0.559	0.505
4.50	0.158	0.425	0.548	0.491
5.00	0.143	0.410	0.536	0.478
5.50	0.130	0.397	0.526	0.467
6.00	0.119	0.384	0.516	0.455
7.00	0.099	0.361	0.497	0.435
8.00	0.083	0.340	0.481	0.416
9.00	0.071	0.322	0.465	0.399
10.00	0.060	0.305	0.450	0.384
12.00	0.044	0.276	0.424	0.356
14.00	0.032	0.251	0.401	0.332
16.00	0.024	0.229	0.379	0.310
18.00	0.017	0.210	0.360	0.291
20.00	0.013	0.194	0.343	0.274

Table 6. Counting yield $Y_b(x)$ of plane beta(+) sources as a function of the source depth x in an aluminum backing.

x (microns)	6C11	11Na22	21Sc44	26Fe52	27Co56	29Cu64
0.00	0.693	0.693	0.692	0.693	0.692	0.693
0.05	0.692	0.691	0.691	0.692	0.691	0.692
0.10	0.691	0.689	0.691	0.692	0.691	0.692
0.15	0.690	0.687	0.691	0.691	0.691	0.691
0.20	0.689	0.686	0.690	0.690	0.690	0.690
0.25	0.689	0.684	0.690	0.690	0.690	0.689
0.30	0.688	0.682	0.690	0.689	0.690	0.688
0.40	0.686	0.679	0.689	0.688	0.689	0.687
0.50	0.685	0.677	0.689	0.687	0.688	0.685
0.60	0.684	0.674	0.688	0.685	0.688	0.684
0.70	0.682	0.671	0.688	0.684	0.687	0.682
0.80	0.681	0.669	0.687	0.683	0.686	0.681
0.90	0.680	0.666	0.687	0.682	0.686	0.679
1.00	0.679	0.664	0.686	0.681	0.685	0.678
1.25	0.676	0.658	0.685	0.678	0.684	0.674
1.50	0.673	0.652	0.684	0.676	0.682	0.671
1.75	0.670	0.647	0.682	0.673	0.681	0.668
2.00	0.668	0.642	0.681	0.670	0.680	0.664
2.50	0.663	0.632	0.679	0.665	0.677	0.658
3.00	0.658	0.623	0.677	0.661	0.674	0.652
3.50	0.653	0.615	0.675	0.656	0.672	0.646
4.00	0.649	0.607	0.673	0.652	0.669	0.641
4.50	0.645	0.599	0.671	0.647	0.667	0.635
5.00	0.641	0.592	0.669	0.643	0.665	0.630
5.50	0.637	0.584	0.667	0.639	0.663	0.625
6.00	0.633	0.578	0.665	0.635	0.660	0.620
7.00	0.626	0.565	0.661	0.627	0.656	0.610
8.00	0.619	0.552	0.657	0.620	0.652	0.601
9.00	0.612	0.541	0.654	0.613	0.648	0.592
10.00	0.606	0.530	0.650	0.606	0.644	0.584
12.00	0.594	0.510	0.643	0.592	0.636	0.568
14.00	0.583	0.491	0.637	0.580	0.629	0.553
16.00	0.572	0.474	0.630	0.568	0.622	0.539
18.00	0.562	0.458	0.624	0.557	0.615	0.525
20.00	0.552	0.443	0.619	0.546	0.609	0.513

Table 6, continued.

x (microns)	33As74	37Rb84	39Y86	43Tc95	53I119	55Cs125
0.00	0.693	0.692	0.691	0.693	0.689	0.690
0.05	0.692	0.691	0.691	0.693	0.689	0.690
0.10	0.692	0.691	0.691	0.692	0.689	0.690
0.15	0.691	0.691	0.691	0.691	0.689	0.690
0.20	0.691	0.690	0.690	0.690	0.689	0.689
0.25	0.690	0.690	0.690	0.690	0.689	0.689
0.30	0.690	0.689	0.690	0.689	0.689	0.689
0.40	0.689	0.689	0.690	0.688	0.688	0.689
0.50	0.688	0.688	0.689	0.686	0.688	0.689
0.60	0.687	0.687	0.689	0.685	0.688	0.688
0.70	0.687	0.687	0.688	0.684	0.688	0.688
0.80	0.686	0.686	0.688	0.682	0.687	0.688
0.90	0.685	0.685	0.688	0.681	0.687	0.688
1.00	0.684	0.684	0.687	0.680	0.687	0.687
1.25	0.682	0.683	0.686	0.677	0.686	0.687
1.50	0.681	0.681	0.685	0.674	0.686	0.686
1.75	0.679	0.680	0.684	0.671	0.685	0.685
2.00	0.677	0.678	0.683	0.668	0.685	0.685
2.50	0.673	0.675	0.682	0.662	0.684	0.683
3.00	0.670	0.672	0.680	0.657	0.682	0.682
3.50	0.667	0.669	0.678	0.651	0.681	0.681
4.00	0.663	0.666	0.676	0.646	0.680	0.680
4.50	0.660	0.663	0.674	0.641	0.679	0.678
5.00	0.657	0.660	0.673	0.636	0.678	0.677
5.50	0.654	0.658	0.671	0.631	0.677	0.676
6.00	0.651	0.655	0.669	0.627	0.676	0.675
7.00	0.645	0.650	0.666	0.617	0.674	0.672
8.00	0.640	0.645	0.663	0.609	0.672	0.670
9.00	0.634	0.640	0.660	0.600	0.670	0.668
10.00	0.629	0.635	0.657	0.592	0.668	0.665
12.00	0.619	0.626	0.650	0.577	0.664	0.661
14.00	0.609	0.618	0.645	0.562	0.660	0.657
16.00	0.600	0.610	0.639	0.548	0.656	0.652
18.00	0.591	0.602	0.633	0.535	0.652	0.648
20.00	0.582	0.594	0.628	0.523	0.649	0.644

Table 7. Counting yield $Y_b(x)$ of plane beta(+) sources as a function of the source depth x in an iron backing.

x (microns)	6C11	11Na22	21Sc44	26Fe52	27Co56	29Cu64
0.00	0.747	0.745	0.748	0.747	0.748	0.747
0.05	0.744	0.740	0.748	0.745	0.747	0.744
0.10	0.742	0.736	0.747	0.743	0.746	0.742
0.15	0.740	0.732	0.746	0.742	0.745	0.740
0.20	0.739	0.729	0.745	0.740	0.745	0.738
0.25	0.737	0.725	0.745	0.739	0.744	0.736
0.30	0.735	0.722	0.744	0.737	0.743	0.734
0.40	0.732	0.715	0.742	0.734	0.741	0.730
0.50	0.729	0.709	0.741	0.731	0.740	0.726
0.60	0.726	0.703	0.740	0.728	0.738	0.723
0.70	0.723	0.697	0.738	0.725	0.737	0.719
0.80	0.720	0.692	0.737	0.722	0.735	0.716
0.90	0.717	0.687	0.736	0.720	0.734	0.712
1.00	0.715	0.682	0.735	0.717	0.732	0.709
1.25	0.708	0.670	0.732	0.711	0.729	0.701
1.50	0.702	0.658	0.729	0.705	0.725	0.693
1.75	0.697	0.648	0.726	0.699	0.722	0.686
2.00	0.691	0.638	0.723	0.693	0.719	0.679
2.50	0.681	0.620	0.718	0.682	0.713	0.665
3.00	0.671	0.603	0.712	0.672	0.707	0.653
3.50	0.662	0.587	0.707	0.662	0.701	0.641
4.00	0.654	0.572	0.703	0.652	0.696	0.629
4.50	0.645	0.559	0.698	0.643	0.691	0.618
5.00	0.637	0.546	0.693	0.635	0.686	0.608
5.50	0.630	0.534	0.689	0.626	0.681	0.598
6.00	0.623	0.522	0.685	0.619	0.676	0.589
7.00	0.609	0.501	0.676	0.603	0.667	0.570
8.00	0.596	0.481	0.668	0.589	0.658	0.554
9.00	0.584	0.463	0.660	0.576	0.650	0.538
10.00	0.572	0.446	0.653	0.563	0.641	0.523
12.00	0.551	0.416	0.639	0.539	0.626	0.496
14.00	0.531	0.389	0.625	0.517	0.612	0.471
16.00	0.513	0.365	0.613	0.498	0.599	0.449
18.00	0.496	0.344	0.601	0.479	0.586	0.428
20.00	0.481	0.324	0.589	0.462	0.574	0.409

Table 7, continued.

x (microns)	33As74	37Rb84	39Y86	43Tc95	53I119	55Cs125
0.00	0.747	0.748	0.749	0.747	0.749	0.749
0.05	0.746	0.747	0.748	0.745	0.749	0.748
0.10	0.745	0.746	0.747	0.743	0.748	0.748
0.15	0.744	0.745	0.747	0.741	0.748	0.748
0.20	0.743	0.744	0.746	0.740	0.748	0.747
0.25	0.742	0.743	0.746	0.738	0.747	0.747
0.30	0.741	0.742	0.745	0.736	0.747	0.747
0.40	0.738	0.740	0.744	0.733	0.746	0.746
0.50	0.736	0.738	0.743	0.729	0.746	0.745
0.60	0.734	0.736	0.742	0.726	0.745	0.744
0.70	0.732	0.735	0.741	0.723	0.744	0.744
0.80	0.730	0.733	0.740	0.719	0.744	0.743
0.90	0.728	0.731	0.739	0.716	0.743	0.742
1.00	0.726	0.729	0.738	0.713	0.742	0.741
1.25	0.722	0.725	0.735	0.706	0.741	0.740
1.50	0.717	0.721	0.733	0.699	0.739	0.738
1.75	0.713	0.717	0.730	0.692	0.738	0.736
2.00	0.709	0.714	0.728	0.685	0.736	0.734
2.50	0.701	0.706	0.723	0.672	0.733	0.731
3.00	0.693	0.699	0.719	0.660	0.730	0.727
3.50	0.685	0.693	0.714	0.649	0.727	0.724
4.00	0.678	0.686	0.710	0.638	0.724	0.721
4.50	0.671	0.680	0.706	0.627	0.721	0.718
5.00	0.664	0.674	0.701	0.617	0.719	0.715
5.50	0.658	0.668	0.697	0.608	0.716	0.712
6.00	0.651	0.663	0.693	0.598	0.713	0.709
7.00	0.639	0.652	0.686	0.581	0.708	0.703
8.00	0.628	0.642	0.678	0.564	0.703	0.697
9.00	0.617	0.632	0.671	0.549	0.698	0.691
10.00	0.606	0.622	0.664	0.534	0.693	0.686
12.00	0.587	0.605	0.651	0.508	0.683	0.676
14.00	0.568	0.588	0.638	0.483	0.674	0.665
16.00	0.551	0.573	0.626	0.461	0.665	0.656
18.00	0.536	0.559	0.615	0.440	0.657	0.647
20.00	0.520	0.545	0.604	0.421	0.648	0.638

Table 8. Counting yield $Y_b(x/r_{\max})$ of plane beta(-) sources as a function of the scaled depth x/r_{\max} in a beryllium backing.

x/r_{\max}	1H3	6C14	13Al28	15P32	16S35	17Cl36
0.000000	0.627	0.630	0.628	0.630	0.630	0.631
0.000100	0.607	0.613	0.626	0.626	0.607	0.620
0.000150	0.602	0.608	0.625	0.625	0.601	0.618
0.000200	0.597	0.604	0.625	0.624	0.596	0.615
0.000300	0.590	0.597	0.623	0.622	0.587	0.611
0.000400	0.584	0.592	0.622	0.620	0.580	0.607
0.000500	0.578	0.586	0.621	0.618	0.574	0.603
0.000600	0.573	0.582	0.620	0.616	0.568	0.600
0.000800	0.564	0.573	0.618	0.613	0.558	0.595
0.001000	0.556	0.566	0.616	0.610	0.549	0.589
0.001500	0.539	0.549	0.612	0.604	0.531	0.578
0.002000	0.525	0.536	0.607	0.598	0.516	0.569
0.003000	0.502	0.513	0.600	0.588	0.491	0.552
0.004000	0.482	0.495	0.593	0.578	0.471	0.539
0.005000	0.465	0.478	0.586	0.570	0.454	0.526
0.006000	0.450	0.464	0.580	0.562	0.439	0.515
0.008000	0.424	0.439	0.568	0.548	0.413	0.495
0.010000	0.402	0.418	0.557	0.534	0.391	0.478
0.015000	0.357	0.375	0.532	0.505	0.349	0.441
0.020000	0.322	0.342	0.511	0.481	0.316	0.412
0.030000	0.270	0.291	0.474	0.439	0.266	0.364
0.040000	0.232	0.252	0.442	0.404	0.230	0.327
0.050000	0.201	0.222	0.414	0.375	0.201	0.296
0.060000	0.176	0.197	0.389	0.348	0.178	0.270
0.080000	0.138	0.158	0.345	0.303	0.141	0.226
0.100000	0.110	0.128	0.307	0.266	0.114	0.192
0.150000	0.065	0.079	0.229	0.191	0.069	0.129
0.200000	0.040	0.049	0.169	0.137	0.043	0.086
0.250000	0.024	0.031	0.123	0.096	0.027	0.058
0.300000	0.015	0.019	0.087	0.066	0.017	0.038
0.350000	0.009	0.012	0.060	0.045	0.010	0.024
0.400000	0.005	0.007	0.040	0.029	0.006	0.015
0.450000	0.003	0.004	0.026	0.018	0.004	0.009
0.500000	0.002	0.002	0.016	0.011	0.002	0.005

Table 8, continued.

x/r_{\max}	19K43	20Ca45	21Sc49	22Ti51	26Fe59	27Co60
0.000000	0.631	0.630	0.629	0.629	0.630	0.630
0.000100	0.615	0.609	0.626	0.626	0.577	0.610
0.000150	0.610	0.604	0.625	0.624	0.563	0.605
0.000200	0.606	0.600	0.624	0.623	0.552	0.600
0.000300	0.599	0.592	0.622	0.622	0.533	0.593
0.000400	0.593	0.585	0.620	0.620	0.517	0.586
0.000500	0.587	0.579	0.618	0.618	0.503	0.581
0.000600	0.582	0.574	0.617	0.617	0.491	0.575
0.000800	0.573	0.565	0.614	0.614	0.470	0.566
0.001000	0.565	0.557	0.611	0.611	0.452	0.558
0.001500	0.547	0.539	0.605	0.605	0.417	0.542
0.002000	0.532	0.525	0.600	0.600	0.388	0.528
0.003000	0.506	0.502	0.590	0.590	0.345	0.505
0.004000	0.485	0.483	0.581	0.581	0.311	0.486
0.005000	0.466	0.467	0.573	0.573	0.284	0.470
0.006000	0.450	0.452	0.565	0.565	0.261	0.456
0.008000	0.421	0.428	0.552	0.551	0.224	0.431
0.010000	0.396	0.407	0.539	0.539	0.195	0.411
0.015000	0.346	0.365	0.511	0.511	0.143	0.370
0.020000	0.307	0.332	0.487	0.486	0.109	0.337
0.030000	0.247	0.283	0.446	0.446	0.066	0.289
0.040000	0.202	0.246	0.413	0.412	0.042	0.252
0.050000	0.167	0.217	0.383	0.382	0.027	0.222
0.060000	0.138	0.193	0.357	0.356	0.018	0.198
0.080000	0.095	0.155	0.313	0.311	0.007	0.160
0.100000	0.065	0.127	0.275	0.273	0.003	0.131
0.150000	0.025	0.079	0.200	0.198	0.000	0.082
0.200000	0.009	0.050	0.144	0.142	0.000	0.052
0.250000	0.004	0.031	0.102	0.100	0.000	0.033
0.300000	0.002	0.020	0.071	0.069	0.000	0.021
0.350000	0.001	0.012	0.048	0.047	0.000	0.013
0.400000	0.001	0.007	0.031	0.031	0.000	0.008
0.450000	0.000	0.004	0.020	0.019	0.000	0.004
0.500000	0.000	0.002	0.012	0.012	0.000	0.002

Table 8, continued.

x/r_{\max}	29Cu64	38Sr90	39Y90	43Tc99	47Ag110	51Sb124
0.000000	0.631	0.631	0.629	0.630	0.629	0.630
0.000100	0.616	0.617	0.624	0.608	0.476	0.596
0.000150	0.612	0.613	0.623	0.602	0.444	0.587
0.000200	0.609	0.610	0.621	0.597	0.418	0.579
0.000300	0.603	0.604	0.619	0.589	0.381	0.566
0.000400	0.598	0.599	0.617	0.582	0.353	0.556
0.000500	0.594	0.595	0.615	0.576	0.330	0.547
0.000600	0.590	0.591	0.613	0.570	0.312	0.539
0.000800	0.583	0.585	0.610	0.560	0.282	0.525
0.001000	0.576	0.579	0.607	0.552	0.260	0.512
0.001500	0.563	0.566	0.600	0.534	0.220	0.488
0.002000	0.552	0.556	0.594	0.519	0.194	0.468
0.003000	0.533	0.538	0.584	0.495	0.161	0.437
0.004000	0.517	0.523	0.574	0.475	0.142	0.412
0.005000	0.503	0.510	0.566	0.458	0.128	0.392
0.006000	0.490	0.498	0.558	0.443	0.119	0.375
0.008000	0.469	0.478	0.544	0.418	0.106	0.346
0.010000	0.450	0.461	0.531	0.397	0.097	0.322
0.015000	0.412	0.424	0.503	0.355	0.079	0.278
0.020000	0.381	0.395	0.479	0.322	0.066	0.245
0.030000	0.333	0.350	0.439	0.273	0.048	0.199
0.040000	0.296	0.314	0.406	0.237	0.035	0.166
0.050000	0.266	0.285	0.377	0.208	0.026	0.142
0.060000	0.240	0.260	0.352	0.185	0.020	0.124
0.080000	0.199	0.220	0.309	0.148	0.011	0.098
0.100000	0.167	0.188	0.273	0.121	0.006	0.081
0.150000	0.109	0.128	0.203	0.075	0.002	0.054
0.200000	0.072	0.089	0.150	0.047	0.001	0.038
0.250000	0.047	0.060	0.109	0.030	0.001	0.026
0.300000	0.031	0.040	0.078	0.019	0.000	0.018
0.350000	0.019	0.026	0.055	0.011	0.000	0.012
0.400000	0.012	0.017	0.037	0.007	0.000	0.007
0.450000	0.007	0.010	0.024	0.004	0.000	0.005
0.500000	0.004	0.006	0.015	0.002	0.000	0.003

Table 8, continued.

x/r_{\max}	53I131	55Cs137	61Pm147	77Ir192	79Au198	81Tl204
0.000000	0.630	0.630	0.630	0.630	0.631	0.631
0.000100	0.609	0.603	0.605	0.610	0.618	0.614
0.000150	0.603	0.596	0.599	0.605	0.614	0.609
0.000200	0.598	0.589	0.593	0.600	0.611	0.606
0.000300	0.589	0.579	0.584	0.592	0.605	0.599
0.000400	0.582	0.570	0.576	0.586	0.601	0.594
0.000500	0.576	0.562	0.570	0.580	0.597	0.589
0.000600	0.570	0.555	0.564	0.575	0.593	0.585
0.000800	0.560	0.543	0.553	0.565	0.587	0.577
0.001000	0.551	0.532	0.544	0.557	0.581	0.570
0.001500	0.533	0.510	0.524	0.540	0.568	0.556
0.002000	0.517	0.491	0.508	0.526	0.557	0.544
0.003000	0.492	0.461	0.483	0.502	0.539	0.524
0.004000	0.471	0.437	0.462	0.483	0.524	0.507
0.005000	0.453	0.417	0.444	0.467	0.511	0.493
0.006000	0.438	0.399	0.429	0.452	0.499	0.481
0.008000	0.411	0.368	0.402	0.428	0.478	0.459
0.010000	0.388	0.343	0.380	0.407	0.460	0.440
0.015000	0.343	0.293	0.337	0.365	0.423	0.402
0.020000	0.309	0.255	0.304	0.332	0.394	0.372
0.030000	0.257	0.200	0.255	0.282	0.347	0.326
0.040000	0.219	0.160	0.219	0.245	0.310	0.290
0.050000	0.188	0.130	0.191	0.216	0.280	0.261
0.060000	0.164	0.105	0.169	0.192	0.254	0.237
0.080000	0.126	0.070	0.133	0.154	0.213	0.198
0.100000	0.097	0.047	0.108	0.125	0.180	0.168
0.150000	0.052	0.017	0.065	0.077	0.120	0.113
0.200000	0.028	0.007	0.040	0.048	0.081	0.078
0.250000	0.014	0.004	0.025	0.030	0.054	0.053
0.300000	0.007	0.002	0.015	0.018	0.035	0.035
0.350000	0.003	0.002	0.009	0.011	0.023	0.023
0.400000	0.001	0.001	0.005	0.006	0.014	0.015
0.450000	0.000	0.001	0.003	0.004	0.009	0.009
0.500000	0.000	0.000	0.002	0.002	0.005	0.005

Table 9. Counting yield $Y_b(x/r_{\max})$ of plane beta(-) sources as a function of the scaled depth x/r_{\max} in a carbon backing.

x/r_{\max}	1H3	6C14	13Al28	15P32	16S35	17Cl36
0.000000	0.648	0.650	0.645	0.648	0.650	0.650
0.000100	0.627	0.632	0.643	0.644	0.626	0.639
0.000150	0.621	0.627	0.642	0.643	0.619	0.636
0.000200	0.617	0.623	0.642	0.641	0.614	0.633
0.000300	0.609	0.615	0.640	0.639	0.605	0.628
0.000400	0.602	0.609	0.639	0.637	0.597	0.624
0.000500	0.596	0.604	0.638	0.635	0.590	0.621
0.000600	0.591	0.598	0.637	0.633	0.584	0.617
0.000800	0.581	0.589	0.635	0.630	0.573	0.611
0.001000	0.573	0.581	0.632	0.627	0.564	0.606
0.001500	0.554	0.564	0.627	0.620	0.544	0.594
0.002000	0.539	0.549	0.623	0.614	0.528	0.583
0.003000	0.514	0.525	0.615	0.603	0.502	0.566
0.004000	0.493	0.505	0.607	0.592	0.480	0.551
0.005000	0.475	0.487	0.600	0.583	0.462	0.537
0.006000	0.459	0.472	0.593	0.575	0.446	0.525
0.008000	0.431	0.445	0.580	0.559	0.418	0.504
0.010000	0.407	0.423	0.568	0.544	0.395	0.485
0.015000	0.359	0.377	0.542	0.513	0.350	0.446
0.020000	0.323	0.342	0.518	0.486	0.315	0.414
0.030000	0.268	0.288	0.478	0.442	0.263	0.364
0.040000	0.227	0.248	0.444	0.404	0.225	0.324
0.050000	0.196	0.216	0.414	0.373	0.196	0.292
0.060000	0.170	0.191	0.387	0.345	0.172	0.264
0.080000	0.132	0.150	0.340	0.297	0.135	0.219
0.100000	0.104	0.121	0.300	0.257	0.107	0.183
0.150000	0.059	0.072	0.219	0.181	0.063	0.119
0.200000	0.035	0.043	0.158	0.126	0.038	0.078
0.250000	0.021	0.026	0.112	0.086	0.023	0.050
0.300000	0.012	0.016	0.077	0.057	0.014	0.032
0.350000	0.007	0.009	0.051	0.037	0.008	0.020
0.400000	0.004	0.005	0.033	0.023	0.004	0.012
0.450000	0.002	0.003	0.021	0.014	0.002	0.007
0.500000	0.001	0.002	0.012	0.008	0.001	0.004

Table 9, continued.

x/r_{\max}	19K43	20Ca45	21Sc49	22Ti51	26Fe59	27Co60
0.000000	0.650	0.650	0.648	0.647	0.650	0.650
0.000100	0.633	0.628	0.644	0.643	0.593	0.629
0.000150	0.628	0.623	0.642	0.642	0.578	0.623
0.000200	0.623	0.618	0.641	0.641	0.566	0.618
0.000300	0.616	0.609	0.639	0.639	0.545	0.610
0.000400	0.609	0.602	0.637	0.637	0.529	0.603
0.000500	0.603	0.596	0.635	0.635	0.514	0.597
0.000600	0.598	0.590	0.634	0.633	0.501	0.591
0.000800	0.588	0.580	0.631	0.630	0.479	0.582
0.001000	0.579	0.571	0.628	0.628	0.460	0.573
0.001500	0.560	0.553	0.621	0.621	0.422	0.555
0.002000	0.543	0.538	0.615	0.615	0.392	0.540
0.003000	0.516	0.513	0.605	0.604	0.345	0.516
0.004000	0.493	0.493	0.595	0.595	0.310	0.496
0.005000	0.473	0.475	0.586	0.586	0.282	0.479
0.006000	0.455	0.460	0.578	0.578	0.258	0.463
0.008000	0.424	0.433	0.563	0.563	0.219	0.438
0.010000	0.398	0.411	0.549	0.549	0.190	0.415
0.015000	0.344	0.367	0.519	0.518	0.137	0.372
0.020000	0.303	0.332	0.493	0.492	0.103	0.338
0.030000	0.240	0.281	0.449	0.449	0.061	0.286
0.040000	0.194	0.242	0.413	0.412	0.038	0.248
0.050000	0.158	0.212	0.382	0.380	0.024	0.217
0.060000	0.129	0.187	0.354	0.353	0.015	0.192
0.080000	0.087	0.148	0.307	0.305	0.006	0.154
0.100000	0.058	0.120	0.267	0.265	0.002	0.124
0.150000	0.020	0.072	0.190	0.187	0.000	0.076
0.200000	0.007	0.044	0.133	0.131	0.000	0.047
0.250000	0.003	0.027	0.092	0.090	0.000	0.029
0.300000	0.001	0.016	0.062	0.060	0.000	0.017
0.350000	0.001	0.010	0.040	0.039	0.000	0.010
0.400000	0.001	0.005	0.025	0.025	0.000	0.006
0.450000	0.000	0.003	0.015	0.015	0.000	0.003
0.500000	0.000	0.002	0.009	0.009	0.000	0.002

Table 9, continued.

x/r_{\max}	29Cu64	38Sr90	39Y90	43Tc99	47Ag110	51Sb124
0.000000	0.650	0.650	0.647	0.650	0.650	0.649
0.000100	0.635	0.635	0.642	0.627	0.486	0.612
0.000150	0.631	0.631	0.640	0.620	0.451	0.603
0.000200	0.627	0.628	0.639	0.615	0.425	0.594
0.000300	0.621	0.622	0.636	0.606	0.385	0.581
0.000400	0.615	0.617	0.634	0.599	0.356	0.570
0.000500	0.611	0.612	0.632	0.592	0.333	0.560
0.000600	0.607	0.608	0.630	0.586	0.313	0.551
0.000800	0.599	0.601	0.626	0.575	0.283	0.536
0.001000	0.592	0.595	0.623	0.566	0.260	0.523
0.001500	0.578	0.581	0.616	0.547	0.219	0.497
0.002000	0.565	0.570	0.609	0.531	0.193	0.476
0.003000	0.545	0.551	0.598	0.505	0.161	0.443
0.004000	0.528	0.535	0.588	0.484	0.141	0.417
0.005000	0.513	0.521	0.578	0.466	0.128	0.396
0.006000	0.500	0.508	0.570	0.450	0.119	0.377
0.008000	0.476	0.486	0.554	0.424	0.106	0.347
0.010000	0.456	0.468	0.540	0.401	0.096	0.322
0.015000	0.415	0.429	0.510	0.356	0.078	0.276
0.020000	0.383	0.398	0.485	0.322	0.064	0.243
0.030000	0.332	0.350	0.442	0.271	0.045	0.195
0.040000	0.293	0.312	0.406	0.233	0.033	0.162
0.050000	0.261	0.281	0.376	0.203	0.024	0.138
0.060000	0.234	0.255	0.349	0.179	0.018	0.120
0.080000	0.192	0.213	0.304	0.142	0.010	0.094
0.100000	0.159	0.180	0.266	0.114	0.005	0.077
0.150000	0.101	0.120	0.193	0.068	0.001	0.051
0.200000	0.065	0.080	0.139	0.042	0.001	0.034
0.250000	0.041	0.053	0.099	0.025	0.000	0.023
0.300000	0.026	0.034	0.069	0.015	0.000	0.015
0.350000	0.016	0.022	0.047	0.009	0.000	0.010
0.400000	0.009	0.013	0.031	0.005	0.000	0.006
0.450000	0.005	0.008	0.019	0.003	0.000	0.004
0.500000	0.003	0.004	0.012	0.002	0.000	0.002
0.700000	0.000	0.000	0.001	0.000	0.000	0.000

Table 9, continued.

x/r_{\max}	53I131	55Cs137	61Pm147	77Ir192	79Au198	81Tl204
0.000000	0.650	0.650	0.650	0.650	0.650	0.650
0.000100	0.627	0.621	0.624	0.628	0.636	0.632
0.000150	0.620	0.613	0.617	0.623	0.632	0.627
0.000200	0.615	0.606	0.611	0.618	0.629	0.623
0.000300	0.606	0.595	0.601	0.609	0.623	0.617
0.000400	0.598	0.585	0.593	0.602	0.618	0.611
0.000500	0.591	0.577	0.586	0.596	0.614	0.605
0.000600	0.585	0.570	0.579	0.590	0.610	0.601
0.000800	0.575	0.556	0.568	0.580	0.603	0.592
0.001000	0.565	0.545	0.558	0.572	0.596	0.585
0.001500	0.545	0.521	0.537	0.553	0.583	0.570
0.002000	0.529	0.501	0.520	0.538	0.571	0.557
0.003000	0.501	0.469	0.493	0.513	0.552	0.536
0.004000	0.479	0.443	0.470	0.493	0.536	0.518
0.005000	0.460	0.421	0.451	0.475	0.521	0.503
0.006000	0.444	0.402	0.435	0.460	0.509	0.489
0.008000	0.415	0.370	0.407	0.433	0.486	0.466
0.010000	0.391	0.343	0.384	0.411	0.467	0.446
0.015000	0.344	0.290	0.338	0.366	0.427	0.406
0.020000	0.307	0.251	0.303	0.332	0.396	0.374
0.030000	0.253	0.194	0.252	0.280	0.346	0.325
0.040000	0.213	0.153	0.215	0.241	0.307	0.287
0.050000	0.182	0.122	0.186	0.211	0.275	0.257
0.060000	0.157	0.098	0.163	0.186	0.249	0.232
0.080000	0.118	0.063	0.127	0.147	0.206	0.192
0.100000	0.090	0.041	0.101	0.118	0.172	0.161
0.150000	0.047	0.014	0.059	0.070	0.112	0.106
0.200000	0.024	0.006	0.036	0.042	0.073	0.070
0.250000	0.011	0.003	0.021	0.025	0.047	0.046
0.300000	0.005	0.002	0.013	0.015	0.030	0.030
0.350000	0.002	0.001	0.007	0.009	0.018	0.019
0.400000	0.001	0.001	0.004	0.005	0.011	0.012
0.450000	0.000	0.001	0.002	0.003	0.006	0.007
0.500000	0.000	0.000	0.001	0.001	0.004	0.004

Table 10. Counting yield $Y_b(x/r_{\max})$ of plane beta(-) sources as a function of the scaled depth x/r_{\max} in an aluminum backing.

x/r_{\max}	1H3	6C14	13Al28	15P32	16S35	17Cl36
0.000000	0.701	0.701	0.689	0.695	0.701	0.699
0.000100	0.677	0.681	0.687	0.690	0.674	0.687
0.000150	0.671	0.675	0.686	0.688	0.666	0.683
0.000200	0.666	0.670	0.685	0.687	0.660	0.680
0.000300	0.657	0.661	0.683	0.684	0.649	0.674
0.000400	0.649	0.654	0.682	0.682	0.640	0.669
0.000500	0.642	0.647	0.680	0.680	0.632	0.665
0.000600	0.636	0.641	0.679	0.678	0.625	0.661
0.000800	0.625	0.630	0.676	0.674	0.612	0.654
0.001000	0.615	0.620	0.674	0.670	0.601	0.647
0.001500	0.595	0.599	0.668	0.661	0.577	0.633
0.002000	0.577	0.582	0.663	0.654	0.558	0.620
0.003000	0.547	0.553	0.652	0.640	0.527	0.599
0.004000	0.522	0.529	0.643	0.628	0.501	0.581
0.005000	0.501	0.508	0.634	0.617	0.480	0.565
0.006000	0.482	0.490	0.626	0.606	0.461	0.551
0.008000	0.449	0.459	0.610	0.587	0.429	0.525
0.010000	0.421	0.432	0.596	0.570	0.402	0.503
0.015000	0.366	0.379	0.563	0.532	0.350	0.457
0.020000	0.323	0.338	0.535	0.500	0.310	0.419
0.030000	0.260	0.277	0.486	0.446	0.252	0.360
0.040000	0.215	0.233	0.445	0.401	0.211	0.315
0.050000	0.181	0.198	0.409	0.364	0.179	0.277
0.060000	0.154	0.171	0.377	0.332	0.153	0.246
0.080000	0.113	0.129	0.323	0.278	0.115	0.197
0.100000	0.086	0.100	0.278	0.234	0.088	0.159
0.150000	0.044	0.054	0.191	0.153	0.047	0.095
0.200000	0.023	0.029	0.129	0.098	0.026	0.057
0.250000	0.012	0.016	0.084	0.062	0.014	0.033
0.300000	0.007	0.008	0.053	0.037	0.007	0.019
0.350000	0.003	0.004	0.032	0.022	0.004	0.010
0.400000	0.002	0.002	0.019	0.012	0.002	0.005
0.450000	0.001	0.001	0.010	0.006	0.001	0.003
0.500000	0.000	0.000	0.005	0.003	0.000	0.001

Table 10. continued.

x/r_{\max}	19K43	20Ca45	21Sc49	22Ti51	26Fe59	27Co60
0.000000	0.699	0.701	0.694	0.693	0.701	0.701
0.000100	0.679	0.676	0.689	0.689	0.635	0.676
0.000150	0.673	0.669	0.688	0.687	0.617	0.669
0.000200	0.668	0.663	0.686	0.686	0.603	0.664
0.000300	0.659	0.653	0.684	0.683	0.579	0.654
0.000400	0.651	0.645	0.681	0.681	0.559	0.646
0.000500	0.644	0.637	0.679	0.679	0.542	0.638
0.000600	0.637	0.631	0.677	0.677	0.527	0.632
0.000800	0.626	0.619	0.674	0.673	0.502	0.620
0.001000	0.615	0.608	0.670	0.670	0.480	0.610
0.001500	0.593	0.587	0.662	0.662	0.436	0.589
0.002000	0.573	0.569	0.655	0.655	0.401	0.571
0.003000	0.541	0.539	0.642	0.642	0.349	0.542
0.004000	0.514	0.515	0.631	0.630	0.309	0.519
0.005000	0.490	0.495	0.620	0.620	0.277	0.499
0.006000	0.469	0.477	0.610	0.610	0.250	0.481
0.008000	0.433	0.446	0.592	0.591	0.209	0.450
0.010000	0.402	0.420	0.575	0.575	0.177	0.425
0.015000	0.340	0.368	0.539	0.538	0.123	0.374
0.020000	0.293	0.329	0.507	0.506	0.088	0.335
0.030000	0.223	0.271	0.455	0.453	0.049	0.277
0.040000	0.174	0.228	0.411	0.410	0.028	0.234
0.050000	0.137	0.195	0.374	0.373	0.017	0.201
0.060000	0.108	0.169	0.342	0.340	0.010	0.174
0.080000	0.068	0.128	0.288	0.286	0.004	0.133
0.100000	0.042	0.100	0.244	0.242	0.001	0.104
0.150000	0.013	0.054	0.162	0.160	0.000	0.058
0.200000	0.004	0.030	0.105	0.104	0.000	0.032
0.250000	0.002	0.016	0.067	0.065	0.000	0.018
0.300000	0.001	0.009	0.041	0.040	0.000	0.010
0.350000	0.000	0.005	0.024	0.024	0.000	0.005
0.400000	0.000	0.002	0.014	0.013	0.000	0.002
0.450000	0.000	0.001	0.007	0.007	0.000	0.001
0.500000	0.000	0.001	0.004	0.004	0.000	0.001

Table 10, continued.

x/rmax	29Cu64	38Sr90	39Y90	43Tc99	47Ag110	51Sb124
0.000000	0.700	0.700	0.692	0.701	0.701	0.698
0.000100	0.682	0.683	0.686	0.674	0.513	0.655
0.000150	0.677	0.678	0.684	0.666	0.473	0.644
0.000200	0.673	0.674	0.683	0.660	0.444	0.634
0.000300	0.665	0.667	0.680	0.649	0.399	0.618
0.000400	0.659	0.661	0.677	0.641	0.366	0.605
0.000500	0.654	0.655	0.675	0.633	0.340	0.594
0.000600	0.649	0.651	0.672	0.626	0.319	0.584
0.000800	0.640	0.642	0.668	0.613	0.287	0.567
0.001000	0.632	0.635	0.664	0.602	0.262	0.552
0.001500	0.614	0.618	0.655	0.580	0.220	0.522
0.002000	0.600	0.605	0.648	0.561	0.193	0.498
0.003000	0.576	0.582	0.634	0.530	0.161	0.460
0.004000	0.555	0.563	0.622	0.506	0.141	0.430
0.005000	0.538	0.547	0.611	0.484	0.128	0.406
0.006000	0.522	0.532	0.601	0.466	0.119	0.385
0.008000	0.494	0.506	0.582	0.435	0.105	0.351
0.010000	0.470	0.484	0.565	0.408	0.094	0.324
0.015000	0.422	0.439	0.529	0.357	0.073	0.273
0.020000	0.384	0.403	0.498	0.318	0.059	0.236
0.030000	0.326	0.346	0.447	0.260	0.040	0.186
0.040000	0.281	0.303	0.405	0.219	0.027	0.152
0.050000	0.246	0.268	0.370	0.187	0.019	0.128
0.060000	0.216	0.239	0.339	0.161	0.013	0.110
0.080000	0.171	0.193	0.287	0.122	0.007	0.085
0.100000	0.136	0.157	0.246	0.094	0.003	0.069
0.150000	0.079	0.096	0.168	0.052	0.001	0.043
0.200000	0.046	0.059	0.113	0.029	0.001	0.027
0.250000	0.026	0.035	0.075	0.016	0.000	0.017
0.300000	0.015	0.020	0.048	0.008	0.000	0.010
0.350000	0.008	0.011	0.029	0.004	0.000	0.006
0.400000	0.004	0.006	0.017	0.002	0.000	0.003
0.450000	0.002	0.003	0.010	0.001	0.000	0.002
0.500000	0.001	0.001	0.005	0.000	0.000	0.001

Table 11. Counting yield $Y_b(x/r_{\max})$ of plane beta(-) sources as a function of the scaled depth x/r_{\max} in an iron backing.

x/r_{\max}	1H3	6C14	13Al28	15P32	16S35	17Cl36
0.000000	0.752	0.752	0.735	0.743	0.752	0.750
0.000100	0.725	0.729	0.732	0.737	0.721	0.735
0.000150	0.718	0.722	0.731	0.735	0.712	0.730
0.000200	0.712	0.716	0.730	0.733	0.705	0.726
0.000300	0.703	0.706	0.728	0.730	0.692	0.720
0.000400	0.694	0.697	0.726	0.727	0.682	0.714
0.000500	0.686	0.689	0.724	0.724	0.672	0.708
0.000600	0.679	0.682	0.722	0.722	0.663	0.703
0.000800	0.667	0.669	0.719	0.717	0.648	0.695
0.001000	0.656	0.657	0.716	0.712	0.635	0.687
0.001500	0.632	0.632	0.709	0.702	0.607	0.669
0.002000	0.611	0.612	0.702	0.693	0.585	0.654
0.003000	0.577	0.577	0.690	0.676	0.547	0.628
0.004000	0.548	0.548	0.678	0.661	0.517	0.606
0.005000	0.522	0.523	0.667	0.647	0.492	0.587
0.006000	0.500	0.502	0.657	0.634	0.470	0.569
0.008000	0.461	0.464	0.638	0.611	0.432	0.539
0.010000	0.429	0.433	0.620	0.589	0.401	0.512
0.015000	0.364	0.371	0.580	0.543	0.341	0.456
0.020000	0.316	0.324	0.544	0.503	0.296	0.411
0.030000	0.245	0.255	0.484	0.437	0.231	0.342
0.040000	0.196	0.206	0.433	0.384	0.186	0.289
0.050000	0.160	0.170	0.389	0.339	0.152	0.248
0.060000	0.132	0.142	0.351	0.301	0.126	0.214
0.080000	0.092	0.101	0.288	0.240	0.089	0.162
0.100000	0.065	0.073	0.238	0.192	0.064	0.124
0.150000	0.030	0.034	0.147	0.111	0.030	0.064
0.200000	0.014	0.016	0.089	0.063	0.014	0.033
0.250000	0.006	0.007	0.052	0.035	0.006	0.017
0.300000	0.003	0.003	0.029	0.018	0.003	0.008
0.350000	0.001	0.001	0.015	0.009	0.001	0.004
0.400000	0.001	0.001	0.007	0.004	0.001	0.002
0.450000	0.000	0.000	0.004	0.002	0.000	0.001
0.500000	0.000	0.000	0.001	0.001	0.000	0.000

Table 11, continued.

x/r_{\max}	19K43	20Ca45	21Sc49	22Ti51	26Fe59	27Co60
0.000000	0.749	0.752	0.741	0.740	0.751	0.752
0.000100	0.725	0.723	0.735	0.735	0.674	0.724
0.000150	0.718	0.715	0.734	0.733	0.653	0.715
0.000200	0.712	0.708	0.732	0.731	0.636	0.709
0.000300	0.701	0.697	0.729	0.728	0.608	0.697
0.000400	0.691	0.687	0.726	0.725	0.584	0.687
0.000500	0.683	0.678	0.724	0.723	0.564	0.679
0.000600	0.675	0.670	0.721	0.720	0.547	0.671
0.000800	0.661	0.656	0.717	0.716	0.516	0.657
0.001000	0.648	0.643	0.712	0.712	0.491	0.645
0.001500	0.621	0.617	0.703	0.702	0.439	0.620
0.002000	0.597	0.596	0.694	0.693	0.399	0.599
0.003000	0.558	0.561	0.678	0.678	0.339	0.564
0.004000	0.525	0.532	0.664	0.664	0.294	0.536
0.005000	0.497	0.508	0.651	0.650	0.258	0.512
0.006000	0.472	0.486	0.639	0.638	0.230	0.491
0.008000	0.428	0.450	0.616	0.615	0.185	0.455
0.010000	0.392	0.419	0.596	0.595	0.152	0.424
0.015000	0.320	0.359	0.551	0.550	0.099	0.365
0.020000	0.267	0.314	0.512	0.511	0.067	0.320
0.030000	0.191	0.249	0.448	0.446	0.033	0.255
0.040000	0.140	0.202	0.395	0.393	0.017	0.208
0.050000	0.104	0.167	0.351	0.349	0.009	0.173
0.060000	0.078	0.140	0.313	0.311	0.005	0.145
0.080000	0.043	0.100	0.251	0.249	0.001	0.105
0.100000	0.024	0.073	0.203	0.201	0.001	0.077
0.150000	0.006	0.035	0.119	0.118	0.000	0.037
0.200000	0.002	0.016	0.069	0.068	0.000	0.018
0.250000	0.001	0.008	0.039	0.038	0.000	0.008
0.300000	0.000	0.003	0.021	0.020	0.000	0.004
0.350000	0.000	0.001	0.010	0.010	0.000	0.002
0.400000	0.000	0.001	0.005	0.005	0.000	0.001
0.450000	0.000	0.000	0.002	0.002	0.000	0.000
0.500000	0.000	0.000	0.001	0.001	0.000	0.000

Table 11, continued.

x/r_{\max}	29Cu64	38Sr90	39Y90	43Tc99	47Ag110	51Sb124
0.000000	0.750	0.750	0.739	0.752	0.752	0.748
0.000100	0.730	0.730	0.732	0.721	0.534	0.697
0.000150	0.724	0.725	0.730	0.712	0.489	0.683
0.000200	0.719	0.720	0.728	0.705	0.455	0.672
0.000300	0.710	0.711	0.724	0.692	0.405	0.654
0.000400	0.702	0.704	0.721	0.682	0.368	0.638
0.000500	0.696	0.698	0.718	0.672	0.340	0.625
0.000600	0.689	0.692	0.715	0.664	0.317	0.613
0.000800	0.678	0.682	0.710	0.649	0.282	0.592
0.001000	0.669	0.673	0.705	0.636	0.256	0.575
0.001500	0.648	0.653	0.695	0.609	0.214	0.540
0.002000	0.631	0.637	0.685	0.586	0.188	0.512
0.003000	0.601	0.610	0.669	0.550	0.156	0.468
0.004000	0.577	0.587	0.654	0.521	0.138	0.434
0.005000	0.555	0.567	0.640	0.496	0.125	0.406
0.006000	0.536	0.549	0.628	0.474	0.115	0.383
0.008000	0.503	0.518	0.605	0.437	0.099	0.345
0.010000	0.475	0.492	0.585	0.407	0.087	0.314
0.015000	0.418	0.438	0.540	0.347	0.064	0.259
0.020000	0.373	0.395	0.503	0.303	0.049	0.220
0.030000	0.306	0.329	0.441	0.238	0.030	0.168
0.040000	0.256	0.280	0.391	0.193	0.019	0.134
0.050000	0.217	0.241	0.348	0.159	0.012	0.111
0.060000	0.185	0.209	0.312	0.133	0.008	0.094
0.080000	0.138	0.159	0.254	0.095	0.004	0.071
0.100000	0.104	0.123	0.208	0.069	0.002	0.055
0.150000	0.053	0.066	0.128	0.033	0.001	0.031
0.200000	0.027	0.035	0.078	0.016	0.000	0.018
0.250000	0.013	0.018	0.045	0.007	0.000	0.010
0.300000	0.006	0.009	0.025	0.003	0.000	0.005
0.350000	0.003	0.004	0.014	0.001	0.000	0.002
0.400000	0.001	0.002	0.007	0.001	0.000	0.001
0.450000	0.000	0.001	0.003	0.000	0.000	0.001
0.500000	0.000	0.000	0.001	0.000	0.000	0.000

Table 12. Counting yield $Y_b(x/r_{\max})$ of plane beta(-) sources as a function of the scaled depth x/r_{\max} in sand (silica, SiO_2).

x/r_{\max}	1H3	6C14	13Al28	15P32	16S35	17Cl36
0.000000	0.688	0.688	0.678	0.683	0.688	0.687
0.000100	0.664	0.668	0.676	0.678	0.661	0.674
0.000150	0.658	0.663	0.675	0.677	0.654	0.671
0.000200	0.653	0.658	0.674	0.675	0.648	0.668
0.000300	0.645	0.650	0.672	0.673	0.638	0.663
0.000400	0.637	0.642	0.671	0.670	0.629	0.658
0.000500	0.631	0.636	0.669	0.668	0.621	0.654
0.000600	0.625	0.630	0.668	0.666	0.614	0.650
0.000800	0.614	0.620	0.666	0.662	0.602	0.643
0.001000	0.605	0.610	0.663	0.659	0.591	0.637
0.001500	0.584	0.591	0.658	0.651	0.569	0.623
0.002000	0.567	0.574	0.652	0.644	0.551	0.611
0.003000	0.539	0.546	0.643	0.631	0.521	0.591
0.004000	0.515	0.523	0.634	0.619	0.496	0.574
0.005000	0.495	0.504	0.625	0.608	0.476	0.559
0.006000	0.476	0.486	0.617	0.599	0.458	0.545
0.008000	0.445	0.456	0.603	0.580	0.427	0.521
0.010000	0.418	0.431	0.589	0.564	0.401	0.499
0.015000	0.365	0.380	0.558	0.528	0.351	0.455
0.020000	0.324	0.340	0.531	0.497	0.313	0.419
0.030000	0.263	0.281	0.484	0.445	0.256	0.363
0.040000	0.219	0.238	0.445	0.403	0.215	0.319
0.050000	0.185	0.204	0.411	0.367	0.184	0.283
0.060000	0.159	0.177	0.380	0.336	0.159	0.252
0.080000	0.119	0.136	0.328	0.284	0.121	0.204
0.100000	0.091	0.106	0.285	0.241	0.094	0.167
0.150000	0.048	0.058	0.199	0.161	0.052	0.102
0.200000	0.026	0.033	0.136	0.106	0.029	0.063
0.250000	0.014	0.018	0.091	0.068	0.016	0.038
0.300000	0.008	0.010	0.059	0.042	0.009	0.022
0.350000	0.004	0.005	0.037	0.025	0.005	0.012
0.400000	0.002	0.003	0.022	0.014	0.002	0.007
0.450000	0.001	0.001	0.012	0.008	0.001	0.003
0.500000	0.001	0.001	0.007	0.004	0.001	0.002

Table 12, continued.

x/r_{\max}	19K43	20Ca45	21Sc49	22Ti51	26Fe59	27Co60
0.000000	0.686	0.688	0.682	0.681	0.688	0.688
0.000100	0.667	0.664	0.677	0.677	0.624	0.664
0.000150	0.661	0.657	0.676	0.675	0.607	0.658
0.000200	0.656	0.651	0.674	0.674	0.594	0.652
0.000300	0.648	0.642	0.672	0.672	0.571	0.643
0.000400	0.640	0.634	0.670	0.670	0.552	0.635
0.000500	0.634	0.627	0.668	0.668	0.536	0.628
0.000600	0.627	0.621	0.666	0.666	0.521	0.622
0.000800	0.616	0.609	0.663	0.662	0.497	0.611
0.001000	0.606	0.599	0.659	0.659	0.476	0.601
0.001500	0.585	0.578	0.652	0.651	0.433	0.581
0.002000	0.566	0.561	0.645	0.645	0.400	0.564
0.003000	0.535	0.533	0.633	0.632	0.349	0.536
0.004000	0.509	0.510	0.622	0.621	0.310	0.514
0.005000	0.486	0.490	0.612	0.611	0.279	0.494
0.006000	0.466	0.473	0.602	0.602	0.254	0.477
0.008000	0.431	0.443	0.585	0.584	0.213	0.448
0.010000	0.402	0.419	0.569	0.568	0.182	0.424
0.015000	0.342	0.369	0.534	0.533	0.127	0.375
0.020000	0.297	0.331	0.504	0.503	0.093	0.337
0.030000	0.229	0.274	0.454	0.453	0.052	0.280
0.040000	0.180	0.233	0.413	0.411	0.031	0.239
0.050000	0.143	0.200	0.377	0.376	0.019	0.206
0.060000	0.114	0.174	0.346	0.345	0.011	0.180
0.080000	0.073	0.134	0.294	0.292	0.004	0.140
0.100000	0.046	0.105	0.251	0.249	0.001	0.110
0.150000	0.014	0.059	0.169	0.167	0.000	0.063
0.200000	0.005	0.034	0.113	0.111	0.000	0.036
0.250000	0.002	0.019	0.073	0.072	0.000	0.021
0.300000	0.001	0.011	0.046	0.045	0.000	0.012
0.350000	0.001	0.006	0.028	0.027	0.000	0.006
0.400000	0.000	0.003	0.016	0.016	0.000	0.003
0.450000	0.000	0.001	0.009	0.009	0.000	0.002
0.500000	0.000	0.001	0.004	0.004	0.000	0.001

Table 12, continued.

x/r_{\max}	29Cu64	38Sr90	39Y90	43Tc99	47Ag110	51Sb124
0.000000	0.687	0.687	0.681	0.688	0.688	0.685
0.000100	0.670	0.670	0.675	0.662	0.507	0.644
0.000150	0.665	0.666	0.673	0.655	0.469	0.633
0.000200	0.661	0.662	0.671	0.649	0.440	0.624
0.000300	0.654	0.655	0.669	0.638	0.397	0.609
0.000400	0.648	0.650	0.666	0.630	0.365	0.596
0.000500	0.643	0.645	0.664	0.623	0.340	0.586
0.000600	0.638	0.640	0.661	0.616	0.319	0.576
0.000800	0.629	0.632	0.657	0.604	0.287	0.559
0.001000	0.622	0.625	0.654	0.593	0.262	0.545
0.001500	0.605	0.609	0.645	0.572	0.221	0.516
0.002000	0.591	0.596	0.638	0.554	0.194	0.493
0.003000	0.568	0.575	0.625	0.525	0.161	0.456
0.004000	0.549	0.557	0.613	0.501	0.142	0.428
0.005000	0.532	0.541	0.603	0.481	0.129	0.404
0.006000	0.517	0.527	0.593	0.463	0.119	0.384
0.008000	0.491	0.502	0.575	0.433	0.105	0.351
0.010000	0.468	0.481	0.559	0.408	0.095	0.324
0.015000	0.422	0.437	0.525	0.358	0.075	0.274
0.020000	0.385	0.403	0.495	0.320	0.061	0.238
0.030000	0.329	0.349	0.446	0.264	0.041	0.188
0.040000	0.286	0.307	0.406	0.224	0.029	0.155
0.050000	0.251	0.273	0.372	0.192	0.020	0.130
0.060000	0.223	0.245	0.342	0.167	0.014	0.112
0.080000	0.177	0.199	0.292	0.128	0.007	0.087
0.100000	0.143	0.164	0.252	0.100	0.004	0.071
0.150000	0.086	0.103	0.175	0.056	0.001	0.045
0.200000	0.051	0.065	0.120	0.032	0.001	0.029
0.250000	0.030	0.040	0.081	0.018	0.000	0.018
0.300000	0.017	0.024	0.053	0.010	0.000	0.011
0.350000	0.010	0.014	0.034	0.005	0.000	0.007
0.400000	0.005	0.007	0.020	0.003	0.000	0.004
0.450000	0.003	0.004	0.012	0.001	0.000	0.002
0.500000	0.001	0.002	0.006	0.001	0.000	0.001

Table 12, continued.

x/r_{\max}	53I131	55Cs137	61Pm147	77Ir192	79Au198	81Tl204
0.000000	0.687	0.687	0.688	0.687	0.686	0.687
0.000100	0.661	0.654	0.659	0.663	0.671	0.667
0.000150	0.654	0.645	0.651	0.656	0.666	0.661
0.000200	0.648	0.638	0.645	0.651	0.663	0.657
0.000300	0.638	0.625	0.633	0.641	0.656	0.649
0.000400	0.629	0.615	0.624	0.633	0.650	0.642
0.000500	0.621	0.605	0.616	0.626	0.646	0.637
0.000600	0.614	0.597	0.609	0.620	0.641	0.632
0.000800	0.602	0.582	0.596	0.609	0.633	0.622
0.001000	0.592	0.569	0.584	0.599	0.626	0.614
0.001500	0.569	0.542	0.561	0.578	0.610	0.596
0.002000	0.550	0.520	0.542	0.561	0.598	0.582
0.003000	0.520	0.484	0.511	0.533	0.576	0.558
0.004000	0.495	0.455	0.486	0.510	0.557	0.538
0.005000	0.474	0.431	0.465	0.490	0.541	0.521
0.006000	0.455	0.409	0.446	0.473	0.527	0.506
0.008000	0.423	0.373	0.415	0.443	0.502	0.479
0.010000	0.397	0.343	0.389	0.418	0.480	0.457
0.015000	0.344	0.286	0.339	0.369	0.435	0.412
0.020000	0.304	0.243	0.301	0.331	0.399	0.377
0.030000	0.245	0.182	0.245	0.274	0.344	0.322
0.040000	0.202	0.140	0.205	0.232	0.301	0.281
0.050000	0.170	0.109	0.175	0.200	0.267	0.249
0.060000	0.144	0.085	0.150	0.174	0.238	0.222
0.080000	0.105	0.052	0.114	0.133	0.192	0.179
0.100000	0.077	0.032	0.088	0.104	0.156	0.146
0.150000	0.036	0.010	0.048	0.058	0.096	0.091
0.200000	0.016	0.004	0.027	0.032	0.059	0.057
0.250000	0.007	0.003	0.015	0.018	0.035	0.035
0.300000	0.003	0.002	0.008	0.010	0.021	0.021
0.350000	0.001	0.001	0.004	0.005	0.012	0.012
0.400000	0.000	0.001	0.002	0.003	0.006	0.007
0.450000	0.000	0.000	0.001	0.001	0.003	0.004
0.500000	0.000	0.000	0.001	0.001	0.002	0.002

Table 13. Counting yield $Y_b(x/r_{\max})$ of plane beta(-) sources as a function of the scaled depth x/r_{\max} in loam.

x/r_{\max}	1H3	6C14	13Al28	15P32	16S35	17Cl36
0.000000	0.678	0.678	0.669	0.674	0.678	0.677
0.000100	0.654	0.658	0.667	0.669	0.652	0.665
0.000150	0.648	0.653	0.666	0.667	0.645	0.661
0.000200	0.643	0.648	0.665	0.666	0.639	0.659
0.000300	0.635	0.640	0.664	0.664	0.629	0.653
0.000400	0.627	0.633	0.662	0.661	0.620	0.649
0.000500	0.621	0.627	0.661	0.659	0.613	0.645
0.000600	0.615	0.622	0.660	0.657	0.606	0.641
0.000800	0.605	0.611	0.657	0.654	0.594	0.634
0.001000	0.596	0.602	0.655	0.650	0.584	0.628
0.001500	0.576	0.583	0.650	0.643	0.562	0.615
0.002000	0.559	0.567	0.645	0.636	0.544	0.604
0.003000	0.532	0.540	0.635	0.623	0.516	0.585
0.004000	0.509	0.518	0.627	0.612	0.492	0.568
0.005000	0.489	0.499	0.619	0.602	0.472	0.553
0.006000	0.471	0.482	0.611	0.592	0.455	0.540
0.008000	0.440	0.453	0.597	0.575	0.425	0.517
0.010000	0.414	0.428	0.584	0.559	0.400	0.496
0.015000	0.363	0.379	0.554	0.524	0.351	0.453
0.020000	0.323	0.341	0.528	0.495	0.314	0.419
0.030000	0.264	0.283	0.483	0.445	0.259	0.364
0.040000	0.221	0.241	0.446	0.405	0.218	0.321
0.050000	0.188	0.208	0.413	0.370	0.188	0.286
0.060000	0.162	0.181	0.383	0.340	0.163	0.257
0.080000	0.122	0.140	0.333	0.289	0.125	0.209
0.100000	0.094	0.110	0.290	0.246	0.098	0.172
0.150000	0.051	0.062	0.205	0.167	0.055	0.108
0.200000	0.028	0.036	0.143	0.112	0.031	0.067
0.250000	0.016	0.020	0.097	0.073	0.018	0.041
0.300000	0.009	0.011	0.064	0.046	0.010	0.025
0.350000	0.005	0.006	0.041	0.028	0.005	0.014
0.400000	0.002	0.003	0.025	0.017	0.003	0.008
0.450000	0.001	0.002	0.014	0.009	0.001	0.004
0.500000	0.001	0.001	0.008	0.005	0.001	0.002

Table 13, continued.

x/r_{\max}	19K43	20Ca45	21Sc49	22Ti51	26Fe59	27Co60
0.000000	0.676	0.678	0.673	0.672	0.678	0.678
0.000100	0.658	0.654	0.668	0.668	0.616	0.655
0.000150	0.652	0.648	0.667	0.666	0.600	0.648
0.000200	0.647	0.642	0.665	0.665	0.586	0.643
0.000300	0.639	0.633	0.663	0.663	0.564	0.634
0.000400	0.632	0.625	0.661	0.661	0.546	0.626
0.000500	0.626	0.618	0.659	0.659	0.530	0.620
0.000600	0.620	0.612	0.657	0.657	0.516	0.614
0.000800	0.609	0.601	0.654	0.654	0.492	0.603
0.001000	0.599	0.592	0.651	0.650	0.472	0.594
0.001500	0.578	0.572	0.644	0.643	0.431	0.574
0.002000	0.561	0.555	0.637	0.637	0.399	0.558
0.003000	0.531	0.528	0.625	0.625	0.349	0.531
0.004000	0.505	0.506	0.615	0.614	0.311	0.509
0.005000	0.484	0.486	0.605	0.605	0.281	0.490
0.006000	0.464	0.470	0.596	0.595	0.256	0.474
0.008000	0.430	0.441	0.579	0.579	0.216	0.445
0.010000	0.401	0.417	0.564	0.563	0.185	0.422
0.015000	0.344	0.369	0.531	0.530	0.131	0.374
0.020000	0.299	0.332	0.502	0.501	0.096	0.338
0.030000	0.233	0.276	0.454	0.453	0.055	0.282
0.040000	0.185	0.236	0.414	0.412	0.033	0.242
0.050000	0.148	0.204	0.380	0.378	0.020	0.210
0.060000	0.119	0.178	0.350	0.348	0.012	0.184
0.080000	0.077	0.139	0.299	0.297	0.005	0.144
0.100000	0.050	0.109	0.256	0.255	0.002	0.114
0.150000	0.016	0.063	0.176	0.174	0.000	0.066
0.200000	0.005	0.037	0.119	0.117	0.000	0.039
0.250000	0.002	0.021	0.078	0.077	0.000	0.023
0.300000	0.001	0.012	0.050	0.049	0.000	0.013
0.350000	0.001	0.007	0.031	0.030	0.000	0.007
0.400000	0.000	0.004	0.018	0.018	0.000	0.004
0.450000	0.000	0.002	0.010	0.010	0.000	0.002
0.500000	0.000	0.001	0.005	0.005	0.000	0.001

* Assumed composition (percentage by weight):

0.02 N₂; 9.04 H₂O; 16.87 Al₂O₃; 45.60 SiO₂; 1.37 Fe₂O₃; 1.34 CaCO₃;
1.10 Na₂O; 0.67 K₂O; 7.92 C₉H₁₂; 16.08 C₆H₁₀O₅. Density 1.5 g/cm³.

Table 13, continued.

x/r_{\max}	29Cu64	38Sr90	39Y90	43Tc99	47Ag110	51Sb124
0.000000	0.677	0.677	0.672	0.678	0.678	0.676
0.000100	0.660	0.661	0.666	0.652	0.501	0.636
0.000150	0.656	0.657	0.664	0.645	0.464	0.625
0.000200	0.652	0.653	0.663	0.640	0.436	0.616
0.000300	0.645	0.646	0.660	0.630	0.394	0.602
0.000400	0.639	0.641	0.657	0.622	0.363	0.590
0.000500	0.634	0.636	0.655	0.614	0.338	0.579
0.000600	0.629	0.632	0.653	0.608	0.318	0.570
0.000800	0.621	0.624	0.649	0.596	0.286	0.553
0.001000	0.614	0.617	0.646	0.586	0.262	0.540
0.001500	0.598	0.602	0.637	0.565	0.221	0.511
0.002000	0.585	0.589	0.630	0.548	0.194	0.489
0.003000	0.562	0.568	0.618	0.519	0.161	0.453
0.004000	0.544	0.551	0.607	0.496	0.142	0.426
0.005000	0.527	0.536	0.596	0.477	0.129	0.403
0.006000	0.513	0.522	0.587	0.460	0.119	0.383
0.008000	0.487	0.498	0.570	0.431	0.106	0.351
0.010000	0.465	0.478	0.555	0.406	0.095	0.325
0.015000	0.421	0.436	0.521	0.358	0.076	0.276
0.020000	0.385	0.402	0.493	0.321	0.062	0.241
0.030000	0.330	0.350	0.446	0.266	0.043	0.191
0.040000	0.288	0.309	0.407	0.227	0.030	0.157
0.050000	0.255	0.276	0.374	0.196	0.022	0.133
0.060000	0.227	0.248	0.345	0.170	0.015	0.115
0.080000	0.182	0.204	0.297	0.132	0.008	0.090
0.100000	0.148	0.169	0.257	0.104	0.004	0.073
0.150000	0.090	0.108	0.180	0.060	0.001	0.047
0.200000	0.055	0.069	0.126	0.035	0.001	0.031
0.250000	0.033	0.043	0.086	0.020	0.000	0.020
0.300000	0.020	0.027	0.057	0.011	0.000	0.012
0.350000	0.011	0.016	0.037	0.006	0.000	0.007
0.400000	0.006	0.009	0.023	0.003	0.000	0.004
0.450000	0.003	0.005	0.014	0.002	0.000	0.002
0.500000	0.002	0.002	0.008	0.001	0.000	0.001

* Assumed composition (percentage by weight):

0.02 N₂; 9.04 H₂O; 16.87 Al₂O₃; 45.60 SiO₂; 1.37 Fe₂O₃; 1.34 CaCO₃;
1.10 Na₂O; 0.67 K₂O; 7.92 C₉H₁₂; 16.08 C₆H₁₀O₅. Density 1.5 g/cm³.

Table 13, continued.

x/r_{\max}	53I131	55Cs137	61Pm147	77Ir192	79Au198	81Tl204
0.000000	0.677	0.677	0.678	0.677	0.676	0.677
0.000100	0.652	0.645	0.649	0.654	0.661	0.658
0.000150	0.645	0.637	0.642	0.647	0.657	0.652
0.000200	0.639	0.629	0.636	0.642	0.653	0.648
0.000300	0.629	0.617	0.625	0.633	0.647	0.640
0.000400	0.621	0.607	0.616	0.625	0.642	0.634
0.000500	0.613	0.598	0.608	0.618	0.637	0.628
0.000600	0.607	0.590	0.601	0.612	0.633	0.623
0.000800	0.595	0.576	0.588	0.601	0.625	0.614
0.001000	0.585	0.563	0.577	0.592	0.618	0.606
0.001500	0.563	0.537	0.554	0.572	0.603	0.590
0.002000	0.545	0.516	0.536	0.555	0.591	0.576
0.003000	0.515	0.481	0.506	0.528	0.570	0.552
0.004000	0.491	0.453	0.482	0.506	0.552	0.533
0.005000	0.471	0.429	0.461	0.486	0.536	0.516
0.006000	0.453	0.408	0.443	0.470	0.522	0.502
0.008000	0.422	0.373	0.413	0.441	0.498	0.476
0.010000	0.396	0.344	0.388	0.417	0.477	0.455
0.015000	0.345	0.288	0.339	0.369	0.434	0.411
0.020000	0.306	0.246	0.302	0.332	0.399	0.377
0.030000	0.248	0.186	0.247	0.276	0.345	0.324
0.040000	0.206	0.144	0.208	0.235	0.304	0.284
0.050000	0.174	0.113	0.178	0.203	0.270	0.252
0.060000	0.148	0.089	0.154	0.178	0.242	0.225
0.080000	0.109	0.056	0.118	0.138	0.197	0.183
0.100000	0.081	0.035	0.092	0.109	0.162	0.151
0.150000	0.039	0.012	0.051	0.062	0.101	0.096
0.200000	0.019	0.005	0.029	0.035	0.063	0.061
0.250000	0.008	0.003	0.017	0.020	0.039	0.038
0.300000	0.003	0.002	0.009	0.011	0.023	0.023
0.350000	0.001	0.001	0.005	0.006	0.014	0.014
0.400000	0.000	0.001	0.003	0.003	0.007	0.008
0.450000	0.000	0.000	0.001	0.002	0.004	0.004
0.500000	0.000	0.000	0.001	0.001	0.002	0.002

* Assumed composition (percentage by weight:

0.02 N₂; 9.04 H₂O; 16.87 Al₂O₃; 45.60 SiO₂; 1.37 Fe₂O₃; 1.34 CaCO₃;
1.10 Na₂O; 0.67 K₂O; 7.92 C₉H₁₂; 16.08 C₆H₁₀O₅. Density 1.5 g/cm³.

Table 14. Counting yield $Y_b(x/r_{\max})$ of plane beta(-) sources as a function of the scaled depth x/r_{\max} in dry soil.

x/r_{\max}	1H3	6C14	13Al28	15P32	16S35	17Cl36
0.000000	0.695	0.695	0.684	0.689	0.695	0.693
0.000100	0.671	0.675	0.682	0.684	0.668	0.681
0.000150	0.665	0.669	0.680	0.683	0.660	0.677
0.000200	0.660	0.664	0.680	0.681	0.654	0.674
0.000300	0.651	0.655	0.678	0.679	0.643	0.669
0.000400	0.643	0.648	0.677	0.676	0.635	0.664
0.000500	0.637	0.641	0.675	0.674	0.627	0.660
0.000600	0.631	0.636	0.674	0.672	0.620	0.656
0.000800	0.620	0.625	0.671	0.668	0.607	0.649
0.001000	0.610	0.615	0.669	0.665	0.596	0.642
0.001500	0.589	0.595	0.663	0.656	0.573	0.628
0.002000	0.572	0.578	0.658	0.649	0.554	0.616
0.003000	0.543	0.550	0.648	0.636	0.524	0.596
0.004000	0.519	0.526	0.639	0.624	0.499	0.578
0.005000	0.498	0.506	0.630	0.613	0.478	0.562
0.006000	0.479	0.488	0.622	0.603	0.459	0.548
0.008000	0.447	0.457	0.607	0.584	0.428	0.523
0.010000	0.419	0.431	0.593	0.567	0.402	0.502
0.015000	0.365	0.379	0.561	0.530	0.351	0.456
0.020000	0.323	0.339	0.533	0.499	0.312	0.420
0.030000	0.261	0.279	0.486	0.446	0.254	0.362
0.040000	0.217	0.235	0.445	0.403	0.213	0.317
0.050000	0.183	0.201	0.410	0.366	0.181	0.281
0.060000	0.156	0.174	0.379	0.335	0.156	0.250
0.080000	0.116	0.132	0.326	0.281	0.118	0.201
0.100000	0.088	0.102	0.282	0.238	0.091	0.163
0.150000	0.046	0.056	0.195	0.157	0.049	0.099
0.200000	0.025	0.031	0.132	0.102	0.027	0.060
0.250000	0.013	0.017	0.087	0.065	0.015	0.035
0.300000	0.007	0.009	0.056	0.040	0.008	0.020
0.350000	0.004	0.005	0.034	0.023	0.004	0.011
0.400000	0.002	0.002	0.020	0.013	0.002	0.006
0.450000	0.001	0.001	0.011	0.007	0.001	0.003
0.500000	0.000	0.001	0.006	0.004	0.000	0.001

Table 14, continued.

x/r_{\max}	19K43	20Ca45	21Sc49	22Ti51	26Fe59	27Co60
0.000000	0.693	0.695	0.688	0.688	0.694	0.695
0.000100	0.673	0.670	0.683	0.683	0.630	0.670
0.000150	0.668	0.663	0.682	0.682	0.613	0.664
0.000200	0.663	0.657	0.681	0.680	0.599	0.658
0.000300	0.654	0.648	0.678	0.678	0.575	0.649
0.000400	0.646	0.640	0.676	0.675	0.556	0.641
0.000500	0.639	0.632	0.674	0.674	0.540	0.633
0.000600	0.633	0.626	0.672	0.672	0.525	0.627
0.000800	0.622	0.614	0.668	0.668	0.500	0.616
0.001000	0.611	0.604	0.665	0.665	0.478	0.606
0.001500	0.589	0.583	0.657	0.657	0.435	0.585
0.002000	0.571	0.565	0.650	0.650	0.401	0.568
0.003000	0.539	0.536	0.638	0.637	0.350	0.540
0.004000	0.512	0.513	0.627	0.626	0.310	0.516
0.005000	0.489	0.493	0.616	0.616	0.279	0.497
0.006000	0.468	0.475	0.607	0.606	0.253	0.479
0.008000	0.433	0.445	0.589	0.588	0.212	0.449
0.010000	0.403	0.419	0.573	0.572	0.180	0.424
0.015000	0.342	0.369	0.537	0.536	0.126	0.374
0.020000	0.296	0.330	0.506	0.505	0.091	0.336
0.030000	0.227	0.273	0.455	0.454	0.051	0.279
0.040000	0.178	0.230	0.413	0.411	0.030	0.236
0.050000	0.141	0.198	0.376	0.375	0.018	0.204
0.060000	0.112	0.171	0.345	0.343	0.011	0.177
0.080000	0.071	0.131	0.292	0.290	0.004	0.137
0.100000	0.044	0.102	0.248	0.246	0.001	0.107
0.150000	0.014	0.057	0.166	0.164	0.000	0.060
0.200000	0.004	0.032	0.109	0.108	0.000	0.034
0.250000	0.002	0.018	0.070	0.069	0.000	0.019
0.300000	0.001	0.010	0.043	0.043	0.000	0.010
0.350000	0.001	0.005	0.026	0.025	0.000	0.006
0.400000	0.000	0.003	0.015	0.014	0.000	0.003
0.450000	0.000	0.001	0.008	0.008	0.000	0.001
0.500000	0.000	0.001	0.004	0.004	0.000	0.001

Table 14, continued.

x/r_{\max}	29Cu64	38Sr90	39Y90	43Tc99	47Ag110	51Sb124
0.000000	0.694	0.694	0.687	0.695	0.695	0.692
0.000100	0.676	0.677	0.681	0.668	0.510	0.650
0.000150	0.671	0.672	0.679	0.661	0.472	0.639
0.000200	0.667	0.668	0.677	0.655	0.442	0.630
0.000300	0.660	0.661	0.674	0.644	0.398	0.614
0.000400	0.654	0.655	0.672	0.635	0.366	0.601
0.000500	0.649	0.650	0.669	0.628	0.341	0.590
0.000600	0.643	0.646	0.667	0.621	0.320	0.581
0.000800	0.635	0.637	0.663	0.609	0.287	0.564
0.001000	0.627	0.630	0.659	0.598	0.263	0.549
0.001500	0.610	0.614	0.651	0.576	0.221	0.520
0.002000	0.596	0.601	0.643	0.557	0.194	0.496
0.003000	0.572	0.579	0.630	0.527	0.161	0.459
0.004000	0.552	0.560	0.618	0.503	0.142	0.430
0.005000	0.535	0.544	0.607	0.483	0.129	0.406
0.006000	0.520	0.530	0.597	0.465	0.119	0.385
0.008000	0.493	0.504	0.579	0.434	0.105	0.352
0.010000	0.470	0.483	0.563	0.408	0.094	0.325
0.015000	0.423	0.438	0.527	0.358	0.075	0.275
0.020000	0.385	0.403	0.497	0.319	0.060	0.238
0.030000	0.328	0.348	0.447	0.262	0.041	0.188
0.040000	0.284	0.305	0.406	0.221	0.028	0.154
0.050000	0.249	0.271	0.371	0.189	0.020	0.130
0.060000	0.220	0.242	0.341	0.164	0.014	0.112
0.080000	0.174	0.196	0.290	0.125	0.007	0.087
0.100000	0.140	0.161	0.249	0.097	0.004	0.070
0.150000	0.083	0.100	0.171	0.054	0.001	0.044
0.200000	0.049	0.062	0.117	0.030	0.001	0.028
0.250000	0.029	0.038	0.078	0.017	0.000	0.018
0.300000	0.016	0.022	0.050	0.009	0.000	0.011
0.350000	0.009	0.013	0.031	0.005	0.000	0.006
0.400000	0.005	0.007	0.019	0.002	0.000	0.004
0.450000	0.002	0.004	0.011	0.001	0.000	0.002
0.500000	0.001	0.002	0.006	0.001	0.000	0.001

Table 14, continued.

x/r_{\max}	53I131	55Cs137	61Pm147	77Ir192	79Au198	81Tl204
0.000000	0.694	0.694	0.695	0.694	0.693	0.693
0.000100	0.667	0.660	0.665	0.669	0.677	0.673
0.000150	0.660	0.651	0.657	0.662	0.672	0.668
0.000200	0.654	0.644	0.650	0.657	0.669	0.663
0.000300	0.643	0.631	0.639	0.647	0.662	0.655
0.000400	0.634	0.620	0.629	0.639	0.656	0.648
0.000500	0.627	0.610	0.621	0.632	0.651	0.642
0.000600	0.620	0.602	0.614	0.625	0.647	0.637
0.000800	0.607	0.587	0.600	0.614	0.638	0.627
0.001000	0.596	0.574	0.589	0.604	0.631	0.619
0.001500	0.573	0.546	0.565	0.582	0.615	0.601
0.002000	0.554	0.524	0.545	0.565	0.602	0.586
0.003000	0.523	0.487	0.513	0.536	0.580	0.562
0.004000	0.498	0.457	0.488	0.513	0.561	0.542
0.005000	0.476	0.432	0.466	0.493	0.545	0.524
0.006000	0.457	0.411	0.447	0.475	0.530	0.509
0.008000	0.424	0.374	0.416	0.445	0.504	0.482
0.010000	0.397	0.343	0.389	0.419	0.482	0.459
0.015000	0.344	0.285	0.338	0.369	0.436	0.413
0.020000	0.303	0.242	0.299	0.330	0.400	0.377
0.030000	0.243	0.180	0.243	0.272	0.343	0.322
0.040000	0.200	0.138	0.203	0.230	0.300	0.280
0.050000	0.167	0.106	0.172	0.197	0.265	0.247
0.060000	0.141	0.083	0.148	0.171	0.236	0.219
0.080000	0.102	0.051	0.111	0.131	0.189	0.176
0.100000	0.075	0.031	0.086	0.102	0.154	0.144
0.150000	0.035	0.010	0.046	0.056	0.093	0.089
0.200000	0.015	0.004	0.025	0.031	0.056	0.055
0.250000	0.007	0.002	0.014	0.017	0.034	0.033
0.300000	0.002	0.001	0.007	0.009	0.019	0.020
0.350000	0.001	0.001	0.004	0.005	0.011	0.011
0.400000	0.000	0.000	0.002	0.002	0.006	0.006
0.450000	0.000	0.000	0.001	0.001	0.003	0.003
0.500000	0.000	0.000	0.000	0.001	0.001	0.002

Table 15. Counting yield $Y_b(x/r_{\max})$ of plane beta(-) sources as a function of the scaled depth x/r_{\max} in human skin.

x/r_{\max}	1H3	6C14	13A128	15P32	16S35	17C136
0.000000	0.652	0.653	0.648	0.651	0.653	0.653
0.000100	0.629	0.635	0.646	0.647	0.628	0.642
0.000150	0.624	0.630	0.645	0.645	0.622	0.639
0.000200	0.619	0.625	0.644	0.644	0.617	0.636
0.000300	0.611	0.618	0.643	0.642	0.607	0.631
0.000400	0.604	0.612	0.642	0.640	0.599	0.627
0.000500	0.598	0.606	0.640	0.638	0.592	0.623
0.000600	0.593	0.601	0.639	0.636	0.586	0.620
0.000800	0.583	0.591	0.637	0.633	0.576	0.614
0.001000	0.575	0.583	0.635	0.630	0.566	0.608
0.001500	0.556	0.566	0.630	0.623	0.546	0.596
0.002000	0.541	0.551	0.625	0.616	0.530	0.586
0.003000	0.515	0.526	0.617	0.605	0.503	0.568
0.004000	0.494	0.506	0.609	0.595	0.481	0.553
0.005000	0.475	0.488	0.602	0.586	0.463	0.539
0.006000	0.459	0.473	0.595	0.577	0.446	0.527
0.008000	0.431	0.446	0.582	0.561	0.419	0.506
0.010000	0.407	0.423	0.570	0.546	0.396	0.487
0.015000	0.359	0.377	0.543	0.515	0.350	0.448
0.020000	0.322	0.342	0.520	0.488	0.315	0.416
0.030000	0.266	0.287	0.479	0.442	0.263	0.365
0.040000	0.226	0.247	0.444	0.405	0.225	0.325
0.050000	0.194	0.215	0.414	0.373	0.195	0.292
0.060000	0.169	0.189	0.387	0.345	0.171	0.264
0.080000	0.130	0.149	0.339	0.297	0.134	0.219
0.100000	0.102	0.119	0.299	0.257	0.106	0.183
0.150000	0.058	0.071	0.217	0.180	0.062	0.119
0.200000	0.034	0.043	0.156	0.124	0.037	0.077
0.250000	0.020	0.025	0.110	0.085	0.022	0.050
0.300000	0.012	0.015	0.075	0.056	0.013	0.031
0.350000	0.007	0.009	0.050	0.036	0.008	0.019
0.400000	0.004	0.005	0.032	0.023	0.004	0.011
0.450000	0.002	0.003	0.020	0.013	0.002	0.006
0.500000	0.001	0.001	0.012	0.008	0.001	0.004

Table 15, continued.

x/r_{\max}	19K43	20Ca45	21Sc49	22Ti51	26Fe59	27Co60
0.000000	0.653	0.653	0.650	0.650	0.653	0.653
0.000100	0.636	0.631	0.646	0.646	0.596	0.632
0.000150	0.631	0.625	0.645	0.645	0.581	0.626
0.000200	0.626	0.620	0.644	0.644	0.568	0.621
0.000300	0.618	0.612	0.642	0.641	0.548	0.613
0.000400	0.612	0.604	0.640	0.640	0.531	0.606
0.000500	0.606	0.598	0.638	0.638	0.516	0.599
0.000600	0.600	0.592	0.636	0.636	0.503	0.594
0.000800	0.590	0.582	0.633	0.633	0.481	0.584
0.001000	0.581	0.573	0.630	0.630	0.462	0.575
0.001500	0.562	0.555	0.624	0.623	0.424	0.557
0.002000	0.546	0.540	0.618	0.618	0.394	0.542
0.003000	0.518	0.514	0.607	0.607	0.347	0.517
0.004000	0.495	0.494	0.597	0.597	0.311	0.497
0.005000	0.475	0.476	0.589	0.588	0.283	0.480
0.006000	0.457	0.461	0.580	0.580	0.259	0.465
0.008000	0.426	0.434	0.565	0.565	0.220	0.438
0.010000	0.399	0.412	0.551	0.551	0.190	0.416
0.015000	0.345	0.367	0.521	0.520	0.138	0.372
0.020000	0.304	0.332	0.495	0.494	0.103	0.338
0.030000	0.241	0.280	0.450	0.449	0.061	0.286
0.040000	0.194	0.242	0.414	0.413	0.038	0.248
0.050000	0.158	0.211	0.382	0.381	0.024	0.217
0.060000	0.129	0.186	0.354	0.353	0.015	0.192
0.080000	0.086	0.148	0.306	0.305	0.006	0.153
0.100000	0.057	0.119	0.266	0.264	0.002	0.123
0.150000	0.020	0.071	0.188	0.186	0.000	0.075
0.200000	0.007	0.043	0.132	0.130	0.000	0.046
0.250000	0.003	0.026	0.090	0.089	0.000	0.028
0.300000	0.001	0.016	0.060	0.059	0.000	0.017
0.350000	0.001	0.009	0.039	0.038	0.000	0.010
0.400000	0.000	0.005	0.025	0.024	0.000	0.006
0.450000	0.000	0.003	0.015	0.014	0.000	0.003
0.500000	0.000	0.002	0.009	0.008	0.000	0.002

Table 15, continued.

x/r_{\max}	29Cu64	38Sr90	39Y90	43Tc99	47Ag110	51Sb124
0.000000	0.653	0.653	0.650	0.653	0.653	0.652
0.000100	0.638	0.638	0.644	0.629	0.488	0.615
0.000150	0.633	0.634	0.643	0.623	0.453	0.605
0.000200	0.630	0.631	0.641	0.618	0.427	0.597
0.000300	0.623	0.624	0.639	0.609	0.387	0.583
0.000400	0.618	0.619	0.636	0.601	0.357	0.572
0.000500	0.613	0.615	0.634	0.594	0.334	0.562
0.000600	0.609	0.611	0.632	0.588	0.315	0.553
0.000800	0.601	0.604	0.629	0.578	0.284	0.539
0.001000	0.595	0.597	0.626	0.568	0.261	0.526
0.001500	0.580	0.584	0.618	0.549	0.220	0.499
0.002000	0.568	0.572	0.612	0.533	0.194	0.478
0.003000	0.547	0.553	0.600	0.507	0.161	0.445
0.004000	0.530	0.537	0.590	0.485	0.142	0.419
0.005000	0.515	0.523	0.581	0.467	0.129	0.397
0.006000	0.502	0.510	0.572	0.451	0.119	0.379
0.008000	0.478	0.488	0.557	0.424	0.106	0.348
0.010000	0.458	0.469	0.542	0.402	0.096	0.324
0.015000	0.417	0.430	0.512	0.357	0.078	0.277
0.020000	0.384	0.399	0.486	0.322	0.064	0.243
0.030000	0.333	0.350	0.443	0.271	0.045	0.195
0.040000	0.293	0.313	0.407	0.232	0.033	0.162
0.050000	0.261	0.282	0.376	0.203	0.024	0.138
0.060000	0.235	0.255	0.349	0.178	0.018	0.119
0.080000	0.192	0.213	0.304	0.141	0.009	0.094
0.100000	0.158	0.179	0.266	0.113	0.005	0.077
0.150000	0.101	0.119	0.192	0.068	0.001	0.051
0.200000	0.064	0.079	0.138	0.041	0.001	0.034
0.250000	0.041	0.052	0.098	0.025	0.000	0.023
0.300000	0.025	0.034	0.068	0.015	0.000	0.015
0.350000	0.015	0.021	0.046	0.009	0.000	0.009
0.400000	0.009	0.013	0.030	0.005	0.000	0.006
0.450000	0.005	0.007	0.019	0.003	0.000	0.004
0.500000	0.003	0.004	0.011	0.001	0.000	0.002

Table 15, continued.

x/r_{\max}	53I131	55Cs137	61Pm147	77Ir192	79Au198	81Tl204
0.000000	0.653	0.653	0.653	0.653	0.653	0.653
0.000100	0.630	0.623	0.626	0.631	0.639	0.635
0.000150	0.623	0.615	0.619	0.625	0.635	0.630
0.000200	0.618	0.609	0.613	0.620	0.631	0.626
0.000300	0.609	0.597	0.604	0.612	0.626	0.619
0.000400	0.601	0.588	0.595	0.605	0.621	0.613
0.000500	0.594	0.580	0.588	0.598	0.616	0.608
0.000600	0.588	0.572	0.581	0.593	0.612	0.603
0.000800	0.577	0.559	0.570	0.583	0.605	0.595
0.001000	0.567	0.547	0.560	0.574	0.599	0.588
0.001500	0.547	0.523	0.539	0.555	0.585	0.572
0.002000	0.531	0.503	0.522	0.540	0.574	0.559
0.003000	0.503	0.471	0.494	0.515	0.554	0.538
0.004000	0.481	0.445	0.471	0.494	0.538	0.520
0.005000	0.462	0.423	0.452	0.477	0.524	0.505
0.006000	0.445	0.404	0.436	0.461	0.511	0.491
0.008000	0.417	0.371	0.408	0.435	0.488	0.468
0.010000	0.393	0.344	0.384	0.412	0.469	0.448
0.015000	0.345	0.291	0.338	0.367	0.429	0.407
0.020000	0.308	0.252	0.303	0.333	0.397	0.375
0.030000	0.253	0.194	0.252	0.280	0.347	0.326
0.040000	0.213	0.153	0.214	0.241	0.308	0.288
0.050000	0.182	0.122	0.185	0.211	0.276	0.257
0.060000	0.157	0.098	0.162	0.186	0.249	0.232
0.080000	0.118	0.063	0.126	0.147	0.206	0.192
0.100000	0.090	0.041	0.100	0.118	0.172	0.160
0.150000	0.046	0.014	0.058	0.070	0.111	0.105
0.200000	0.023	0.006	0.035	0.042	0.072	0.070
0.250000	0.011	0.003	0.021	0.025	0.046	0.046
0.300000	0.005	0.002	0.012	0.014	0.029	0.029
0.350000	0.002	0.001	0.007	0.008	0.018	0.019
0.400000	0.001	0.001	0.004	0.005	0.011	0.011
0.450000	0.000	0.001	0.002	0.002	0.006	0.007
0.500000	0.000	0.000	0.001	0.001	0.003	0.004

Table 16. Counting yield $Y_b(x/r_{\max})$ of plane beta(+) sources as a function of the scaled depth x/r_{\max} in an aluminum backing.

x/r_{\max}	6C11	11Na22	21Sc44	26Fe52	27Co56	29Cu64
0.000000	0.693	0.693	0.692	0.693	0.692	0.693
0.000100	0.689	0.689	0.690	0.691	0.689	0.691
0.000150	0.688	0.688	0.689	0.690	0.688	0.690
0.000200	0.686	0.686	0.688	0.689	0.687	0.689
0.000300	0.684	0.683	0.686	0.687	0.685	0.687
0.000400	0.681	0.680	0.684	0.685	0.683	0.685
0.000500	0.679	0.677	0.683	0.683	0.682	0.684
0.000600	0.676	0.675	0.681	0.682	0.680	0.682
0.000800	0.672	0.670	0.678	0.678	0.676	0.678
0.001000	0.668	0.665	0.676	0.675	0.673	0.675
0.001500	0.658	0.654	0.669	0.667	0.665	0.667
0.002000	0.650	0.644	0.662	0.659	0.658	0.660
0.003000	0.634	0.627	0.650	0.646	0.645	0.645
0.004000	0.620	0.611	0.640	0.633	0.633	0.632
0.005000	0.607	0.596	0.629	0.621	0.621	0.620
0.006000	0.595	0.583	0.619	0.609	0.611	0.609
0.008000	0.573	0.558	0.601	0.589	0.591	0.587
0.010000	0.554	0.537	0.584	0.570	0.573	0.568
0.015000	0.512	0.491	0.547	0.528	0.534	0.526
0.020000	0.476	0.453	0.515	0.493	0.501	0.489
0.030000	0.419	0.391	0.461	0.434	0.446	0.430
0.040000	0.372	0.343	0.417	0.387	0.401	0.381
0.050000	0.334	0.304	0.379	0.347	0.363	0.341
0.060000	0.301	0.271	0.345	0.312	0.331	0.306
0.080000	0.247	0.217	0.290	0.256	0.277	0.250
0.100000	0.204	0.176	0.244	0.211	0.234	0.205
0.150000	0.128	0.106	0.160	0.132	0.153	0.126
0.200000	0.079	0.063	0.103	0.081	0.098	0.077
0.250000	0.048	0.037	0.064	0.049	0.061	0.046
0.300000	0.028	0.021	0.039	0.029	0.037	0.026
0.350000	0.016	0.012	0.022	0.016	0.021	0.015
0.400000	0.009	0.006	0.012	0.009	0.012	0.008
0.450000	0.004	0.003	0.006	0.004	0.006	0.004
0.500000	0.002	0.001	0.003	0.002	0.003	0.002

Table 16, continued.

x/r_{\max}	33As74	37Rb84	39Y86	43Tc95	53I119	55Cs125
0.000000	0.693	0.692	0.691	0.693	0.689	0.690
0.000100	0.690	0.689	0.690	0.691	0.688	0.689
0.000150	0.688	0.688	0.689	0.690	0.688	0.688
0.000200	0.687	0.686	0.688	0.689	0.687	0.687
0.000300	0.684	0.684	0.687	0.688	0.686	0.686
0.000400	0.681	0.681	0.686	0.686	0.685	0.685
0.000500	0.679	0.679	0.684	0.684	0.684	0.684
0.000600	0.676	0.676	0.683	0.682	0.683	0.682
0.000800	0.672	0.672	0.681	0.679	0.680	0.680
0.001000	0.667	0.667	0.678	0.675	0.678	0.678
0.001500	0.656	0.657	0.672	0.667	0.673	0.672
0.002000	0.646	0.647	0.667	0.660	0.668	0.667
0.003000	0.627	0.630	0.656	0.645	0.659	0.656
0.004000	0.610	0.614	0.646	0.632	0.650	0.646
0.005000	0.594	0.599	0.636	0.619	0.641	0.637
0.006000	0.579	0.585	0.627	0.608	0.633	0.628
0.008000	0.553	0.559	0.610	0.586	0.617	0.611
0.010000	0.528	0.537	0.594	0.565	0.603	0.595
0.015000	0.476	0.488	0.558	0.521	0.570	0.559
0.020000	0.433	0.448	0.527	0.483	0.540	0.528
0.030000	0.364	0.383	0.474	0.421	0.489	0.474
0.040000	0.309	0.333	0.430	0.370	0.447	0.429
0.050000	0.265	0.292	0.391	0.329	0.409	0.390
0.060000	0.228	0.257	0.358	0.293	0.376	0.356
0.080000	0.170	0.204	0.301	0.235	0.320	0.298
0.100000	0.127	0.164	0.255	0.190	0.273	0.251
0.150000	0.060	0.101	0.168	0.113	0.183	0.162
0.200000	0.029	0.065	0.108	0.067	0.120	0.102
0.250000	0.014	0.042	0.068	0.040	0.077	0.063
0.300000	0.007	0.026	0.041	0.023	0.047	0.038
0.350000	0.004	0.016	0.024	0.013	0.028	0.022
0.400000	0.002	0.009	0.013	0.007	0.016	0.012
0.450000	0.001	0.005	0.007	0.004	0.008	0.006
0.500000	0.001	0.002	0.003	0.002	0.004	0.003

Table 17. Counting yield $Y_b(x/r_{\max})$ of plane beta(+) sources as a function of the scaled depth x/r_{\max} in an iron backing.

x/r_{\max}	6C11	11Na22	21Sc44	26Fe52	27Co56	29Cu64
0.000000	0.747	0.745	0.748	0.747	0.748	0.747
0.000100	0.743	0.741	0.746	0.745	0.746	0.744
0.000150	0.742	0.740	0.746	0.744	0.745	0.743
0.000200	0.740	0.738	0.745	0.743	0.744	0.743
0.000300	0.738	0.735	0.743	0.741	0.742	0.741
0.000400	0.735	0.733	0.741	0.739	0.740	0.739
0.000500	0.733	0.730	0.739	0.737	0.738	0.737
0.000600	0.730	0.727	0.738	0.735	0.736	0.735
0.000800	0.726	0.722	0.735	0.732	0.732	0.732
0.001000	0.721	0.718	0.732	0.728	0.729	0.728
0.001500	0.711	0.706	0.724	0.720	0.721	0.720
0.002000	0.702	0.696	0.718	0.712	0.713	0.712
0.003000	0.686	0.678	0.705	0.697	0.699	0.697
0.004000	0.671	0.661	0.693	0.684	0.686	0.683
0.005000	0.658	0.646	0.682	0.671	0.674	0.671
0.006000	0.645	0.632	0.672	0.660	0.663	0.659
0.008000	0.622	0.607	0.653	0.638	0.642	0.637
0.010000	0.602	0.584	0.635	0.618	0.623	0.616
0.015000	0.558	0.536	0.596	0.575	0.583	0.572
0.020000	0.522	0.497	0.563	0.539	0.548	0.535
0.030000	0.462	0.434	0.506	0.479	0.490	0.474
0.040000	0.414	0.384	0.460	0.430	0.444	0.425
0.050000	0.375	0.344	0.421	0.389	0.405	0.384
0.060000	0.341	0.310	0.387	0.354	0.371	0.348
0.080000	0.285	0.254	0.330	0.296	0.316	0.290
0.100000	0.241	0.211	0.283	0.250	0.271	0.244
0.150000	0.161	0.136	0.197	0.166	0.188	0.160
0.200000	0.107	0.088	0.136	0.110	0.130	0.105
0.250000	0.071	0.056	0.092	0.072	0.088	0.068
0.300000	0.046	0.035	0.061	0.047	0.058	0.044
0.350000	0.029	0.022	0.039	0.029	0.038	0.027
0.400000	0.017	0.013	0.024	0.018	0.023	0.016
0.450000	0.010	0.007	0.014	0.010	0.014	0.009
0.500000	0.006	0.004	0.008	0.006	0.008	0.005

Table 17, continued.

x/r_{\max}	33As74	37Rb84	39Y86	43Tc95	53I119	55Cs125
0.000000	0.747	0.748	0.749	0.747	0.749	0.749
0.000100	0.744	0.745	0.747	0.745	0.748	0.748
0.000150	0.743	0.744	0.746	0.744	0.747	0.747
0.000200	0.741	0.742	0.746	0.743	0.746	0.746
0.000300	0.738	0.739	0.744	0.741	0.745	0.745
0.000400	0.736	0.737	0.743	0.739	0.744	0.743
0.000500	0.733	0.734	0.741	0.737	0.743	0.742
0.000600	0.730	0.732	0.740	0.736	0.742	0.741
0.000800	0.725	0.727	0.737	0.732	0.739	0.738
0.001000	0.721	0.723	0.735	0.729	0.737	0.736
0.001500	0.709	0.712	0.728	0.720	0.731	0.729
0.002000	0.698	0.701	0.722	0.712	0.726	0.724
0.003000	0.679	0.683	0.711	0.697	0.716	0.712
0.004000	0.661	0.666	0.700	0.683	0.706	0.702
0.005000	0.645	0.650	0.690	0.670	0.697	0.692
0.006000	0.629	0.636	0.680	0.657	0.688	0.682
0.008000	0.601	0.610	0.662	0.635	0.671	0.664
0.010000	0.576	0.586	0.645	0.613	0.655	0.647
0.015000	0.523	0.536	0.608	0.568	0.620	0.609
0.020000	0.478	0.494	0.575	0.529	0.588	0.575
0.030000	0.407	0.428	0.519	0.465	0.535	0.519
0.040000	0.352	0.375	0.473	0.414	0.490	0.472
0.050000	0.307	0.333	0.434	0.371	0.451	0.432
0.060000	0.269	0.297	0.400	0.335	0.417	0.397
0.080000	0.208	0.240	0.342	0.275	0.361	0.339
0.100000	0.162	0.197	0.295	0.228	0.314	0.291
0.150000	0.086	0.127	0.206	0.145	0.223	0.200
0.200000	0.045	0.086	0.143	0.093	0.157	0.137
0.250000	0.023	0.059	0.097	0.060	0.108	0.091
0.300000	0.012	0.040	0.064	0.038	0.073	0.059
0.350000	0.007	0.027	0.041	0.023	0.047	0.038
0.400000	0.004	0.017	0.026	0.014	0.030	0.023
0.450000	0.002	0.011	0.015	0.008	0.018	0.014
0.500000	0.001	0.006	0.009	0.005	0.010	0.008

Table 18, continued.

s	x = 5.0	6.0	8.0	10.0	12.0	16.0	20.0
0.000	1.0000	1.0000	1.0000	1.0000	1.0000	1.0000	1.0000
0.010	0.9957	0.9959	0.9962	0.9964	0.9966	0.9968	0.9968
0.015	0.9938	0.9940	0.9945	0.9948	0.9950	0.9953	0.9952
0.020	0.9918	0.9921	0.9928	0.9933	0.9935	0.9937	0.9938
0.030	0.9881	0.9887	0.9895	0.9900	0.9905	0.9908	0.9911
0.040	0.9842	0.9850	0.9864	0.9873	0.9877	0.9881	0.9885
0.050	0.9804	0.9814	0.9832	0.9842	0.9847	0.9853	0.9859
0.060	0.9767	0.9780	0.9799	0.9811	0.9817	0.9825	0.9832
0.080	0.9693	0.9710	0.9736	0.9751	0.9759	0.9772	0.9782
0.100	0.9622	0.9643	0.9674	0.9692	0.9704	0.9720	0.9727
0.150	0.9447	0.9477	0.9520	0.9543	0.9560	0.9586	0.9598
0.200	0.9277	0.9314	0.9366	0.9399	0.9423	0.9455	0.9469
0.300	0.8942	0.8996	0.9071	0.9114	0.9151	0.9195	0.9221
0.400	0.8624	0.8691	0.8782	0.8836	0.8883	0.8933	0.8974
0.500	0.8318	0.8394	0.8501	0.8569	0.8619	0.8676	0.8723
0.600	0.8021	0.8108	0.8227	0.8308	0.8365	0.8428	0.8482
0.800	0.7472	0.7569	0.7709	0.7808	0.7872	0.7948	0.8017
1.000	0.6967	0.7070	0.7226	0.7335	0.7405	0.7493	0.7567
1.500	0.5864	0.5983	0.6159	0.6277	0.6352	0.6457	0.6533
2.000	0.4960	0.5079	0.5261	0.5377	0.5453	0.5568	0.5632
3.000	0.3584	0.3684	0.3840	0.3950	0.4024	0.4110	0.4139
4.000	0.2604	0.2685	0.2812	0.2902	0.2959	0.3009	0.3015
5.000	0.1895	0.1962	0.2060	0.2122	0.2159	0.2193	0.2191
6.000	0.1378	0.1430	0.1504	0.1544	0.1566	0.1582	0.1567
8.000	0.0716	0.0741	0.0779	0.0799	0.0804	0.0792	0.0763
10.000	0.0360	0.0370	0.0383	0.0388	0.0388	0.0375	0.0349
15.000	0.0047	0.0047	0.0046	0.0045	0.0044	0.0038	0.0029
20.000	0.0003	0.0003	0.0002	0.0002	0.0002	0.0001	0.0001

Table 20. Transmission of $^{13}\text{Al}^{28}$ beta particles through a mylar overlayer of thickness s (mg/cm^2), for plane sources located at depth x (microns) in an aluminum backing.

s	$x = 0.0$	0.5	1.0	1.5	2.0	3.0	4.0
0.000	1.0000	1.0000	1.0000	1.0000	1.0000	1.0000	1.0000
0.010	0.9994	0.9997	0.9998	0.9998	0.9998	0.9998	0.9998
0.015	0.9991	0.9996	0.9996	0.9997	0.9997	0.9997	0.9997
0.020	0.9989	0.9995	0.9995	0.9996	0.9996	0.9996	0.9996
0.030	0.9985	0.9992	0.9993	0.9993	0.9994	0.9994	0.9995
0.040	0.9981	0.9989	0.9991	0.9991	0.9992	0.9992	0.9993
0.050	0.9978	0.9987	0.9988	0.9989	0.9990	0.9991	0.9991
0.060	0.9975	0.9984	0.9986	0.9987	0.9988	0.9989	0.9989
0.080	0.9969	0.9979	0.9982	0.9983	0.9984	0.9985	0.9986
0.100	0.9963	0.9975	0.9977	0.9979	0.9980	0.9981	0.9982
0.150	0.9950	0.9963	0.9967	0.9969	0.9970	0.9973	0.9974
0.200	0.9938	0.9952	0.9957	0.9959	0.9961	0.9964	0.9966
0.300	0.9917	0.9933	0.9938	0.9941	0.9944	0.9947	0.9950
0.400	0.9897	0.9914	0.9920	0.9924	0.9927	0.9932	0.9935
0.500	0.9878	0.9896	0.9903	0.9908	0.9911	0.9917	0.9921
0.600	0.9861	0.9879	0.9887	0.9892	0.9896	0.9902	0.9907
0.800	0.9829	0.9848	0.9857	0.9863	0.9868	0.9875	0.9881
1.000	0.9799	0.9819	0.9828	0.9835	0.9840	0.9849	0.9856
1.500	0.9734	0.9755	0.9766	0.9773	0.9780	0.9790	0.9799
2.000	0.9677	0.9699	0.9711	0.9719	0.9727	0.9739	0.9749
3.000	0.9578	0.9601	0.9614	0.9624	0.9632	0.9646	0.9658
4.000	0.9494	0.9518	0.9531	0.9542	0.9551	0.9566	0.9580
5.000	0.9417	0.9442	0.9456	0.9467	0.9476	0.9493	0.9508
6.000	0.9345	0.9370	0.9384	0.9396	0.9406	0.9424	0.9439
8.000	0.9216	0.9242	0.9256	0.9269	0.9279	0.9298	0.9315
10.000	0.9097	0.9123	0.9138	0.9151	0.9162	0.9182	0.9199
15.000	0.8831	0.8857	0.8872	0.8885	0.8897	0.8918	0.8937
20.000	0.8592	0.8618	0.8633	0.8646	0.8658	0.8680	0.8699
30.000	0.8167	0.8192	0.8208	0.8221	0.8234	0.8256	0.8275
40.000	0.7787	0.7811	0.7826	0.7839	0.7852	0.7873	0.7893
50.000	0.7436	0.7460	0.7474	0.7487	0.7499	0.7521	0.7540
60.000	0.7111	0.7134	0.7148	0.7161	0.7172	0.7194	0.7213
80.000	0.6517	0.6538	0.6552	0.6564	0.6574	0.6594	0.6612
100.000	0.5984	0.6003	0.6016	0.6027	0.6037	0.6055	0.6072

Table 20, continued.

s	x = 5.0	6.0	8.0	10.0	12.0	16.0	20.0
0.000	1.0000	1.0000	1.0000	1.0000	1.0000	1.0000	1.0000
0.010	0.9998	0.9998	0.9998	0.9999	0.9999	0.9999	0.9999
0.015	0.9997	0.9998	0.9998	0.9998	0.9998	0.9998	0.9998
0.020	0.9997	0.9997	0.9997	0.9997	0.9997	0.9998	0.9998
0.030	0.9995	0.9995	0.9995	0.9996	0.9996	0.9996	0.9997
0.040	0.9993	0.9993	0.9994	0.9994	0.9995	0.9995	0.9996
0.050	0.9992	0.9992	0.9993	0.9993	0.9993	0.9994	0.9995
0.060	0.9990	0.9990	0.9991	0.9992	0.9992	0.9993	0.9994
0.080	0.9987	0.9987	0.9988	0.9989	0.9990	0.9991	0.9992
0.100	0.9983	0.9984	0.9985	0.9986	0.9987	0.9988	0.9989
0.150	0.9975	0.9976	0.9978	0.9980	0.9981	0.9983	0.9984
0.200	0.9967	0.9969	0.9971	0.9973	0.9974	0.9977	0.9979
0.300	0.9953	0.9954	0.9958	0.9960	0.9962	0.9966	0.9969
0.400	0.9938	0.9941	0.9945	0.9948	0.9951	0.9955	0.9959
0.500	0.9924	0.9927	0.9932	0.9936	0.9939	0.9945	0.9950
0.600	0.9911	0.9914	0.9920	0.9924	0.9928	0.9935	0.9940
0.800	0.9886	0.9890	0.9897	0.9902	0.9907	0.9916	0.9922
1.000	0.9861	0.9866	0.9874	0.9881	0.9887	0.9897	0.9905
1.500	0.9806	0.9812	0.9823	0.9832	0.9840	0.9853	0.9864
2.000	0.9757	0.9764	0.9777	0.9788	0.9797	0.9813	0.9827
3.000	0.9668	0.9678	0.9694	0.9707	0.9719	0.9740	0.9757
4.000	0.9591	0.9602	0.9620	0.9636	0.9650	0.9674	0.9694
5.000	0.9520	0.9532	0.9552	0.9570	0.9585	0.9612	0.9635
6.000	0.9452	0.9465	0.9487	0.9506	0.9523	0.9552	0.9577
8.000	0.9329	0.9343	0.9367	0.9389	0.9408	0.9441	0.9469
10.000	0.9215	0.9229	0.9255	0.9278	0.9299	0.9336	0.9367
15.000	0.8954	0.8969	0.8998	0.9024	0.9047	0.9089	0.9125
20.000	0.8717	0.8734	0.8764	0.8792	0.8817	0.8862	0.8901
30.000	0.8294	0.8311	0.8343	0.8372	0.8399	0.8448	0.8491
40.000	0.7912	0.7929	0.7961	0.7991	0.8018	0.8068	0.8112
50.000	0.7559	0.7576	0.7608	0.7637	0.7665	0.7715	0.7759
60.000	0.7231	0.7248	0.7279	0.7308	0.7335	0.7385	0.7430
80.000	0.6629	0.6645	0.6674	0.6702	0.6728	0.6776	0.6819
100.000	0.6088	0.6103	0.6131	0.6157	0.6181	0.6227	0.6268

Table 21, continued.

x (microns)	53I131		55Cs137		61Pm147		77Ir192	
	h (mg/cm ²)	Y	h (mg/cm ²)	Y	h (mg/cm ²)	Y	h (mg/cm ²)	Y
0.00	6.65	0.700	6.98	0.700	1.02	0.701	6.33	0.700
0.05	7.02	0.687	7.38	0.688	1.20	0.657	6.72	0.686
0.10	7.22	0.679	7.57	0.681	1.30	0.636	6.92	0.678
0.15	7.37	0.674	7.72	0.675	1.37	0.620	7.07	0.672
0.20	7.49	0.669	7.86	0.670	1.43	0.606	7.20	0.667
0.25	7.61	0.664	7.97	0.666	1.48	0.595	7.32	0.662
0.30	7.71	0.660	8.08	0.662	1.53	0.584	7.42	0.658
0.40	7.89	0.653	8.26	0.655	1.61	0.566	7.61	0.650
0.50	8.06	0.647	8.43	0.648	1.68	0.551	7.77	0.644
0.60	8.20	0.641	8.58	0.643	1.75	0.537	7.92	0.638
0.70	8.34	0.636	8.71	0.638	1.80	0.525	8.06	0.632
0.80	8.47	0.631	8.84	0.633	1.86	0.513	8.19	0.627
0.90	8.59	0.626	8.96	0.628	1.91	0.503	8.31	0.622
1.00	8.70	0.622	9.07	0.624	1.95	0.493	8.43	0.618
1.25	8.96	0.612	9.33	0.614	2.06	0.471	8.69	0.608
1.50	9.19	0.603	9.56	0.605	2.15	0.452	8.93	0.598
1.75	9.40	0.594	9.78	0.598	2.24	0.435	9.15	0.590
2.00	9.60	0.587	9.97	0.590	2.32	0.420	9.35	0.582
2.50	9.95	0.573	10.33	0.576	2.45	0.393	9.71	0.568
3.00	10.27	0.561	10.65	0.564	2.57	0.371	10.03	0.555
3.50	10.56	0.549	10.93	0.553	2.68	0.351	10.32	0.544
4.00	10.82	0.539	11.20	0.543	2.77	0.333	10.59	0.533
4.50	11.07	0.529	11.44	0.534	2.85	0.317	10.84	0.524
5.00	11.29	0.520	11.67	0.525	2.93	0.302	11.08	0.514
5.50	11.51	0.512	11.88	0.517	3.00	0.289	11.30	0.506
6.00	11.71	0.504	12.08	0.509	3.06	0.277	11.50	0.498
7.00	12.09	0.489	12.44	0.495	3.18	0.255	11.89	0.483
8.00	12.42	0.475	12.77	0.481	3.29	0.236	12.23	0.469
9.00	12.73	0.463	13.07	0.469	3.38	0.220	12.55	0.456
10.00	13.02	0.451	13.35	0.457	3.46	0.205	12.84	0.445
12.00	13.53	0.430	13.84	0.437	3.61	0.179	13.37	0.424
14.00	13.99	0.412	14.27	0.418	3.72	0.158	13.84	0.405
16.00	14.39	0.395	14.65	0.401	3.82	0.141	14.27	0.388
18.00	14.76	0.379	14.99	0.386	3.90	0.125	14.65	0.373
20.00	15.08	0.365	15.30	0.372	3.96	0.112	14.99	0.359

Table 21, continued.

x (microns)	79Au198		81Tl204	
	h (mg/cm ²)	Y	h (mg/cm ²)	Y
0.00	16.81	0.699	10.68	0.700
0.05	17.27	0.692	11.16	0.689
0.10	17.50	0.688	11.40	0.683
0.15	17.69	0.685	11.59	0.679
0.20	17.85	0.682	11.75	0.675
0.25	17.99	0.680	11.89	0.671
0.30	18.12	0.678	12.02	0.668
0.40	18.35	0.674	12.25	0.662
0.50	18.55	0.670	12.46	0.657
0.60	18.74	0.667	12.64	0.653
0.70	18.91	0.664	12.81	0.649
0.80	19.07	0.661	12.97	0.645
0.90	19.22	0.658	13.12	0.641
1.00	19.37	0.656	13.27	0.638
1.25	19.70	0.650	13.60	0.630
1.50	20.01	0.645	13.90	0.623
1.75	20.29	0.640	14.17	0.616
2.00	20.56	0.635	14.43	0.610
2.50	21.04	0.626	14.89	0.599
3.00	21.47	0.619	15.29	0.589
3.50	21.87	0.612	15.67	0.580
4.00	22.24	0.605	16.01	0.571
4.50	22.58	0.599	16.33	0.563
5.00	22.91	0.593	16.64	0.556
5.50	23.22	0.587	16.93	0.549
6.00	23.51	0.582	17.20	0.543
7.00	24.06	0.572	17.71	0.530
8.00	24.56	0.562	18.17	0.519
9.00	25.02	0.553	18.60	0.508
10.00	25.45	0.545	18.99	0.499
12.00	26.22	0.530	19.69	0.481
14.00	26.91	0.516	20.32	0.465
16.00	27.54	0.503	20.89	0.450
18.00	28.11	0.492	21.40	0.437
20.00	28.62	0.481	21.88	0.424

Table 21. Relation between x (depth of source in Al), h (half-value layer in mylar) and Y (counting yield), for beta(-) sources. The quantity h represents the thickness of a mylar overlayer which reduces the transmission by a 50 percent (70 percent for 13Al28).

x (microns)	6C14		13Al28		15P32		16S35	
	h (mg/cm ²)	Y	h (mg/cm ²)	Y	h (mg/cm ²)	Y	h (mg/cm ²)	Y
0.00	0.77	0.701	63.59	0.689	63.87	0.695	0.70	0.701
0.05	0.90	0.658	63.73	0.689	64.12	0.694	0.85	0.648
0.10	0.96	0.636	63.83	0.689	64.26	0.693	0.92	0.623
0.15	1.01	0.619	63.91	0.689	64.38	0.692	0.98	0.605
0.20	1.05	0.604	63.98	0.688	64.48	0.692	1.02	0.589
0.25	1.08	0.591	64.04	0.688	64.58	0.691	1.06	0.575
0.30	1.11	0.580	64.10	0.688	64.66	0.691	1.10	0.563
0.40	1.17	0.559	64.21	0.688	64.83	0.690	1.16	0.542
0.50	1.22	0.542	64.32	0.687	64.98	0.689	1.22	0.524
0.60	1.26	0.526	64.42	0.687	65.11	0.688	1.27	0.508
0.70	1.30	0.512	64.51	0.687	65.24	0.687	1.31	0.494
0.80	1.34	0.499	64.61	0.687	65.37	0.687	1.35	0.481
0.90	1.37	0.487	64.69	0.686	65.49	0.686	1.39	0.469
1.00	1.40	0.475	64.78	0.686	65.60	0.685	1.42	0.458
1.25	1.47	0.450	64.99	0.685	65.88	0.684	1.50	0.433
1.50	1.53	0.428	65.18	0.685	66.13	0.682	1.57	0.412
1.75	1.58	0.408	65.37	0.684	66.38	0.680	1.63	0.393
2.00	1.63	0.391	65.56	0.683	66.61	0.679	1.68	0.376
2.50	1.71	0.360	65.90	0.682	67.04	0.676	1.78	0.346
3.00	1.77	0.333	66.23	0.681	67.44	0.674	1.85	0.321
3.50	1.83	0.310	66.54	0.680	67.81	0.671	1.92	0.300
4.00	1.89	0.290	66.84	0.679	68.17	0.669	1.99	0.280
4.50	1.93	0.272	67.13	0.678	68.51	0.667	2.04	0.264
5.00	1.98	0.256	67.42	0.677	68.84	0.665	2.09	0.248
5.50	2.01	0.241	67.69	0.676	69.15	0.663	2.14	0.234
6.00	2.05	0.228	67.96	0.675	69.46	0.660	2.18	0.222
7.00	2.11	0.204	68.48	0.673	70.04	0.656	2.25	0.199
8.00	2.16	0.184	68.97	0.671	70.58	0.653	2.31	0.180
9.00	2.20	0.166	69.44	0.669	71.09	0.649	2.36	0.164
10.00	2.23	0.150	69.90	0.668	71.58	0.645	2.41	0.149
12.00	2.28	0.125	70.78	0.664	72.49	0.639	2.48	0.125
14.00	2.32	0.104	71.60	0.661	73.34	0.632	2.53	0.106
16.00	2.36	0.087	72.39	0.658	74.12	0.626	2.58	0.090
18.00	2.38	0.074	73.14	0.655	74.86	0.620	2.61	0.076
20.00	2.39	0.062	73.86	0.652	75.54	0.614	2.63	0.065

Table 21, continued.

x (microns)	17Cl36		19K43		20Ca45		21Sc49	
	h (mg/cm ²)	Y	h (mg/cm ²)	Y	h (mg/cm ²)	Y	h (mg/cm ²)	Y
0.00	12.98	0.699	17.45	0.699	1.60	0.701	80.23	0.694
0.05	13.30	0.693	17.79	0.695	1.81	0.668	80.49	0.693
0.10	13.47	0.689	17.97	0.692	1.91	0.652	80.64	0.692
0.15	13.60	0.686	18.11	0.689	1.99	0.639	80.76	0.692
0.20	13.71	0.683	18.23	0.687	2.06	0.629	80.86	0.691
0.25	13.81	0.680	18.34	0.684	2.12	0.619	80.96	0.691
0.30	13.91	0.678	18.45	0.683	2.17	0.611	81.05	0.690
0.40	14.08	0.674	18.63	0.679	2.26	0.596	81.22	0.689
0.50	14.22	0.670	18.80	0.676	2.34	0.584	81.37	0.689
0.60	14.36	0.667	18.95	0.673	2.42	0.572	81.51	0.688
0.70	14.49	0.664	19.09	0.671	2.48	0.562	81.64	0.687
0.80	14.61	0.661	19.22	0.668	2.54	0.552	81.77	0.687
0.90	14.72	0.658	19.34	0.666	2.60	0.544	81.89	0.686
1.00	14.83	0.655	19.46	0.664	2.65	0.535	82.01	0.686
1.25	15.07	0.649	19.74	0.658	2.78	0.516	82.29	0.684
1.50	15.30	0.643	19.99	0.653	2.88	0.500	82.55	0.683
1.75	15.51	0.638	20.23	0.649	2.98	0.485	82.80	0.682
2.00	15.70	0.633	20.45	0.645	3.07	0.472	83.03	0.680
2.50	16.06	0.623	20.85	0.637	3.23	0.447	83.48	0.678
3.00	16.38	0.615	21.22	0.629	3.37	0.426	83.89	0.676
3.50	16.67	0.607	21.55	0.623	3.49	0.408	84.28	0.674
4.00	16.94	0.599	21.86	0.616	3.59	0.391	84.65	0.672
4.50	17.19	0.592	22.16	0.610	3.69	0.376	85.00	0.670
5.00	17.43	0.586	22.43	0.605	3.78	0.362	85.35	0.668
5.50	17.65	0.579	22.70	0.599	3.86	0.349	85.68	0.667
6.00	17.86	0.573	22.95	0.594	3.93	0.337	85.99	0.665
7.00	18.26	0.562	23.41	0.584	4.07	0.315	86.60	0.662
8.00	18.61	0.551	23.83	0.575	4.20	0.296	87.18	0.658
9.00	18.94	0.541	24.22	0.566	4.30	0.279	87.73	0.655
10.00	19.24	0.531	24.58	0.558	4.40	0.263	88.26	0.652
12.00	19.77	0.514	25.23	0.543	4.56	0.236	89.25	0.647
14.00	20.23	0.498	25.80	0.529	4.70	0.213	90.17	0.641
16.00	20.65	0.483	26.32	0.516	4.82	0.194	91.03	0.636
18.00	21.02	0.470	26.79	0.504	4.92	0.177	91.84	0.631
20.00	21.36	0.457	27.21	0.492	5.01	0.161	92.60	0.626

Table 21, continued

x (microns)	²² Ti51		²⁶ Fe59		²⁷ Co60		³¹ Ga72	
	h (mg/cm ²)	Y	h (mg/cm ²)	Y	h (mg/cm ²)	Y	h (mg/cm ²)	Y
0.00	86.34	0.693	2.96	0.701	2.31	0.701	23.11	0.697
0.05	86.59	0.692	3.25	0.683	2.56	0.674	23.59	0.694
0.10	86.76	0.692	3.39	0.671	2.68	0.661	23.90	0.691
0.15	86.87	0.691	3.50	0.661	2.77	0.650	24.15	0.688
0.20	86.98	0.691	3.60	0.653	2.85	0.641	24.35	0.686
0.25	87.08	0.690	3.68	0.646	2.93	0.634	24.50	0.684
0.30	87.17	0.690	3.76	0.640	2.99	0.627	24.65	0.682
0.40	87.34	0.689	3.89	0.629	3.10	0.614	24.92	0.679
0.50	87.49	0.689	4.01	0.619	3.20	0.604	25.17	0.676
0.60	87.64	0.688	4.12	0.610	3.29	0.594	25.40	0.673
0.70	87.78	0.687	4.21	0.602	3.37	0.585	25.61	0.671
0.80	87.90	0.687	4.31	0.595	3.44	0.577	25.81	0.668
0.90	88.03	0.686	4.39	0.588	3.51	0.570	26.00	0.666
1.00	88.15	0.686	4.47	0.581	3.58	0.562	26.18	0.664
1.25	88.44	0.684	4.66	0.566	3.73	0.546	26.60	0.659
1.50	88.70	0.683	4.83	0.553	3.86	0.532	26.98	0.654
1.75	88.96	0.682	4.98	0.541	3.99	0.519	27.33	0.650
2.00	89.20	0.681	5.13	0.530	4.10	0.507	27.66	0.646
2.50	89.65	0.679	5.38	0.511	4.30	0.486	28.28	0.639
3.00	90.08	0.677	5.60	0.494	4.47	0.467	28.83	0.632
3.50	90.48	0.675	5.80	0.479	4.63	0.450	29.34	0.626
4.00	90.86	0.673	5.98	0.465	4.76	0.435	29.82	0.620
4.50	91.23	0.671	6.15	0.452	4.89	0.421	30.27	0.615
5.00	91.58	0.669	6.31	0.440	5.00	0.409	30.69	0.610
5.50	91.92	0.668	6.46	0.429	5.11	0.397	31.10	0.605
6.00	92.25	0.666	6.60	0.419	5.21	0.386	31.49	0.600
7.00	92.88	0.663	6.86	0.400	5.40	0.365	32.22	0.592
8.00	93.47	0.660	7.09	0.383	5.56	0.347	32.90	0.584
9.00	94.03	0.657	7.30	0.368	5.71	0.331	33.53	0.576
10.00	94.57	0.654	7.50	0.354	5.84	0.316	34.12	0.569
12.00	95.59	0.649	7.85	0.329	6.07	0.290	35.21	0.556
14.00	96.53	0.644	8.16	0.307	6.26	0.267	36.20	0.544
16.00	97.40	0.639	8.44	0.288	6.43	0.247	37.11	0.532
18.00	98.22	0.634	8.70	0.271	6.58	0.230	37.95	0.522
20.00	98.99	0.629	8.93	0.256	6.71	0.214	38.74	0.512

Table 21, continued

x (microns)	38Sr90 39Y90		43Tc99		47Ag110		51Sb124	
	h (mg/cm ²)	Y	h (mg/cm ²)	Y	h (mg/cm ²)	Y	h (mg/cm ²)	Y
0.00	24.66	0.696	1.80	0.701	0.36	0.701	12.36	0.698
0.05	25.35	0.690	2.03	0.669	0.53	0.641	13.03	0.690
0.10	25.71	0.686	2.15	0.654	0.61	0.603	13.45	0.684
0.15	25.99	0.684	2.24	0.642	0.68	0.575	13.72	0.679
0.20	26.23	0.681	2.31	0.632	0.74	0.553	13.94	0.675
0.25	26.45	0.679	2.38	0.623	0.79	0.535	14.15	0.671
0.30	26.64	0.677	2.44	0.615	0.85	0.519	14.35	0.668
0.40	26.99	0.674	2.54	0.601	0.94	0.492	14.70	0.662
0.50	27.31	0.670	2.64	0.589	1.03	0.470	15.01	0.657
0.60	27.59	0.668	2.72	0.578	1.12	0.451	15.29	0.652
0.70	27.86	0.665	2.80	0.568	1.20	0.435	15.55	0.647
0.80	28.11	0.662	2.87	0.559	1.29	0.420	15.78	0.643
0.90	28.34	0.660	2.93	0.550	1.37	0.407	16.00	0.640
1.00	28.57	0.658	2.99	0.542	1.45	0.395	16.21	0.636
1.25	29.09	0.653	3.13	0.525	1.65	0.370	16.71	0.628
1.50	29.57	0.648	3.25	0.509	1.86	0.349	17.17	0.621
1.75	30.01	0.644	3.37	0.495	2.08	0.331	17.59	0.614
2.00	30.43	0.640	3.47	0.482	2.32	0.315	17.97	0.608
2.50	31.20	0.632	3.66	0.459	2.83	0.290	18.68	0.597
3.00	31.89	0.626	3.82	0.439	3.40	0.270	19.33	0.587
3.50	32.54	0.620	3.96	0.421	4.02	0.253	19.92	0.578
4.00	33.14	0.614	4.09	0.405	4.66	0.239	20.47	0.570
4.50	33.71	0.609	4.21	0.391	5.31	0.227	20.99	0.563
5.00	34.25	0.604	4.31	0.377	5.95	0.217	21.48	0.556
5.50	34.77	0.599	4.41	0.365	6.56	0.207	21.95	0.549
6.00	35.26	0.594	4.51	0.353	7.13	0.199	22.40	0.543
7.00	36.20	0.586	4.67	0.332	8.15	0.186	23.24	0.531
8.00	37.07	0.578	4.82	0.314	9.03	0.175	24.03	0.521
9.00	37.89	0.571	4.96	0.297	9.78	0.166	24.75	0.511
10.00	38.66	0.563	5.08	0.282	10.42	0.158	25.44	0.502
12.00	40.09	0.551	5.29	0.256	11.45	0.146	26.70	0.486
14.00	41.41	0.539	5.47	0.234	12.22	0.136	27.86	0.472
16.00	42.66	0.529	5.63	0.214	12.83	0.129	28.93	0.458
18.00	43.83	0.519	5.76	0.198	13.30	0.123	29.94	0.447
20.00	44.96	0.509	5.88	0.183	13.68	0.117	30.89	0.436

Table 22. Counting yield $\langle Y_b(x_0) \rangle$ of beta (-) sources distributed uniformly to depth x_0 in sand (silica, SiO_2).

$x_0, \text{g/cm}^2$	1H3	6C14	13Al28	15P32	16S35	17Cl36
0.0000	0.688	0.688	0.678	0.683	0.688	0.687
0.0002	0.175	0.566	0.677	0.678	0.552	0.665
0.0004	0.092	0.511	0.675	0.675	0.495	0.653
0.0006	0.061	0.471	0.674	0.673	0.456	0.643
0.0008	0.046	0.440	0.673	0.671	0.426	0.635
0.0010	0.037	0.415	0.673	0.669	0.401	0.627
0.0012	0.031	0.393	0.672	0.667	0.379	0.621
0.0014	0.026	0.373	0.671	0.665	0.361	0.614
0.0016	0.023	0.356	0.670	0.663	0.344	0.608
0.0018	0.020	0.340	0.669	0.661	0.329	0.603
0.0020	0.018	0.326	0.669	0.660	0.316	0.598
0.0022	0.017	0.313	0.668	0.658	0.304	0.593
0.0024	0.015	0.301	0.667	0.656	0.292	0.588
0.0026	0.014	0.290	0.666	0.655	0.282	0.583
0.0028	0.013	0.280	0.666	0.653	0.272	0.579
0.0030	0.012	0.271	0.665	0.652	0.263	0.575
0.0032	0.012	0.262	0.664	0.650	0.255	0.570
0.0034	0.011	0.253	0.664	0.649	0.247	0.566
0.0036	0.010	0.246	0.663	0.648	0.239	0.562
0.0038	0.010	0.238	0.662	0.646	0.232	0.559
0.0040	0.009	0.231	0.662	0.645	0.226	0.555
0.0042	0.009	0.225	0.661	0.644	0.219	0.551
0.0044	0.008	0.218	0.660	0.642	0.214	0.548
0.0046	0.008	0.212	0.660	0.641	0.208	0.544
0.0048	0.008	0.207	0.659	0.640	0.202	0.541
0.0050	0.007	0.201	0.659	0.638	0.197	0.538
0.0052	0.007	0.196	0.658	0.637	0.192	0.535
0.0054	0.007	0.191	0.657	0.636	0.188	0.532
0.0056	0.007	0.186	0.657	0.635	0.183	0.528
0.0058	0.006	0.182	0.656	0.634	0.179	0.525
0.0060	0.006	0.177	0.656	0.632	0.175	0.523
0.0064	0.006	0.169	0.654	0.630	0.167	0.517
0.0068	0.005	0.162	0.653	0.628	0.160	0.511
0.0072	0.005	0.155	0.652	0.626	0.153	0.506
0.0076	0.005	0.148	0.651	0.623	0.147	0.501
0.0080	0.005	0.142	0.650	0.621	0.141	0.496
0.0084	0.004	0.137	0.649	0.619	0.136	0.491
0.0088	0.004	0.132	0.648	0.617	0.131	0.486
0.0092	0.004	0.127	0.647	0.615	0.126	0.482
0.0096	0.004	0.122	0.646	0.613	0.122	0.477
0.0100	0.004	0.118	0.644	0.611	0.118	0.473

Table 22, continued.

$x_O, g/cm^2$	19K43	20Ca45	21Sc49	22Ti51	26Fe59	27Co60
0.0000	0.686	0.688	0.682	0.681	0.688	0.688
0.0002	0.669	0.598	0.678	0.678	0.625	0.614
0.0004	0.659	0.558	0.676	0.676	0.595	0.579
0.0006	0.651	0.528	0.673	0.674	0.572	0.554
0.0008	0.644	0.505	0.672	0.672	0.553	0.534
0.0010	0.638	0.485	0.670	0.670	0.537	0.516
0.0012	0.632	0.468	0.668	0.669	0.524	0.501
0.0014	0.627	0.452	0.667	0.667	0.511	0.487
0.0016	0.622	0.438	0.665	0.666	0.500	0.475
0.0018	0.617	0.426	0.664	0.664	0.489	0.463
0.0020	0.613	0.414	0.662	0.663	0.479	0.453
0.0022	0.609	0.403	0.661	0.662	0.470	0.443
0.0024	0.605	0.393	0.660	0.661	0.462	0.434
0.0026	0.601	0.383	0.658	0.659	0.454	0.425
0.0028	0.597	0.374	0.657	0.658	0.446	0.417
0.0030	0.593	0.366	0.656	0.657	0.439	0.409
0.0032	0.590	0.358	0.655	0.656	0.432	0.402
0.0034	0.586	0.350	0.654	0.655	0.425	0.395
0.0036	0.583	0.343	0.652	0.654	0.419	0.388
0.0038	0.579	0.336	0.651	0.653	0.413	0.381
0.0040	0.576	0.330	0.650	0.651	0.407	0.375
0.0042	0.573	0.323	0.649	0.650	0.401	0.369
0.0044	0.570	0.317	0.648	0.649	0.396	0.363
0.0046	0.567	0.312	0.647	0.648	0.391	0.358
0.0048	0.564	0.306	0.646	0.647	0.386	0.353
0.0050	0.561	0.301	0.645	0.646	0.381	0.348
0.0052	0.559	0.296	0.644	0.645	0.376	0.343
0.0054	0.556	0.291	0.643	0.644	0.372	0.338
0.0056	0.553	0.286	0.642	0.643	0.367	0.333
0.0058	0.551	0.281	0.641	0.642	0.363	0.329
0.0060	0.548	0.277	0.640	0.642	0.359	0.324
0.0064	0.543	0.268	0.638	0.640	0.351	0.316
0.0068	0.538	0.260	0.636	0.638	0.344	0.308
0.0072	0.533	0.252	0.634	0.636	0.336	0.300
0.0076	0.529	0.245	0.632	0.634	0.330	0.293
0.0080	0.524	0.238	0.630	0.633	0.323	0.287
0.0084	0.520	0.232	0.628	0.631	0.317	0.280
0.0088	0.516	0.226	0.627	0.629	0.311	0.274
0.0092	0.512	0.220	0.625	0.628	0.305	0.268
0.0096	0.508	0.214	0.623	0.626	0.300	0.262
0.0100	0.504	0.209	0.621	0.624	0.294	0.257

Table 22, continued.

$x_0, \text{g/cm}^2$	29Cu64	38Sr90	39Y90	43Tc99	47Ag110	51Sb124
0.0000	0.687	0.687	0.681	0.688	0.688	0.685
0.0002	0.652	0.652	0.676	0.602	0.510	0.654
0.0004	0.634	0.635	0.673	0.563	0.444	0.637
0.0006	0.621	0.621	0.671	0.535	0.402	0.625
0.0008	0.609	0.610	0.669	0.513	0.371	0.615
0.0010	0.599	0.600	0.667	0.494	0.348	0.606
0.0012	0.590	0.591	0.666	0.477	0.329	0.598
0.0014	0.582	0.583	0.664	0.463	0.312	0.591
0.0016	0.574	0.576	0.662	0.449	0.299	0.584
0.0018	0.567	0.569	0.661	0.437	0.287	0.578
0.0020	0.560	0.562	0.659	0.426	0.276	0.572
0.0022	0.554	0.556	0.658	0.416	0.267	0.567
0.0024	0.547	0.550	0.657	0.406	0.258	0.562
0.0026	0.542	0.544	0.655	0.397	0.251	0.557
0.0028	0.536	0.539	0.654	0.388	0.244	0.552
0.0030	0.531	0.534	0.653	0.380	0.238	0.548
0.0032	0.526	0.529	0.652	0.373	0.232	0.544
0.0034	0.521	0.524	0.651	0.365	0.227	0.540
0.0036	0.516	0.519	0.649	0.358	0.222	0.536
0.0038	0.511	0.515	0.648	0.352	0.217	0.532
0.0040	0.507	0.510	0.647	0.345	0.213	0.529
0.0042	0.502	0.506	0.646	0.339	0.209	0.525
0.0044	0.498	0.502	0.645	0.333	0.205	0.522
0.0046	0.494	0.498	0.644	0.328	0.202	0.518
0.0048	0.490	0.494	0.643	0.322	0.198	0.515
0.0050	0.486	0.491	0.642	0.317	0.195	0.512
0.0052	0.482	0.487	0.641	0.312	0.192	0.509
0.0054	0.479	0.483	0.640	0.307	0.189	0.506
0.0056	0.475	0.480	0.639	0.303	0.187	0.503
0.0058	0.471	0.476	0.638	0.298	0.184	0.500
0.0060	0.468	0.473	0.637	0.294	0.182	0.498
0.0064	0.461	0.466	0.635	0.286	0.177	0.492
0.0068	0.455	0.460	0.633	0.278	0.173	0.487
0.0072	0.449	0.454	0.631	0.270	0.169	0.483
0.0076	0.443	0.448	0.629	0.263	0.165	0.478
0.0080	0.437	0.443	0.628	0.256	0.162	0.473
0.0084	0.431	0.437	0.626	0.250	0.159	0.469
0.0088	0.426	0.432	0.624	0.244	0.156	0.465
0.0092	0.421	0.427	0.623	0.238	0.153	0.461
0.0096	0.416	0.422	0.621	0.233	0.150	0.457
0.0100	0.411	0.418	0.619	0.228	0.148	0.453

Table 22, continued.

$x_0, \text{g/cm}^2$	53I131	55Cs137	61Pm147	77Ir192	79Au198	81Tl204
0.0000	0.687	0.687	0.688	0.687	0.686	0.687
0.0002	0.646	0.648	0.573	0.644	0.664	0.655
0.0004	0.626	0.628	0.523	0.623	0.653	0.638
0.0006	0.611	0.613	0.489	0.607	0.644	0.626
0.0008	0.598	0.601	0.462	0.594	0.636	0.616
0.0010	0.587	0.590	0.440	0.583	0.629	0.607
0.0012	0.577	0.580	0.420	0.572	0.623	0.599
0.0014	0.568	0.571	0.403	0.563	0.618	0.592
0.0016	0.559	0.563	0.388	0.555	0.612	0.585
0.0018	0.552	0.555	0.375	0.547	0.607	0.579
0.0020	0.544	0.548	0.362	0.539	0.603	0.573
0.0022	0.538	0.542	0.351	0.532	0.598	0.567
0.0024	0.531	0.535	0.340	0.526	0.594	0.562
0.0026	0.525	0.529	0.330	0.520	0.590	0.557
0.0028	0.519	0.523	0.321	0.514	0.586	0.552
0.0030	0.513	0.518	0.312	0.508	0.582	0.547
0.0032	0.508	0.513	0.304	0.502	0.578	0.543
0.0034	0.503	0.508	0.296	0.497	0.575	0.539
0.0036	0.498	0.503	0.289	0.492	0.571	0.534
0.0038	0.493	0.498	0.282	0.487	0.568	0.530
0.0040	0.488	0.493	0.276	0.483	0.565	0.526
0.0042	0.484	0.489	0.269	0.478	0.562	0.523
0.0044	0.479	0.485	0.263	0.474	0.559	0.519
0.0046	0.475	0.480	0.258	0.469	0.556	0.515
0.0048	0.471	0.476	0.252	0.465	0.553	0.512
0.0050	0.467	0.472	0.247	0.461	0.550	0.509
0.0052	0.463	0.469	0.242	0.457	0.547	0.505
0.0054	0.459	0.465	0.237	0.453	0.544	0.502
0.0056	0.456	0.461	0.233	0.450	0.542	0.499
0.0058	0.452	0.458	0.228	0.446	0.539	0.496
0.0060	0.449	0.454	0.224	0.443	0.537	0.493
0.0064	0.442	0.447	0.216	0.436	0.532	0.487
0.0068	0.435	0.441	0.208	0.429	0.527	0.481
0.0072	0.429	0.435	0.201	0.423	0.522	0.476
0.0076	0.423	0.429	0.195	0.417	0.517	0.471
0.0080	0.417	0.423	0.188	0.411	0.513	0.466
0.0084	0.412	0.418	0.182	0.406	0.509	0.461
0.0088	0.406	0.412	0.177	0.400	0.505	0.456
0.0092	0.401	0.407	0.172	0.395	0.501	0.452
0.0096	0.396	0.402	0.167	0.390	0.497	0.447
0.0100	0.391	0.397	0.162	0.385	0.493	0.443

Table 23. Counting yield $\langle Y_b(x_0) \rangle$ of beta (-) sources distributed uniformly to depth x_0 in dry soil.

$x_0, \text{g/cm}^2$	1H3	6C14	13Al28	15P32	16S35	17Cl36
0.0000	0.695	0.695	0.684	0.689	0.695	0.693
0.0002	0.176	0.571	0.682	0.685	0.557	0.671
0.0004	0.092	0.515	0.681	0.682	0.499	0.659
0.0006	0.062	0.475	0.680	0.679	0.460	0.649
0.0008	0.046	0.444	0.679	0.677	0.429	0.641
0.0010	0.037	0.417	0.678	0.675	0.403	0.633
0.0012	0.031	0.395	0.678	0.673	0.382	0.626
0.0014	0.026	0.375	0.677	0.671	0.363	0.620
0.0016	0.023	0.358	0.676	0.669	0.346	0.614
0.0018	0.021	0.342	0.675	0.667	0.331	0.608
0.0020	0.019	0.328	0.674	0.665	0.317	0.603
0.0022	0.017	0.315	0.674	0.664	0.305	0.598
0.0024	0.015	0.303	0.673	0.662	0.293	0.593
0.0026	0.014	0.291	0.672	0.661	0.283	0.588
0.0028	0.013	0.281	0.671	0.659	0.273	0.584
0.0030	0.012	0.272	0.671	0.658	0.264	0.579
0.0032	0.012	0.263	0.670	0.656	0.256	0.575
0.0034	0.011	0.254	0.669	0.655	0.248	0.571
0.0036	0.010	0.246	0.669	0.653	0.240	0.567
0.0038	0.010	0.239	0.668	0.652	0.233	0.563
0.0040	0.009	0.232	0.667	0.651	0.226	0.560
0.0042	0.009	0.225	0.667	0.649	0.220	0.556
0.0044	0.008	0.219	0.666	0.648	0.214	0.552
0.0046	0.008	0.213	0.665	0.647	0.208	0.549
0.0048	0.008	0.207	0.665	0.645	0.203	0.545
0.0050	0.007	0.201	0.664	0.644	0.198	0.542
0.0052	0.007	0.196	0.663	0.643	0.193	0.539
0.0054	0.007	0.191	0.663	0.641	0.188	0.536
0.0056	0.007	0.186	0.662	0.640	0.183	0.533
0.0058	0.006	0.182	0.662	0.639	0.179	0.530
0.0060	0.006	0.178	0.661	0.638	0.175	0.527
0.0064	0.006	0.169	0.660	0.635	0.167	0.521
0.0068	0.005	0.162	0.659	0.633	0.160	0.515
0.0072	0.005	0.155	0.657	0.631	0.153	0.510
0.0076	0.005	0.148	0.656	0.629	0.147	0.504
0.0080	0.005	0.142	0.655	0.626	0.141	0.499
0.0084	0.004	0.137	0.654	0.624	0.136	0.494
0.0088	0.004	0.132	0.653	0.622	0.131	0.490
0.0092	0.004	0.127	0.652	0.620	0.126	0.485
0.0096	0.004	0.122	0.651	0.618	0.122	0.480
0.0100	0.004	0.118	0.650	0.616	0.118	0.476

Table 23, continued.

$x_O, \text{g/cm}^2$	19K43	20Ca45	21Sc49	22Ti51	26Fe59	27Co60
0.0000	0.693	0.695	0.688	0.687	0.694	0.694
0.0002	0.675	0.604	0.684	0.684	0.631	0.619
0.0004	0.665	0.562	0.682	0.682	0.600	0.584
0.0006	0.657	0.533	0.680	0.680	0.577	0.559
0.0008	0.650	0.509	0.678	0.678	0.558	0.538
0.0010	0.644	0.489	0.676	0.676	0.542	0.520
0.0012	0.638	0.471	0.674	0.675	0.528	0.505
0.0014	0.633	0.455	0.673	0.673	0.515	0.491
0.0016	0.628	0.441	0.671	0.672	0.503	0.478
0.0018	0.623	0.428	0.670	0.670	0.493	0.467
0.0020	0.618	0.416	0.668	0.669	0.483	0.456
0.0022	0.614	0.405	0.667	0.668	0.474	0.446
0.0024	0.610	0.395	0.666	0.666	0.465	0.437
0.0026	0.606	0.386	0.664	0.665	0.457	0.428
0.0028	0.602	0.376	0.663	0.664	0.449	0.419
0.0030	0.598	0.368	0.662	0.663	0.442	0.412
0.0032	0.595	0.360	0.660	0.662	0.435	0.404
0.0034	0.591	0.352	0.659	0.660	0.428	0.397
0.0036	0.588	0.345	0.658	0.659	0.422	0.390
0.0038	0.584	0.338	0.657	0.658	0.415	0.383
0.0040	0.581	0.331	0.656	0.657	0.410	0.377
0.0042	0.578	0.325	0.655	0.656	0.404	0.371
0.0044	0.575	0.319	0.653	0.655	0.398	0.365
0.0046	0.572	0.313	0.652	0.654	0.393	0.360
0.0048	0.569	0.307	0.651	0.653	0.388	0.354
0.0050	0.566	0.302	0.650	0.652	0.383	0.349
0.0052	0.563	0.297	0.649	0.651	0.378	0.344
0.0054	0.560	0.292	0.648	0.650	0.374	0.339
0.0056	0.558	0.287	0.647	0.649	0.369	0.335
0.0058	0.555	0.282	0.646	0.648	0.365	0.330
0.0060	0.552	0.277	0.645	0.647	0.361	0.326
0.0064	0.547	0.269	0.643	0.645	0.353	0.317
0.0068	0.542	0.261	0.641	0.643	0.345	0.309
0.0072	0.538	0.253	0.639	0.641	0.338	0.301
0.0076	0.533	0.246	0.637	0.640	0.331	0.294
0.0080	0.528	0.239	0.635	0.638	0.324	0.287
0.0084	0.524	0.232	0.634	0.636	0.318	0.281
0.0088	0.520	0.226	0.632	0.634	0.312	0.275
0.0092	0.516	0.220	0.630	0.633	0.306	0.269
0.0096	0.511	0.215	0.628	0.631	0.301	0.263
0.0100	0.508	0.209	0.627	0.629	0.295	0.257

Table 23, continued.

$x_0, \text{g/cm}^2$	29Cu64	38Sr90	39Y90	43Tc99	47Ag110	51Sb124
0.0000	0.694	0.694	0.687	0.695	0.695	0.692
0.0002	0.658	0.658	0.682	0.607	0.515	0.660
0.0004	0.640	0.640	0.679	0.568	0.447	0.643
0.0006	0.626	0.627	0.677	0.540	0.405	0.631
0.0008	0.615	0.615	0.675	0.517	0.374	0.620
0.0010	0.604	0.606	0.673	0.498	0.350	0.611
0.0012	0.595	0.597	0.671	0.481	0.331	0.603
0.0014	0.587	0.588	0.670	0.466	0.314	0.596
0.0016	0.579	0.581	0.668	0.453	0.300	0.589
0.0018	0.572	0.574	0.667	0.440	0.288	0.583
0.0020	0.565	0.567	0.665	0.429	0.278	0.577
0.0022	0.558	0.561	0.664	0.418	0.268	0.572
0.0024	0.552	0.555	0.662	0.409	0.260	0.567
0.0026	0.546	0.549	0.661	0.399	0.252	0.562
0.0028	0.540	0.543	0.660	0.391	0.245	0.557
0.0030	0.535	0.538	0.659	0.382	0.239	0.553
0.0032	0.530	0.533	0.657	0.375	0.233	0.548
0.0034	0.525	0.528	0.656	0.367	0.228	0.544
0.0036	0.520	0.523	0.655	0.360	0.223	0.540
0.0038	0.515	0.519	0.654	0.353	0.218	0.536
0.0040	0.511	0.514	0.653	0.347	0.214	0.533
0.0042	0.506	0.510	0.652	0.341	0.210	0.529
0.0044	0.502	0.506	0.650	0.335	0.206	0.526
0.0046	0.498	0.502	0.649	0.329	0.203	0.522
0.0048	0.494	0.498	0.648	0.324	0.199	0.519
0.0050	0.490	0.494	0.647	0.319	0.196	0.516
0.0052	0.486	0.490	0.646	0.314	0.193	0.513
0.0054	0.482	0.487	0.645	0.309	0.190	0.510
0.0056	0.478	0.483	0.644	0.304	0.188	0.507
0.0058	0.475	0.480	0.643	0.299	0.185	0.504
0.0060	0.471	0.476	0.642	0.295	0.183	0.501
0.0064	0.464	0.470	0.640	0.286	0.178	0.496
0.0068	0.458	0.463	0.638	0.279	0.174	0.491
0.0072	0.452	0.457	0.637	0.271	0.170	0.486
0.0076	0.446	0.451	0.635	0.264	0.166	0.481
0.0080	0.440	0.446	0.633	0.257	0.163	0.477
0.0084	0.434	0.440	0.631	0.251	0.159	0.472
0.0088	0.429	0.435	0.629	0.245	0.156	0.468
0.0092	0.423	0.430	0.628	0.239	0.153	0.464
0.0096	0.418	0.425	0.626	0.233	0.151	0.460
0.0100	0.413	0.420	0.624	0.228	0.148	0.456

Table 23, continued.

$x_0, \text{g/cm}^2$	53I131	55Cs137	61Pm147	77Ir192	79Au198	81Tl204
0.0000	0.694	0.694	0.695	0.694	0.693	0.693
0.0002	0.653	0.654	0.578	0.650	0.671	0.661
0.0004	0.632	0.634	0.528	0.629	0.659	0.644
0.0006	0.616	0.619	0.493	0.613	0.650	0.632
0.0008	0.603	0.606	0.466	0.599	0.642	0.622
0.0010	0.592	0.595	0.443	0.588	0.635	0.613
0.0012	0.582	0.585	0.423	0.577	0.629	0.604
0.0014	0.573	0.576	0.406	0.568	0.623	0.597
0.0016	0.564	0.568	0.391	0.559	0.618	0.590
0.0018	0.556	0.560	0.377	0.551	0.613	0.584
0.0020	0.549	0.553	0.364	0.544	0.608	0.578
0.0022	0.542	0.546	0.352	0.537	0.603	0.572
0.0024	0.535	0.540	0.342	0.530	0.599	0.567
0.0026	0.529	0.533	0.332	0.524	0.595	0.562
0.0028	0.523	0.528	0.322	0.518	0.591	0.557
0.0030	0.517	0.522	0.314	0.512	0.587	0.552
0.0032	0.512	0.517	0.305	0.506	0.583	0.547
0.0034	0.507	0.511	0.298	0.501	0.580	0.543
0.0036	0.502	0.506	0.290	0.496	0.576	0.539
0.0038	0.497	0.502	0.283	0.491	0.573	0.535
0.0040	0.492	0.497	0.277	0.486	0.570	0.531
0.0042	0.487	0.492	0.270	0.482	0.566	0.527
0.0044	0.483	0.488	0.264	0.477	0.563	0.523
0.0046	0.479	0.484	0.259	0.473	0.560	0.519
0.0048	0.474	0.480	0.253	0.469	0.557	0.516
0.0050	0.470	0.476	0.248	0.464	0.554	0.513
0.0052	0.466	0.472	0.243	0.460	0.552	0.509
0.0054	0.463	0.468	0.238	0.457	0.549	0.506
0.0056	0.459	0.464	0.233	0.453	0.546	0.503
0.0058	0.455	0.461	0.229	0.449	0.543	0.500
0.0060	0.452	0.457	0.224	0.446	0.541	0.497
0.0064	0.445	0.450	0.216	0.439	0.536	0.491
0.0068	0.438	0.444	0.209	0.432	0.531	0.485
0.0072	0.432	0.438	0.201	0.426	0.526	0.479
0.0076	0.426	0.431	0.195	0.420	0.521	0.474
0.0080	0.420	0.426	0.189	0.414	0.517	0.469
0.0084	0.414	0.420	0.183	0.408	0.513	0.464
0.0088	0.409	0.415	0.177	0.403	0.508	0.459
0.0092	0.403	0.409	0.172	0.397	0.504	0.455
0.0096	0.398	0.404	0.167	0.392	0.500	0.450
0.0100	0.393	0.399	0.162	0.387	0.496	0.446

Table 24. Counting yield $\langle Y_b(x_0) \rangle$ of beta (-) sources distributed uniformly to depth x_0 in loam.

$x_0, \text{g/cm}^2$	1H3	6C14	13Al28	15P32	16S35	17Cl36
0.0000	0.678	0.678	0.669	0.673	0.678	0.677
0.0002	0.170	0.556	0.668	0.669	0.543	0.655
0.0004	0.089	0.501	0.667	0.666	0.486	0.643
0.0006	0.059	0.463	0.666	0.664	0.448	0.633
0.0008	0.044	0.432	0.665	0.661	0.418	0.625
0.0010	0.036	0.407	0.664	0.659	0.393	0.618
0.0012	0.030	0.385	0.663	0.657	0.372	0.611
0.0014	0.025	0.366	0.662	0.655	0.354	0.605
0.0016	0.022	0.349	0.661	0.654	0.337	0.599
0.0018	0.020	0.333	0.661	0.652	0.323	0.593
0.0020	0.018	0.320	0.660	0.650	0.309	0.588
0.0022	0.016	0.307	0.659	0.649	0.297	0.583
0.0024	0.015	0.295	0.658	0.647	0.286	0.579
0.0026	0.014	0.284	0.658	0.645	0.276	0.574
0.0028	0.013	0.274	0.657	0.644	0.267	0.570
0.0030	0.012	0.265	0.656	0.642	0.258	0.565
0.0032	0.011	0.256	0.656	0.641	0.249	0.561
0.0034	0.010	0.248	0.655	0.640	0.242	0.557
0.0036	0.010	0.240	0.654	0.638	0.234	0.553
0.0038	0.009	0.233	0.654	0.637	0.227	0.550
0.0040	0.009	0.226	0.653	0.636	0.221	0.546
0.0042	0.008	0.220	0.652	0.634	0.215	0.542
0.0044	0.008	0.213	0.652	0.633	0.209	0.539
0.0046	0.008	0.208	0.651	0.632	0.203	0.536
0.0048	0.007	0.202	0.650	0.630	0.198	0.532
0.0050	0.007	0.197	0.650	0.629	0.193	0.529
0.0052	0.007	0.192	0.649	0.628	0.188	0.526
0.0054	0.007	0.187	0.649	0.627	0.184	0.523
0.0056	0.006	0.182	0.648	0.626	0.179	0.520
0.0058	0.006	0.178	0.647	0.624	0.175	0.517
0.0060	0.006	0.173	0.647	0.623	0.171	0.514
0.0064	0.006	0.165	0.646	0.621	0.163	0.508
0.0068	0.005	0.158	0.645	0.619	0.156	0.503
0.0072	0.005	0.151	0.643	0.616	0.150	0.498
0.0076	0.005	0.145	0.642	0.614	0.144	0.493
0.0080	0.004	0.139	0.641	0.612	0.138	0.488
0.0084	0.004	0.133	0.640	0.610	0.133	0.483
0.0088	0.004	0.128	0.639	0.608	0.128	0.478
0.0092	0.004	0.124	0.638	0.606	0.123	0.474
0.0100	0.004	0.115	0.636	0.602	0.115	0.465

Table 24, continued.

$x_O, g/cm^2$	19K43	20Ca45	21Sc49	22Ti51	26Fe59	27Co60
0.0000	0.676	0.678	0.673	0.672	0.678	0.678
0.0002	0.659	0.588	0.669	0.669	0.615	0.604
0.0004	0.649	0.548	0.666	0.666	0.585	0.569
0.0006	0.641	0.519	0.664	0.664	0.562	0.545
0.0008	0.634	0.496	0.662	0.663	0.544	0.525
0.0010	0.628	0.476	0.661	0.661	0.528	0.507
0.0012	0.623	0.459	0.659	0.659	0.515	0.492
0.0014	0.617	0.444	0.657	0.658	0.502	0.479
0.0016	0.613	0.430	0.656	0.657	0.491	0.466
0.0018	0.608	0.418	0.655	0.655	0.481	0.455
0.0020	0.603	0.406	0.653	0.654	0.471	0.445
0.0022	0.599	0.395	0.652	0.653	0.462	0.435
0.0024	0.595	0.386	0.650	0.651	0.453	0.426
0.0026	0.591	0.376	0.649	0.650	0.446	0.417
0.0028	0.587	0.367	0.648	0.649	0.438	0.409
0.0030	0.584	0.359	0.647	0.648	0.431	0.402
0.0032	0.580	0.351	0.646	0.647	0.424	0.394
0.0034	0.577	0.344	0.644	0.646	0.418	0.387
0.0036	0.574	0.337	0.643	0.644	0.411	0.381
0.0038	0.570	0.330	0.642	0.643	0.405	0.374
0.0040	0.567	0.323	0.641	0.642	0.400	0.368
0.0042	0.564	0.317	0.640	0.641	0.394	0.362
0.0044	0.561	0.311	0.639	0.640	0.389	0.357
0.0046	0.558	0.306	0.638	0.639	0.384	0.351
0.0048	0.555	0.300	0.637	0.638	0.379	0.346
0.0050	0.552	0.295	0.636	0.637	0.374	0.341
0.0052	0.550	0.290	0.634	0.636	0.370	0.336
0.0054	0.547	0.285	0.633	0.635	0.365	0.332
0.0056	0.544	0.280	0.632	0.634	0.361	0.327
0.0058	0.542	0.276	0.631	0.633	0.357	0.323
0.0060	0.539	0.271	0.630	0.632	0.353	0.318
0.0064	0.534	0.263	0.629	0.631	0.345	0.310
0.0068	0.529	0.255	0.627	0.629	0.337	0.302
0.0072	0.525	0.247	0.625	0.627	0.330	0.295
0.0076	0.520	0.240	0.623	0.625	0.323	0.288
0.0080	0.516	0.234	0.621	0.624	0.317	0.281
0.0084	0.512	0.227	0.619	0.622	0.311	0.275
0.0088	0.508	0.221	0.618	0.620	0.305	0.269
0.0092	0.504	0.216	0.616	0.619	0.299	0.263
0.0096	0.500	0.210	0.614	0.617	0.294	0.257
0.0100	0.496	0.205	0.612	0.615	0.289	0.252

Table 24, continued.

$x_0, \text{g/cm}^2$	29Cu64	38Sr90	39Y90	43Tc99	47Ag110	51Sb124
0.0000	0.677	0.677	0.672	0.678	0.678	0.676
0.0002	0.642	0.642	0.667	0.592	0.501	0.644
0.0004	0.625	0.625	0.664	0.554	0.435	0.628
0.0006	0.611	0.611	0.662	0.526	0.394	0.616
0.0008	0.600	0.600	0.660	0.504	0.364	0.605
0.0010	0.590	0.591	0.658	0.485	0.341	0.597
0.0012	0.581	0.582	0.656	0.469	0.322	0.589
0.0014	0.572	0.574	0.655	0.454	0.306	0.582
0.0016	0.565	0.566	0.653	0.441	0.293	0.575
0.0018	0.558	0.560	0.652	0.429	0.281	0.569
0.0020	0.551	0.553	0.650	0.418	0.271	0.563
0.0022	0.545	0.547	0.649	0.408	0.261	0.558
0.0024	0.538	0.541	0.648	0.398	0.253	0.553
0.0026	0.533	0.535	0.646	0.390	0.246	0.548
0.0028	0.527	0.530	0.645	0.381	0.239	0.544
0.0030	0.522	0.525	0.644	0.373	0.233	0.539
0.0032	0.517	0.520	0.643	0.366	0.227	0.535
0.0034	0.512	0.515	0.642	0.358	0.222	0.531
0.0036	0.507	0.511	0.640	0.352	0.217	0.528
0.0038	0.503	0.506	0.639	0.345	0.213	0.524
0.0040	0.498	0.502	0.638	0.339	0.209	0.520
0.0042	0.494	0.498	0.637	0.333	0.205	0.517
0.0044	0.490	0.494	0.636	0.327	0.201	0.513
0.0046	0.486	0.490	0.635	0.322	0.198	0.510
0.0048	0.482	0.486	0.634	0.316	0.194	0.507
0.0050	0.478	0.482	0.633	0.311	0.191	0.504
0.0052	0.474	0.479	0.632	0.306	0.188	0.501
0.0054	0.470	0.475	0.631	0.302	0.186	0.498
0.0056	0.467	0.472	0.630	0.297	0.183	0.495
0.0058	0.463	0.468	0.629	0.293	0.180	0.492
0.0060	0.460	0.465	0.628	0.288	0.178	0.490
0.0064	0.453	0.459	0.626	0.280	0.173	0.485
0.0068	0.447	0.452	0.624	0.272	0.169	0.480
0.0072	0.441	0.447	0.622	0.265	0.166	0.475
0.0076	0.435	0.441	0.621	0.258	0.162	0.470
0.0080	0.430	0.435	0.619	0.252	0.159	0.466
0.0084	0.424	0.430	0.617	0.245	0.156	0.462
0.0088	0.419	0.425	0.616	0.239	0.153	0.457
0.0092	0.414	0.420	0.614	0.234	0.150	0.453
0.0096	0.409	0.415	0.612	0.228	0.147	0.450
0.0100	0.404	0.410	0.611	0.223	0.145	0.446

Table 24, continued.

$x_0, \text{g/cm}^2$	53I131	55Cs137	61Pm147	77Ir192	79Au198	81Tl204
0.0000	0.677	0.677	0.678	0.677	0.676	0.677
0.0002	0.637	0.638	0.563	0.634	0.655	0.645
0.0004	0.616	0.618	0.514	0.613	0.643	0.629
0.0006	0.601	0.603	0.480	0.598	0.634	0.617
0.0008	0.588	0.591	0.454	0.585	0.627	0.606
0.0010	0.577	0.580	0.432	0.573	0.620	0.598
0.0012	0.568	0.571	0.413	0.563	0.614	0.590
0.0014	0.559	0.562	0.396	0.554	0.608	0.582
0.0016	0.550	0.554	0.381	0.546	0.603	0.576
0.0018	0.543	0.546	0.367	0.538	0.598	0.570
0.0020	0.535	0.539	0.355	0.530	0.593	0.564
0.0022	0.529	0.533	0.344	0.524	0.589	0.558
0.0024	0.522	0.526	0.333	0.517	0.585	0.553
0.0026	0.516	0.520	0.324	0.511	0.581	0.548
0.0028	0.510	0.515	0.315	0.505	0.577	0.543
0.0030	0.505	0.509	0.306	0.499	0.573	0.539
0.0032	0.500	0.504	0.298	0.494	0.569	0.534
0.0034	0.494	0.499	0.290	0.489	0.566	0.530
0.0036	0.489	0.494	0.283	0.484	0.562	0.526
0.0038	0.485	0.490	0.277	0.479	0.559	0.522
0.0040	0.480	0.485	0.270	0.474	0.556	0.518
0.0042	0.476	0.481	0.264	0.470	0.553	0.514
0.0044	0.471	0.476	0.258	0.466	0.550	0.511
0.0046	0.467	0.472	0.253	0.461	0.547	0.507
0.0048	0.463	0.468	0.247	0.457	0.544	0.504
0.0050	0.459	0.464	0.242	0.453	0.541	0.500
0.0052	0.455	0.461	0.237	0.450	0.538	0.497
0.0054	0.452	0.457	0.232	0.446	0.536	0.494
0.0056	0.448	0.453	0.228	0.442	0.533	0.491
0.0058	0.444	0.450	0.224	0.439	0.530	0.488
0.0060	0.441	0.446	0.219	0.435	0.528	0.485
0.0064	0.434	0.440	0.211	0.428	0.523	0.479
0.0068	0.428	0.433	0.204	0.422	0.518	0.474
0.0072	0.422	0.427	0.197	0.416	0.514	0.468
0.0076	0.416	0.421	0.190	0.410	0.509	0.463
0.0080	0.410	0.416	0.184	0.404	0.505	0.458
0.0084	0.405	0.410	0.179	0.399	0.501	0.453
0.0088	0.399	0.405	0.173	0.393	0.497	0.449
0.0092	0.394	0.400	0.168	0.388	0.493	0.444
0.0096	0.389	0.395	0.163	0.383	0.489	0.440
0.0100	0.385	0.390	0.158	0.379	0.485	0.436

Table 25. Counting yield $\langle Y_b(x_0) \rangle$ of beta (-) sources distributed uniformly to depth x_0 in human skin.

$x_0, \text{g/cm}^2$	1H3	6C14	13Al28	15P32	16S35	17Cl36
0.0000	0.652	0.653	0.648	0.651	0.653	0.653
0.0002	0.158	0.533	0.646	0.646	0.520	0.631
0.0004	0.082	0.479	0.645	0.644	0.465	0.619
0.0006	0.055	0.442	0.644	0.641	0.427	0.610
0.0008	0.041	0.412	0.643	0.639	0.398	0.602
0.0010	0.033	0.388	0.643	0.637	0.375	0.594
0.0012	0.027	0.367	0.642	0.635	0.354	0.588
0.0014	0.023	0.348	0.641	0.633	0.337	0.582
0.0016	0.021	0.332	0.640	0.631	0.321	0.576
0.0018	0.018	0.317	0.639	0.629	0.307	0.571
0.0020	0.016	0.304	0.639	0.628	0.294	0.566
0.0022	0.015	0.292	0.638	0.626	0.283	0.561
0.0024	0.014	0.280	0.637	0.625	0.272	0.556
0.0026	0.013	0.270	0.636	0.623	0.262	0.552
0.0028	0.012	0.260	0.636	0.622	0.253	0.547
0.0030	0.011	0.251	0.635	0.620	0.244	0.543
0.0032	0.010	0.243	0.634	0.619	0.236	0.539
0.0034	0.010	0.235	0.634	0.617	0.229	0.535
0.0036	0.009	0.228	0.633	0.616	0.222	0.532
0.0038	0.009	0.221	0.632	0.615	0.215	0.528
0.0040	0.008	0.214	0.632	0.613	0.209	0.525
0.0042	0.008	0.208	0.631	0.612	0.203	0.521
0.0044	0.007	0.202	0.631	0.611	0.198	0.518
0.0046	0.007	0.196	0.630	0.610	0.192	0.514
0.0048	0.007	0.191	0.629	0.608	0.187	0.511
0.0050	0.007	0.186	0.629	0.607	0.182	0.508
0.0052	0.006	0.181	0.628	0.606	0.178	0.505
0.0054	0.006	0.176	0.628	0.605	0.173	0.502
0.0056	0.006	0.172	0.627	0.603	0.169	0.499
0.0058	0.006	0.167	0.626	0.602	0.165	0.496
0.0060	0.005	0.163	0.626	0.601	0.161	0.493
0.0064	0.005	0.156	0.625	0.599	0.154	0.488
0.0068	0.005	0.149	0.623	0.597	0.147	0.483
0.0072	0.005	0.142	0.622	0.595	0.141	0.478
0.0076	0.004	0.136	0.621	0.592	0.135	0.473
0.0080	0.004	0.130	0.620	0.590	0.130	0.468
0.0084	0.004	0.125	0.619	0.588	0.125	0.463
0.0088	0.004	0.120	0.618	0.586	0.120	0.459
0.0092	0.004	0.116	0.617	0.584	0.116	0.454
0.0096	0.003	0.112	0.616	0.582	0.112	0.450
0.0100	0.003	0.108	0.615	0.580	0.108	0.446

Table 25, continued.

$x_o, \text{g/cm}^2$	19K43	20Ca45	21Sc49	22Ti51	26Fe59	27Co60
0.0000	0.653	0.653	0.650	0.650	0.653	0.653
0.0002	0.636	0.565	0.647	0.647	0.592	0.580
0.0004	0.626	0.525	0.644	0.644	0.562	0.546
0.0006	0.618	0.497	0.642	0.642	0.540	0.522
0.0008	0.611	0.475	0.640	0.641	0.522	0.503
0.0010	0.605	0.456	0.638	0.639	0.507	0.486
0.0012	0.600	0.439	0.637	0.637	0.493	0.471
0.0014	0.594	0.424	0.635	0.636	0.481	0.458
0.0016	0.590	0.411	0.634	0.635	0.470	0.446
0.0018	0.585	0.399	0.632	0.633	0.460	0.435
0.0020	0.581	0.388	0.631	0.632	0.451	0.425
0.0022	0.577	0.378	0.630	0.631	0.442	0.416
0.0024	0.573	0.368	0.628	0.629	0.434	0.407
0.0026	0.569	0.359	0.627	0.628	0.426	0.399
0.0028	0.565	0.350	0.626	0.627	0.419	0.391
0.0030	0.562	0.343	0.625	0.626	0.412	0.384
0.0032	0.558	0.335	0.623	0.625	0.406	0.377
0.0034	0.555	0.328	0.622	0.624	0.399	0.370
0.0036	0.552	0.321	0.621	0.623	0.393	0.364
0.0038	0.548	0.314	0.620	0.622	0.388	0.358
0.0040	0.545	0.308	0.619	0.621	0.382	0.352
0.0042	0.542	0.302	0.618	0.619	0.377	0.346
0.0044	0.539	0.297	0.617	0.618	0.372	0.341
0.0046	0.537	0.291	0.616	0.617	0.367	0.335
0.0048	0.534	0.286	0.615	0.616	0.362	0.330
0.0050	0.531	0.281	0.614	0.615	0.358	0.326
0.0052	0.528	0.276	0.613	0.615	0.353	0.321
0.0054	0.526	0.271	0.612	0.614	0.349	0.316
0.0056	0.523	0.267	0.611	0.613	0.345	0.312
0.0058	0.521	0.262	0.610	0.612	0.341	0.308
0.0060	0.518	0.258	0.609	0.611	0.337	0.303
0.0064	0.513	0.250	0.607	0.609	0.329	0.296
0.0068	0.509	0.242	0.605	0.607	0.322	0.288
0.0072	0.504	0.235	0.603	0.605	0.315	0.281
0.0076	0.500	0.228	0.601	0.604	0.309	0.274
0.0080	0.496	0.222	0.599	0.602	0.303	0.268
0.0084	0.491	0.216	0.598	0.600	0.297	0.262
0.0088	0.487	0.210	0.596	0.599	0.291	0.256
0.0092	0.483	0.205	0.594	0.597	0.286	0.250
0.0096	0.480	0.199	0.593	0.596	0.280	0.245
0.0100	0.476	0.194	0.591	0.594	0.275	0.240

Table 25, continued.

$x_O, g/cm^2$	29Cu64	38Sr90	39Y90	43Tc99	47Ag110	51Sb124
0.0000	0.653	0.653	0.650	0.653	0.653	0.652
0.0002	0.619	0.618	0.645	0.568	0.479	0.621
0.0004	0.601	0.601	0.642	0.531	0.415	0.605
0.0006	0.588	0.588	0.640	0.504	0.376	0.593
0.0008	0.577	0.577	0.638	0.483	0.347	0.583
0.0010	0.567	0.568	0.636	0.464	0.325	0.574
0.0012	0.558	0.559	0.635	0.449	0.306	0.567
0.0014	0.550	0.551	0.633	0.435	0.291	0.560
0.0016	0.542	0.544	0.631	0.422	0.278	0.553
0.0018	0.536	0.537	0.630	0.410	0.267	0.548
0.0020	0.529	0.531	0.629	0.400	0.257	0.542
0.0022	0.523	0.525	0.627	0.390	0.248	0.537
0.0024	0.517	0.519	0.626	0.381	0.241	0.532
0.0026	0.511	0.514	0.625	0.372	0.234	0.527
0.0028	0.506	0.509	0.623	0.364	0.227	0.523
0.0030	0.501	0.504	0.622	0.356	0.221	0.519
0.0032	0.496	0.499	0.621	0.349	0.216	0.515
0.0034	0.491	0.494	0.620	0.342	0.211	0.511
0.0036	0.487	0.490	0.619	0.335	0.206	0.507
0.0038	0.482	0.486	0.618	0.329	0.202	0.504
0.0040	0.478	0.482	0.617	0.323	0.198	0.500
0.0042	0.474	0.478	0.615	0.317	0.195	0.497
0.0044	0.470	0.474	0.614	0.312	0.191	0.494
0.0046	0.466	0.470	0.613	0.307	0.188	0.490
0.0048	0.462	0.466	0.612	0.302	0.185	0.487
0.0050	0.458	0.463	0.611	0.297	0.182	0.484
0.0052	0.455	0.459	0.610	0.292	0.179	0.481
0.0054	0.451	0.456	0.609	0.287	0.176	0.479
0.0056	0.448	0.452	0.608	0.283	0.174	0.476
0.0058	0.444	0.449	0.607	0.279	0.172	0.473
0.0060	0.441	0.446	0.607	0.275	0.169	0.471
0.0064	0.435	0.440	0.605	0.267	0.165	0.466
0.0068	0.428	0.434	0.603	0.259	0.161	0.461
0.0072	0.423	0.428	0.601	0.252	0.157	0.456
0.0076	0.417	0.422	0.599	0.246	0.154	0.452
0.0080	0.411	0.417	0.598	0.239	0.151	0.447
0.0084	0.406	0.412	0.596	0.233	0.148	0.443
0.0088	0.401	0.407	0.594	0.227	0.145	0.439
0.0092	0.396	0.402	0.593	0.222	0.143	0.436
0.0096	0.391	0.398	0.591	0.217	0.140	0.432
0.0100	0.387	0.393	0.590	0.212	0.138	0.428

Table 25, continued.

$x_0, \text{g/cm}^2$	53I131	55Cs137	61Pm147	77Ir192	79Au198	81Tl204
0.0000	0.653	0.653	0.653	0.653	0.653	0.653
0.0002	0.613	0.614	0.540	0.611	0.631	0.621
0.0004	0.593	0.595	0.492	0.590	0.620	0.605
0.0006	0.578	0.580	0.459	0.575	0.611	0.593
0.0008	0.566	0.568	0.433	0.562	0.603	0.584
0.0010	0.555	0.558	0.412	0.551	0.597	0.575
0.0012	0.545	0.548	0.394	0.541	0.591	0.567
0.0014	0.536	0.540	0.378	0.532	0.585	0.560
0.0016	0.528	0.532	0.363	0.524	0.580	0.554
0.0018	0.521	0.525	0.350	0.516	0.575	0.548
0.0020	0.514	0.518	0.338	0.509	0.571	0.542
0.0022	0.507	0.511	0.327	0.502	0.567	0.536
0.0024	0.501	0.505	0.317	0.496	0.563	0.531
0.0026	0.495	0.499	0.308	0.490	0.559	0.526
0.0028	0.490	0.494	0.299	0.484	0.555	0.522
0.0030	0.484	0.489	0.291	0.479	0.551	0.517
0.0032	0.479	0.484	0.284	0.474	0.548	0.513
0.0034	0.474	0.479	0.276	0.469	0.544	0.509
0.0036	0.469	0.474	0.269	0.464	0.541	0.505
0.0038	0.465	0.469	0.263	0.459	0.538	0.501
0.0040	0.460	0.465	0.257	0.455	0.535	0.497
0.0042	0.456	0.461	0.251	0.450	0.532	0.494
0.0044	0.452	0.457	0.245	0.446	0.529	0.490
0.0046	0.448	0.453	0.240	0.442	0.526	0.487
0.0048	0.444	0.449	0.235	0.438	0.523	0.483
0.0050	0.440	0.445	0.230	0.434	0.520	0.480
0.0052	0.436	0.441	0.225	0.431	0.517	0.477
0.0054	0.433	0.438	0.221	0.427	0.515	0.474
0.0056	0.429	0.434	0.216	0.424	0.512	0.471
0.0058	0.426	0.431	0.212	0.420	0.510	0.468
0.0060	0.422	0.428	0.208	0.417	0.507	0.465
0.0064	0.416	0.421	0.200	0.410	0.502	0.460
0.0068	0.410	0.415	0.193	0.404	0.498	0.454
0.0072	0.404	0.409	0.187	0.398	0.493	0.449
0.0076	0.398	0.404	0.180	0.392	0.489	0.444
0.0080	0.393	0.398	0.174	0.387	0.485	0.439
0.0084	0.387	0.393	0.169	0.382	0.481	0.435
0.0088	0.382	0.388	0.164	0.377	0.477	0.430
0.0092	0.377	0.383	0.159	0.372	0.473	0.426
0.0096	0.373	0.378	0.154	0.367	0.469	0.422
0.0100	0.368	0.374	0.150	0.362	0.466	0.418

Table 26. Backscattering of alpha particles from backing of atomic weight A.

B = backscattering coefficient
 $B_f = 0.001649 + A^{0.628}$ = fitted backscattering coefficient;
 $Y = (1 + B)/2$ = counting yield
 $Y_f = (1 + B_f)/2$ = fitted counting yield

Z	A	B	B_f	% Diff.	Y	Y_f	% Diff.
3	6.941000	0.005512	0.005569	-1.0349	0.502756	0.502785	-0.0057
4	9.012182	0.006741	0.006562	2.7274	0.503370	0.503281	0.0178
5	10.811000	0.007290	0.007357	-0.9045	0.503645	0.503678	-0.0066
6	12.011000	0.008174	0.007860	4.0057	0.504087	0.503930	0.0312
11	22.989768	0.011398	0.011817	-3.5436	0.505699	0.505909	-0.0414
12	24.305000	0.012650	0.012237	3.3737	0.506325	0.506119	0.0408
13	26.981539	0.013627	0.013067	4.2805	0.506813	0.506534	0.0552
14	28.085500	0.013890	0.013401	3.6475	0.506945	0.506700	0.0482
19	39.098300	0.015695	0.016496	-4.8548	0.507848	0.508248	-0.0788
20	40.078000	0.016501	0.016755	-1.5160	0.508250	0.508377	-0.0250
21	44.955910	0.016837	0.018008	-6.5044	0.508418	0.509004	-0.1151
22	47.880000	0.017777	0.018735	-5.1153	0.508889	0.509368	-0.0941
23	50.941500	0.017951	0.019479	-7.8465	0.508975	0.509740	-0.1499
24	51.996100	0.019287	0.019732	-2.2536	0.509643	0.509866	-0.0436
25	54.938050	0.019944	0.020426	-2.3583	0.509972	0.510213	-0.0472
26	55.847000	0.020435	0.020637	-0.9821	0.510217	0.510319	-0.0199
27	58.933200	0.021504	0.021347	0.7370	0.510752	0.510673	0.0154
28	58.690000	0.022353	0.021291	4.9871	0.511177	0.510646	0.1040
29	63.546000	0.023094	0.022381	3.1818	0.511547	0.511191	0.0697
30	65.390000	0.024008	0.022787	5.3589	0.512004	0.511394	0.1194
31	69.723000	0.024291	0.023724	2.3864	0.512145	0.511862	0.0553
32	72.610000	0.024639	0.024337	1.2426	0.512320	0.512168	0.0295
33	74.921590	0.025484	0.024821	2.6716	0.512742	0.512410	0.0647
34	78.960000	0.026087	0.025653	1.6925	0.513044	0.512826	0.0423
46	106.420000	0.029907	0.030943	-3.3483	0.514953	0.515471	-0.1005
47	107.868200	0.031002	0.031207	-0.6541	0.515501	0.515603	-0.0198
48	112.411000	0.031443	0.032026	-1.8203	0.515721	0.516013	-0.0565
49	114.820000	0.031609	0.032455	-2.6079	0.515804	0.516228	-0.0820
50	118.710000	0.032215	0.033142	-2.7961	0.516107	0.516571	-0.0897
73	180.947900	0.043815	0.043189	1.4503	0.521908	0.521594	0.0600
74	183.850000	0.044614	0.043623	2.2736	0.522307	0.521811	0.0950
78	195.080000	0.047457	0.045278	4.8132	0.523729	0.522639	0.2085
79	196.966540	0.046451	0.045553	1.9727	0.523226	0.522776	0.0859
80	200.590000	0.047573	0.046077	3.2457	0.523786	0.523039	0.1430
81	204.383300	0.047371	0.046623	1.6055	0.523686	0.523311	0.0715
82	207.200000	0.046521	0.047025	-1.0719	0.523261	0.523513	-0.0481
92	238.028900	0.049105	0.051306	-4.2899	0.524553	0.525653	-0.2094

Table 27. Counting yield $Y(0)$ of alpha-particle sources at the surface of a backing of atomic number Z , as a function of the source energy E .

E (MeV)	$Z = 4$	5	6	11	12	13
9.0	0.5031	0.5035	0.5037	0.5055	0.5057	0.5061
8.8	0.5031	0.5035	0.5037	0.5055	0.5057	0.5061
8.6	0.5031	0.5035	0.5037	0.5056	0.5058	0.5061
8.4	0.5031	0.5035	0.5037	0.5056	0.5058	0.5062
8.2	0.5032	0.5035	0.5038	0.5056	0.5058	0.5062
8.0	0.5032	0.5035	0.5038	0.5056	0.5058	0.5062
7.8	0.5032	0.5036	0.5038	0.5057	0.5059	0.5062
7.6	0.5032	0.5036	0.5038	0.5057	0.5059	0.5063
7.4	0.5032	0.5036	0.5038	0.5057	0.5059	0.5063
7.2	0.5032	0.5036	0.5038	0.5057	0.5059	0.5063
7.0	0.5032	0.5036	0.5039	0.5058	0.5060	0.5064
6.8	0.5033	0.5036	0.5039	0.5058	0.5060	0.5064
6.6	0.5033	0.5037	0.5039	0.5058	0.5060	0.5064
6.4	0.5033	0.5037	0.5039	0.5059	0.5061	0.5065
6.2	0.5033	0.5037	0.5039	0.5059	0.5061	0.5065
6.0	0.5033	0.5037	0.5040	0.5059	0.5061	0.5066
5.8	0.5033	0.5037	0.5040	0.5060	0.5062	0.5066
5.6	0.5034	0.5038	0.5040	0.5060	0.5062	0.5066
5.4	0.5034	0.5038	0.5041	0.5061	0.5063	0.5067
5.2	0.5034	0.5038	0.5041	0.5061	0.5063	0.5067
5.0	0.5034	0.5039	0.5041	0.5062	0.5064	0.5068
4.8	0.5035	0.5039	0.5041	0.5062	0.5064	0.5069
4.6	0.5035	0.5039	0.5042	0.5063	0.5065	0.5069
4.4	0.5035	0.5040	0.5042	0.5063	0.5065	0.5070
4.2	0.5036	0.5040	0.5043	0.5064	0.5066	0.5071
4.0	0.5036	0.5040	0.5043	0.5065	0.5067	0.5071
3.8	0.5037	0.5041	0.5044	0.5065	0.5068	0.5072
3.6	0.5037	0.5041	0.5044	0.5066	0.5069	0.5073
3.4	0.5038	0.5042	0.5045	0.5067	0.5070	0.5074
3.2	0.5038	0.5043	0.5046	0.5068	0.5071	0.5075
3.0	0.5039	0.5043	0.5046	0.5069	0.5072	0.5077

Table 27, continued

E (MeV)	Z = 14	19	20	21	22	23
9.0	0.5062	0.5076	0.5078	0.5083	0.5087	0.5090
8.8	0.5063	0.5077	0.5078	0.5084	0.5087	0.5090
8.6	0.5063	0.5077	0.5078	0.5084	0.5087	0.5091
8.4	0.5063	0.5077	0.5079	0.5084	0.5088	0.5091
8.2	0.5063	0.5078	0.5079	0.5085	0.5088	0.5091
8.0	0.5064	0.5078	0.5079	0.5085	0.5088	0.5092
7.8	0.5064	0.5078	0.5080	0.5085	0.5089	0.5092
7.6	0.5064	0.5079	0.5080	0.5086	0.5089	0.5093
7.4	0.5065	0.5079	0.5080	0.5086	0.5090	0.5093
7.2	0.5065	0.5080	0.5081	0.5087	0.5090	0.5094
7.0	0.5065	0.5080	0.5081	0.5087	0.5091	0.5094
6.8	0.5066	0.5080	0.5082	0.5088	0.5091	0.5095
6.6	0.5066	0.5081	0.5082	0.5088	0.5092	0.5095
6.4	0.5066	0.5081	0.5083	0.5089	0.5092	0.5096
6.2	0.5067	0.5082	0.5083	0.5089	0.5093	0.5096
6.0	0.5067	0.5082	0.5084	0.5090	0.5093	0.5097
5.8	0.5068	0.5083	0.5084	0.5090	0.5094	0.5098
5.6	0.5068	0.5084	0.5085	0.5091	0.5095	0.5098
5.4	0.5069	0.5084	0.5085	0.5092	0.5095	0.5099
5.2	0.5069	0.5085	0.5086	0.5093	0.5096	0.5100
5.0	0.5070	0.5086	0.5087	0.5093	0.5097	0.5101
4.8	0.5070	0.5086	0.5088	0.5094	0.5098	0.5102
4.6	0.5071	0.5087	0.5088	0.5095	0.5099	0.5103
4.4	0.5072	0.5088	0.5089	0.5096	0.5100	0.5104
4.2	0.5072	0.5089	0.5090	0.5097	0.5101	0.5105
4.0	0.5073	0.5090	0.5091	0.5098	0.5102	0.5106
3.8	0.5074	0.5091	0.5092	0.5099	0.5103	0.5107
3.6	0.5075	0.5092	0.5094	0.5101	0.5105	0.5109
3.4	0.5076	0.5094	0.5095	0.5102	0.5106	0.5110
3.2	0.5077	0.5095	0.5097	0.5104	0.5108	0.5112
3.0	0.5079	0.5097	0.5098	0.5105	0.5110	0.5114

Table 27, continued

E (MeV)	Z = 24	25	26	27	28	29
9.0	0.5091	0.5094	0.5095	0.5098	0.5098	0.5103
8.8	0.5091	0.5094	0.5095	0.5099	0.5098	0.5103
8.6	0.5092	0.5095	0.5096	0.5099	0.5099	0.5104
8.4	0.5092	0.5095	0.5096	0.5099	0.5099	0.5104
8.2	0.5093	0.5096	0.5097	0.5100	0.5100	0.5105
8.0	0.5093	0.5096	0.5097	0.5100	0.5100	0.5105
7.8	0.5093	0.5097	0.5098	0.5101	0.5101	0.5106
7.6	0.5094	0.5097	0.5098	0.5101	0.5101	0.5106
7.4	0.5094	0.5098	0.5099	0.5102	0.5102	0.5107
7.2	0.5095	0.5098	0.5099	0.5102	0.5102	0.5107
7.0	0.5095	0.5099	0.5100	0.5103	0.5103	0.5108
6.8	0.5096	0.5099	0.5100	0.5104	0.5103	0.5108
6.6	0.5096	0.5100	0.5101	0.5104	0.5104	0.5109
6.4	0.5097	0.5100	0.5101	0.5105	0.5105	0.5110
6.2	0.5098	0.5101	0.5102	0.5105	0.5105	0.5110
6.0	0.5098	0.5102	0.5103	0.5106	0.5106	0.5111
5.8	0.5099	0.5102	0.5103	0.5107	0.5107	0.5112
5.6	0.5100	0.5103	0.5104	0.5108	0.5107	0.5113
5.4	0.5100	0.5104	0.5105	0.5109	0.5108	0.5114
5.2	0.5101	0.5105	0.5106	0.5109	0.5109	0.5115
5.0	0.5102	0.5106	0.5107	0.5110	0.5110	0.5116
4.8	0.5103	0.5107	0.5108	0.5111	0.5111	0.5117
4.6	0.5104	0.5108	0.5109	0.5112	0.5112	0.5118
4.4	0.5105	0.5109	0.5110	0.5114	0.5113	0.5119
4.2	0.5106	0.5110	0.5111	0.5115	0.5114	0.5120
4.0	0.5107	0.5111	0.5112	0.5116	0.5116	0.5122
3.8	0.5109	0.5113	0.5114	0.5118	0.5117	0.5123
3.6	0.5110	0.5114	0.5115	0.5119	0.5119	0.5125
3.4	0.5112	0.5116	0.5117	0.5121	0.5121	0.5127
3.2	0.5114	0.5117	0.5119	0.5123	0.5122	0.5129
3.0	0.5115	0.5119	0.5121	0.5125	0.5124	0.5131

Table 27, continued

E (MeV)	Z = 30	31	32	33	34	42
9.0	0.5105	0.5109	0.5112	0.5114	0.5118	0.5132
8.8	0.5105	0.5109	0.5112	0.5114	0.5118	0.5133
8.6	0.5106	0.5110	0.5113	0.5115	0.5119	0.5134
8.4	0.5106	0.5110	0.5113	0.5115	0.5119	0.5134
8.2	0.5106	0.5111	0.5114	0.5116	0.5120	0.5135
8.0	0.5107	0.5111	0.5114	0.5116	0.5120	0.5135
7.8	0.5107	0.5112	0.5115	0.5117	0.5121	0.5136
7.6	0.5108	0.5112	0.5115	0.5117	0.5121	0.5137
7.4	0.5109	0.5113	0.5116	0.5118	0.5122	0.5137
7.2	0.5109	0.5114	0.5116	0.5119	0.5123	0.5138
7.0	0.5110	0.5114	0.5117	0.5119	0.5123	0.5139
6.8	0.5110	0.5115	0.5118	0.5120	0.5124	0.5140
6.6	0.5111	0.5116	0.5118	0.5121	0.5125	0.5141
6.4	0.5112	0.5116	0.5119	0.5122	0.5126	0.5142
6.2	0.5112	0.5117	0.5120	0.5122	0.5126	0.5142
6.0	0.5113	0.5118	0.5121	0.5123	0.5127	0.5143
5.8	0.5114	0.5119	0.5122	0.5124	0.5128	0.5144
5.6	0.5115	0.5119	0.5123	0.5125	0.5129	0.5146
5.4	0.5116	0.5120	0.5123	0.5126	0.5130	0.5147
5.2	0.5117	0.5121	0.5124	0.5127	0.5131	0.5148
5.0	0.5118	0.5122	0.5126	0.5128	0.5132	0.5149
4.8	0.5119	0.5124	0.5127	0.5129	0.5133	0.5151
4.6	0.5120	0.5125	0.5128	0.5130	0.5135	0.5152
4.4	0.5121	0.5126	0.5129	0.5132	0.5136	0.5154
4.2	0.5122	0.5127	0.5131	0.5133	0.5138	0.5155
4.0	0.5124	0.5129	0.5132	0.5135	0.5139	0.5157
3.8	0.5125	0.5130	0.5134	0.5136	0.5141	0.5159
3.6	0.5127	0.5132	0.5136	0.5138	0.5143	0.5161
3.4	0.5129	0.5134	0.5138	0.5140	0.5145	0.5164
3.2	0.5131	0.5136	0.5140	0.5143	0.5147	0.5166
3.0	0.5133	0.5139	0.5142	0.5145	0.5150	0.5169

Table 27, continued

E (MeV)	Z = 46	47	48	49	50	64
9.0	0.5141	0.5142	0.5146	0.5148	0.5151	0.5179
8.8	0.5142	0.5143	0.5147	0.5148	0.5151	0.5180
8.6	0.5142	0.5143	0.5147	0.5149	0.5152	0.5181
8.4	0.5143	0.5144	0.5148	0.5150	0.5153	0.5182
8.2	0.5144	0.5145	0.5148	0.5150	0.5154	0.5182
8.0	0.5144	0.5145	0.5149	0.5151	0.5154	0.5183
7.8	0.5145	0.5146	0.5150	0.5152	0.5155	0.5184
7.6	0.5146	0.5147	0.5151	0.5153	0.5156	0.5185
7.4	0.5146	0.5148	0.5152	0.5154	0.5157	0.5186
7.2	0.5147	0.5149	0.5152	0.5154	0.5158	0.5187
7.0	0.5148	0.5149	0.5153	0.5155	0.5158	0.5188
6.8	0.5149	0.5150	0.5154	0.5156	0.5159	0.5190
6.6	0.5150	0.5151	0.5155	0.5157	0.5160	0.5191
6.4	0.5151	0.5152	0.5156	0.5158	0.5161	0.5192
6.2	0.5152	0.5153	0.5157	0.5159	0.5162	0.5193
6.0	0.5153	0.5154	0.5158	0.5160	0.5164	0.5195
5.8	0.5154	0.5155	0.5159	0.5161	0.5165	0.5196
5.6	0.5155	0.5157	0.5161	0.5163	0.5166	0.5198
5.4	0.5156	0.5158	0.5162	0.5164	0.5167	0.5199
5.2	0.5158	0.5159	0.5163	0.5165	0.5169	0.5201
5.0	0.5159	0.5160	0.5165	0.5167	0.5170	0.5203
4.8	0.5161	0.5162	0.5166	0.5168	0.5172	0.5205
4.6	0.5162	0.5164	0.5168	0.5170	0.5174	0.5207
4.4	0.5164	0.5165	0.5170	0.5172	0.5175	0.5209
4.2	0.5166	0.5167	0.5171	0.5174	0.5177	0.5211
4.0	0.5168	0.5169	0.5173	0.5176	0.5179	0.5214
3.8	0.5170	0.5171	0.5176	0.5178	0.5182	0.5216
3.6	0.5172	0.5174	0.5178	0.5180	0.5184	0.5219
3.4	0.5175	0.5176	0.5181	0.5183	0.5187	0.5223
3.2	0.5177	0.5179	0.5183	0.5186	0.5190	0.5226
3.0	0.5180	0.5182	0.5187	0.5189	0.5193	0.5230

Table 27, continued

E (MeV)	Z = 73	74	78	79	82	92
9.0	0.5195	0.5197	0.5205	0.5206	0.5212	0.5231
8.8	0.5196	0.5198	0.5205	0.5207	0.5213	0.5232
8.6	0.5197	0.5199	0.5206	0.5208	0.5214	0.5233
8.4	0.5198	0.5200	0.5207	0.5209	0.5215	0.5234
8.2	0.5199	0.5201	0.5208	0.5210	0.5216	0.5235
8.0	0.5200	0.5202	0.5209	0.5211	0.5217	0.5237
7.8	0.5201	0.5203	0.5210	0.5212	0.5218	0.5238
7.6	0.5202	0.5204	0.5212	0.5213	0.5219	0.5239
7.4	0.5203	0.5205	0.5213	0.5214	0.5221	0.5240
7.2	0.5204	0.5206	0.5214	0.5215	0.5222	0.5242
7.0	0.5205	0.5207	0.5215	0.5216	0.5223	0.5243
6.8	0.5207	0.5209	0.5216	0.5218	0.5225	0.5245
6.6	0.5208	0.5210	0.5218	0.5219	0.5226	0.5246
6.4	0.5209	0.5211	0.5219	0.5221	0.5228	0.5248
6.2	0.5211	0.5213	0.5221	0.5222	0.5229	0.5250
6.0	0.5212	0.5214	0.5222	0.5224	0.5231	0.5252
5.8	0.5214	0.5216	0.5224	0.5225	0.5233	0.5253
5.6	0.5216	0.5218	0.5226	0.5227	0.5234	0.5255
5.4	0.5217	0.5219	0.5228	0.5229	0.5236	0.5258
5.2	0.5219	0.5221	0.5230	0.5231	0.5238	0.5260
5.0	0.5221	0.5223	0.5232	0.5233	0.5241	0.5262
4.8	0.5223	0.5225	0.5234	0.5235	0.5243	0.5265
4.6	0.5225	0.5228	0.5236	0.5238	0.5245	0.5267
4.4	0.5228	0.5230	0.5239	0.5240	0.5248	0.5270
4.2	0.5230	0.5233	0.5241	0.5243	0.5251	0.5273
4.0	0.5233	0.5236	0.5244	0.5246	0.5254	0.5277
3.8	0.5236	0.5239	0.5247	0.5249	0.5257	0.5280
3.6	0.5239	0.5242	0.5251	0.5252	0.5260	0.5284
3.4	0.5243	0.5245	0.5255	0.5256	0.5264	0.5288
3.2	0.5247	0.5249	0.5259	0.5260	0.5269	0.5293
3.0	0.5251	0.5254	0.5263	0.5265	0.5273	0.5298

Table 28. Relation between the counting yield of a plane alpha-particle source at the surface of a backing, $Y(0)$, and the yield of a plane source at a depth x below the surface, $Y(x)$. The tabulated quantity is the percentage reduction $100 [1-Y(x)/Y(0)]$, as a function of x , the energy E , and the atomic number Z of the backing.

$E = 9.2 \text{ MeV}$

x (10^{-6} g/cm^2)	$Z = 4$	13	26	47	78	92
0.0	0.00	0.00	0.00	0.00	0.00	0.00
1.0	0.06	0.08	0.08	0.08	0.06	0.07
2.0	0.10	0.12	0.12	0.12	0.09	0.10
3.0	0.13	0.15	0.15	0.15	0.12	0.13
4.0	0.15	0.18	0.18	0.18	0.14	0.15
5.0	0.18	0.20	0.20	0.20	0.17	0.17
6.0	0.20	0.23	0.23	0.23	0.19	0.19
8.0	0.24	0.27	0.27	0.27	0.22	0.22
10.0	0.28	0.31	0.31	0.30	0.26	0.25
12.0	0.31	0.35	0.35	0.34	0.29	0.28
15.0	0.36	0.40	0.40	0.39	0.33	0.32
20.0	0.43	0.48	0.48	0.46	0.40	0.37
25.0	0.50	0.54	0.55	0.52	0.45	0.42
30.0	0.56	0.61	0.61	0.58	0.51	0.47
40.0	0.68	0.72	0.73	0.68	0.61	0.55
50.0	0.78	0.83	0.84	0.78	0.70	0.63

Table 28, continued.

E = 6.4 MeV

x (10^{-6} g/cm 2)	Z = 4	13	26	47	78	92
0.0	0.00	0.00	0.00	0.00	0.00	0.00
1.0	0.09	0.10	0.10	0.09	0.08	0.09
2.0	0.14	0.16	0.16	0.14	0.13	0.14
3.0	0.18	0.21	0.20	0.18	0.17	0.18
4.0	0.22	0.25	0.24	0.22	0.20	0.21
5.0	0.26	0.29	0.28	0.25	0.23	0.24
6.0	0.29	0.32	0.31	0.28	0.26	0.27
8.0	0.35	0.38	0.37	0.34	0.31	0.32
10.0	0.41	0.44	0.43	0.39	0.35	0.37
12.0	0.46	0.50	0.48	0.44	0.40	0.41
15.0	0.54	0.57	0.55	0.50	0.46	0.47
20.0	0.65	0.68	0.66	0.60	0.55	0.56
25.0	0.75	0.78	0.76	0.69	0.63	0.64
30.0	0.85	0.88	0.85	0.77	0.71	0.71
40.0	1.03	1.05	1.01	0.93	0.84	0.85
50.0	1.19	1.20	1.16	1.06	0.97	0.97

E = 5.3 MeV

x (10^{-6} g/cm 2)	Z = 4	13	26	47	78	92
0.0	0.00	0.00	0.00	0.00	0.00	0.00
1.0	0.11	0.12	0.12	0.12	0.10	0.10
2.0	0.17	0.19	0.19	0.18	0.16	0.16
3.0	0.22	0.25	0.24	0.23	0.20	0.20
4.0	0.27	0.30	0.29	0.27	0.24	0.24
5.0	0.31	0.34	0.33	0.31	0.27	0.28
6.0	0.35	0.38	0.37	0.35	0.31	0.31
8.0	0.43	0.46	0.44	0.41	0.36	0.37
10.0	0.50	0.53	0.51	0.47	0.42	0.42
12.0	0.56	0.59	0.57	0.53	0.46	0.47
15.0	0.66	0.68	0.65	0.61	0.53	0.54
20.0	0.80	0.82	0.78	0.72	0.63	0.65
25.0	0.93	0.94	0.90	0.83	0.72	0.75
30.0	1.05	1.06	1.00	0.92	0.81	0.84
40.0	1.27	1.27	1.20	1.10	0.96	1.00
50.0	1.48	1.46	1.37	1.26	1.10	1.14

Table 28, continued.

E = 4 MeV

x (10^{-6} g/cm 2)	Z = 4	13	26	47	78	92
0.0	0.00	0.00	0.00	0.00	0.00	0.00
1.0	0.12	0.16	0.15	0.14	0.13	0.11
2.0	0.20	0.25	0.23	0.21	0.19	0.17
3.0	0.27	0.32	0.30	0.27	0.25	0.22
4.0	0.33	0.39	0.36	0.33	0.30	0.27
5.0	0.39	0.44	0.41	0.37	0.34	0.31
6.0	0.44	0.50	0.46	0.42	0.38	0.35
8.0	0.55	0.60	0.55	0.50	0.45	0.42
10.0	0.64	0.70	0.64	0.57	0.52	0.49
12.0	0.73	0.78	0.72	0.64	0.58	0.55
15.0	0.86	0.90	0.82	0.73	0.66	0.63
20.0	1.05	1.09	0.99	0.87	0.79	0.76
25.0	1.24	1.25	1.13	1.00	0.91	0.87
30.0	1.41	1.41	1.27	1.12	1.02	0.98
40.0	1.73	1.69	1.52	1.33	1.21	1.18
50.0	2.03	1.95	1.75	1.52	1.39	1.36

E = 3 MeV

x (10^{-6} g/cm 2)	Z = 4	13	26	47	78	92
0.0	0.00	0.00	0.00	0.00	0.00	0.00
1.0	0.16	0.17	0.17	0.12	0.14	0.15
2.0	0.27	0.28	0.27	0.20	0.22	0.23
3.0	0.36	0.37	0.35	0.27	0.29	0.29
4.0	0.44	0.45	0.43	0.33	0.34	0.35
5.0	0.52	0.53	0.50	0.39	0.39	0.40
6.0	0.60	0.60	0.56	0.44	0.44	0.45
8.0	0.74	0.73	0.68	0.54	0.52	0.54
10.0	0.87	0.85	0.79	0.64	0.60	0.62
12.0	0.99	0.97	0.89	0.73	0.67	0.69
15.0	1.17	1.14	1.03	0.86	0.77	0.79
20.0	1.45	1.39	1.25	1.06	0.92	0.95
25.0	1.70	1.62	1.45	1.24	1.06	1.09
30.0	1.94	1.84	1.64	1.42	1.18	1.22
40.0	2.40	2.25	1.98	1.75	1.41	1.46
50.0	2.82	2.62	2.29	2.06	1.62	1.67

Table 29. Relation between the counting yield of a plane alpha-particle source at the surface of a backing, $Y(0)$, and the yield of a uniform layer source extending to a depth x_0 below the surface, $Y_{av}(x_0)$. The tabulated quantity is the percentage reduction $100 [1 - Y_{av}(x_0)/Y(0)]$, as a function of x , the particle energy E , and the atomic number Z of the backing.

$E = 9.2 \text{ MeV}$

x_0 (10^{-6} g/cm^2)	$Z = 4$	13	26	47	78	92
0.0	0.00	0.00	0.00	0.00	0.00	0.00
1.0	0.06	0.08	0.08	0.08	0.06	0.07
2.0	0.10	0.12	0.12	0.12	0.09	0.10
3.0	0.13	0.15	0.15	0.15	0.12	0.13
4.0	0.15	0.18	0.18	0.18	0.14	0.15
5.0	0.18	0.20	0.20	0.20	0.17	0.17
6.0	0.20	0.23	0.23	0.23	0.19	0.19
8.0	0.24	0.27	0.27	0.27	0.22	0.22
10.0	0.28	0.31	0.31	0.30	0.26	0.25
12.0	0.31	0.35	0.35	0.34	0.29	0.28
15.0	0.36	0.40	0.40	0.39	0.33	0.32
20.0	0.43	0.48	0.48	0.46	0.40	0.37
25.0	0.50	0.54	0.55	0.52	0.45	0.42
30.0	0.56	0.61	0.61	0.58	0.51	0.47
40.0	0.68	0.72	0.73	0.68	0.61	0.55
50.0	0.78	0.83	0.84	0.78	0.70	0.63

Table 29, continued.

E = 6.4 MeV

$(10^{-6} \frac{x_o}{g/cm^2})$	Z = 4	13	26	47	78	92
0.0	0.00	0.00	0.00	0.00	0.00	0.00
1.0	0.09	0.10	0.10	0.09	0.08	0.09
2.0	0.14	0.16	0.16	0.14	0.13	0.14
3.0	0.18	0.21	0.20	0.18	0.17	0.18
4.0	0.22	0.25	0.24	0.22	0.20	0.21
5.0	0.26	0.29	0.28	0.25	0.23	0.24
6.0	0.29	0.32	0.31	0.28	0.26	0.27
8.0	0.35	0.38	0.37	0.34	0.31	0.32
10.0	0.41	0.44	0.43	0.39	0.35	0.37
12.0	0.46	0.50	0.48	0.44	0.40	0.41
15.0	0.54	0.57	0.55	0.50	0.46	0.47
20.0	0.65	0.68	0.66	0.60	0.55	0.56
25.0	0.75	0.78	0.76	0.69	0.63	0.64
30.0	0.85	0.88	0.85	0.77	0.71	0.71
40.0	1.03	1.05	1.01	0.93	0.84	0.85
50.0	1.19	1.20	1.16	1.06	0.97	0.97

E = 5.3 MeV

$(10^{-6} \frac{x_o}{g/cm^2})$	Z = 4	13	26	47	78	92
0.0	0.00	0.00	0.00	0.00	0.00	0.00
1.0	0.11	0.12	0.12	0.12	0.10	0.10
2.0	0.17	0.19	0.19	0.18	0.16	0.16
3.0	0.22	0.25	0.24	0.23	0.20	0.20
4.0	0.27	0.30	0.29	0.27	0.24	0.24
5.0	0.31	0.34	0.33	0.31	0.27	0.28
6.0	0.35	0.38	0.37	0.35	0.31	0.31
8.0	0.43	0.46	0.44	0.41	0.36	0.37
10.0	0.50	0.53	0.51	0.47	0.42	0.42
12.0	0.56	0.59	0.57	0.53	0.46	0.47
15.0	0.66	0.68	0.65	0.61	0.53	0.54
20.0	0.80	0.82	0.78	0.72	0.63	0.65
25.0	0.93	0.94	0.90	0.83	0.72	0.75
30.0	1.05	1.06	1.00	0.92	0.81	0.84
40.0	1.27	1.27	1.20	1.10	0.96	1.00
50.0	1.48	1.46	1.37	1.26	1.10	1.14

Table 29, continued.

E = 4 MeV

x_{O} (10^{-6} g/cm 2)	Z = 4	13	26	47	78	92
0.0	0.00	0.00	0.00	0.00	0.00	0.00
1.0	0.12	0.16	0.15	0.14	0.13	0.11
2.0	0.20	0.25	0.23	0.21	0.19	0.17
3.0	0.27	0.32	0.30	0.27	0.25	0.22
4.0	0.33	0.39	0.36	0.33	0.30	0.27
5.0	0.39	0.44	0.41	0.37	0.34	0.31
6.0	0.44	0.50	0.46	0.42	0.38	0.35
8.0	0.55	0.60	0.55	0.50	0.45	0.42
10.0	0.64	0.70	0.64	0.57	0.52	0.49
12.0	0.73	0.78	0.72	0.64	0.58	0.55
15.0	0.86	0.90	0.82	0.73	0.66	0.63
20.0	1.05	1.09	0.99	0.87	0.79	0.76
25.0	1.24	1.25	1.13	1.00	0.91	0.87
30.0	1.41	1.41	1.27	1.12	1.02	0.98
40.0	1.73	1.69	1.52	1.33	1.21	1.18
50.0	2.03	1.95	1.75	1.52	1.39	1.36

E = 3 MeV

x_{O} (10^{-6} g/cm 2)	Z = 4	13	26	47	78	92
0.0	0.00	0.00	0.00	0.00	0.00	0.00
1.0	0.16	0.17	0.17	0.12	0.14	0.15
2.0	0.27	0.28	0.27	0.20	0.22	0.23
3.0	0.36	0.37	0.35	0.27	0.29	0.29
4.0	0.44	0.45	0.43	0.33	0.34	0.35
5.0	0.52	0.53	0.50	0.39	0.39	0.40
6.0	0.60	0.60	0.56	0.44	0.44	0.45
8.0	0.74	0.73	0.68	0.54	0.52	0.54
10.0	0.87	0.85	0.79	0.64	0.60	0.62
12.0	0.99	0.97	0.89	0.73	0.67	0.69
15.0	1.17	1.14	1.03	0.86	0.77	0.79
20.0	1.45	1.39	1.25	1.06	0.92	0.95
25.0	1.70	1.62	1.45	1.24	1.06	1.09
30.0	1.94	1.84	1.64	1.42	1.18	1.22
40.0	2.40	2.25	1.98	1.75	1.41	1.46
50.0	2.82	2.62	2.29	2.06	1.62	1.67

Table 30. Effect of surface roughness on the ratio of the counting rates $R = N_{2\pi}/N_{1\pi}$ with 2π and 1π detectors. From an experiment by Hutchinson, Naas, Walker and Mann [21] with a thin Po-210 source mounted on various metal backings.

R_U = ratios obtained with polonium chloride top of unpolished backings
 R_P = ratios obtained with polonium chloride source on top of polished backings
 R_C = ratios obtained with polonium-chloride in collodion film placed on top of polished backings

Backing	% Difference $100 (R_U - R_P)/R_P$	% Difference $100 (R_P - R_C)/R_C$
Be	-2.70	-0.04
Al	0.48	-0.98
Ni	0.12	----
Monel	-0.15	0.51
Cu	-4.96	0.98
Ag	-0.12	-0.08
Cd	----	-0.39
Pt	-0.15	-0.61
Au	0.08	-0.72

Table 31. Counting yields Y_1 and Y_2 for $^{233}\text{UF}_4$ -Si alpha particle sources obtained with two different approximations.

	S o u r c e			
	2002-2	2003-1	3003-3	2004-1
x_o , thickness of UF_4 ($\mu\text{g}/\text{cm}^2$)	7.44	13.08	13.11	20.52
$x_o/\text{range}(\text{Si})$	0.0014	0.0025	0.0025	0.0039
x_o' , equiv.thickness, Si ($\mu\text{g}/\text{cm}^2$)	3.71	6.53	6.54	10.24
$Y(x_o')/Y(0)$ for Si	0.9981	0.9973	0.9973	0.9964
Y_1 (from range-scaling method)	0.5061	0.5057	0.5057	0.5052
$Y(x_o)/Y(0)$ for UF_4	0.9973	0.9962	0.9962	0.9950
Y_2 (appl.of UF_4 reduction factor)	0.5057	0.5051	0.5051	0.5045

Table 32. Comparison of the experimental results of Hutchinson (private communication) and Gilliam [22] pertaining to the activities of $^{233}\text{UF}_4$ (4.81-MeV) alpha-particle sources placed on top of a thick Si backing.

- x: Thickness of UF_4 layer
 Y_L : Counting yield from Lucas model, Ref [23]
 Y_1 : Counting yield from the present calculation (with range scaling)
 Y_2 : Counting yield from the present calculation (with UF_4 reduction factor)
 N_G : Source activity reported by D.M. Gilliam, based on measurements with a narrow-geometry counter, from Ref [22]
 N_H : Source activity reported by J.M.R. Hutchinson, based on measurements with a 2 counter, and assuming a counting yield Y_L from the Lucas model.
 N_1 : Corrected source activity obtained by multiplying N_H by the ratio Y_L/Y_1 .
 N_2 : Corrected source activity obtained by multiplying N_H by the ratio Y_L/Y_2

Source	x ($\mu\text{g}/\text{cm}^2$)	Y_L	Y_1	Y_2	N_G (Bq)	N_H (Bq)	N_1 (Bq)	N_2 (Bq)
2002-2	7.444	0.5026	0.5061	0.5057	6186.7	6238.0	6194.9	6199.8
2003-1	13.055	0.5015	0.5057	0.5051	10870.8	10954.0	10863.0	10875.9
3003-3	13.077	0.5015	0.5057	0.5051	10890.9	10972.0	10880.8	10893.8
2004-1	20.472	0.5011	0.5052	0.5045	17058.1	17178.0	17038.6	17062.2

Source	x ($\mu\text{g}/\text{cm}^2$)	P e r c e n t D i f f e r e n c e		
		$100(N_H - N_G)/N_G$	$100(N_1 - N_G)/N_G$	$100(N_2 - N_G)/N_G$
2002-3	7.444	0.829	0.133	0.212
2003-1	13.055	0.765	-0.072	0.047
3003-3	13.077	0.745	-0.093	0.027
2004-1	20.472	0.703	-0.114	0.024

Table 33. Comparison of experimental and calculated counting yields
 The experimental yields are from measurements by Hutchinson
et al [21] for Po-210 (5.3045 MeV) alpha particle sources
 mounted on various metal backings, interpreted with use
 of Eq(7).

Z	Atomic Weight	Counting Yield		Percent Difference
		Y_{exp}	Y_{calc}	$100 (Y_{exp} - Y_{calc})/Y_{calc}$
4	9.012182	0.5031	0.5034	-0.06
13	26.981539	0.5066	0.5067	-0.02
26	55.27	0.5107	0.5105	0.04
29	63.546	0.5117	0.5114	0.06
47	107.8682	0.5166	0.5158	0.16
48	112.411	0.5170	0.5162	0.15
78	195.080	0.5243	0.5229	0.27
79	196.96654	0.5244	0.5230	0.27

